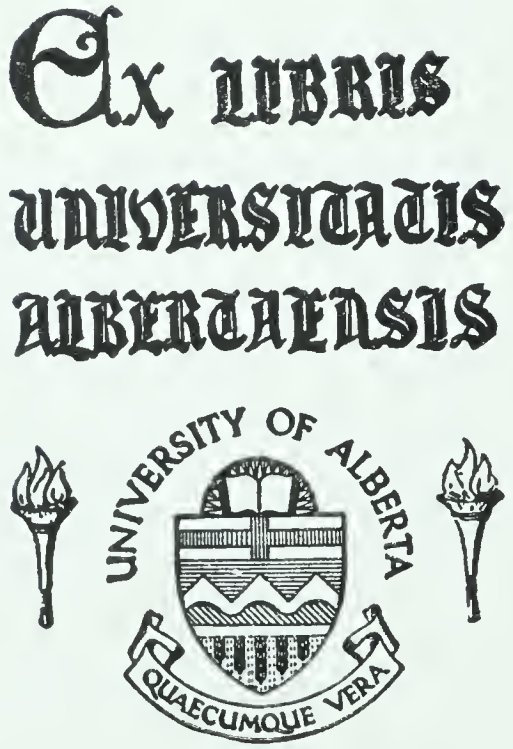

University of Alberta
Printing Department

THE UNIVERSITY OF ALBERTA

AN EXPERIMENTAL STUDY OF INJECTION OF SUPERHEATED STEAM INTO THE COMBUSTION CHAMBER OF A GAS TURBINE

A THESIS

SUBMITTED TO THE FACULTY OF GRADUATE STUDIES

IN PARTIAL FULFILMENT OF THE REQUIREMENTS FOR THE DEGREE OF

MASTER OF SCIENCE

DEPARTMENT OF MECHANICAL ENGINEERING

by

JAMES DOUGLAS DALE, B.Sc. (Alberta)

EDMONTON, ALBERTA

SEPTEMBER, 1963

UNIVERSITY OF ALBERTA

FACULTY OF GRADUATE STUDIES

The undersigned certify that they have read, and recommend to the Faculty of Graduate Studies for acceptance, a thesis entitled "An Experimental Study of Injection of Superheated Steam into the Combustion Chamber of a Gas Turbine" submitted by James Douglas Dale in partial fulfilment of the requirements for the degree of Master of Science.

ABSTRACT

In recent years many authors have published papers discussing the theoretical merits of injecting steam into the gas turbine cycle. This experimental work investigates the problem.

Even though the experimental apparatus was of very low efficiency, the effect of injecting superheated steam was found to improve the thermal efficiency of the cycle. Comparing the experimental results with theoretical calculations for the same cycle, good agreement was obtained, indicating that the effect may have been correctly predicted.

ACKNOWLEDGMENTS

The author wishes to extend his appreciation to Prof. D. Panar for supervising this thesis and for the numerous hours spent helping in the laboratory during the building and running of the equipment.

Thanks must also go to the staff members of the Mechanical Engineering Department Shop for their help and insight in constructing the apparatus.

To Dr. W. C. Eccles and Dr. L. Hertzman of the Department of History the author is indebted for their patience, understanding and interest in translating verbally the papers by P. Chambadal and H. J. Schröder respectively.

He would also like to thank all the members of the Department of Mechanical Engineering for their help and interest, and particularly H. Y. Tso for his help in developing the photographs, and D. G. Bellow for his many helpful suggestions.

TABLE OF CONTENTS

CHAPTER PAGE

LIST OF TABLES

LIST OF FIGURES

NOTATION

°A.P.I.	American Petroleum Institute Gravity Scale
B.T.U.	British Thermal Unit
°C.	degrees Centigrade
c.c.	combustion chamber
comp.	compressor
Cp	constant-pressure specific heat
Cv	constant-volume specific heat
°F.	degrees Fahrenheit
FE	flow energy
H	isentropic heat drop
h	enthalpy
h	heat-transfer coefficient
Hg	mercury
H_2O	water
HP	horsepower
HR	hour
IE	internal energy
J	Joule
k	specific-heat ratio: Cp/Cv
KE	kinetic energy
Kg	kilogram
kCal	kilocalorie

L.H.V.	lower heating value
lbf	pound force
lbm	pound mass
$\dot{m}$	mass rate of flow
P	pressure
PE	potential energy
Ps	static pressure
p.s.i.	pressure
p.s.i.a.	absolute pressure
p.s.i.g.	gauge pressure
P_t	total pressure
Q	total heat transfer
R	gas constant
°R	degrees Rankine
R.P.M.	revolutions per minute
s	specific entropy
sec.	seconds
T	absolute temperature in degrees R
T_t	total absolute temperature in degrees R
turb.	turbine
U	circumferential speed
U	internal energy
v	specific volume

W	work
δ	pressure ratio
η_{ad}	adiabatic efficiency
η_c	compressor adiabatic efficiency

CHAPTER 1

INTRODUCTION

The fundamental problem considered in this experimental investigation is the effect of steam injection on the thermal efficiency of a simple open cycle gas turbine.

1.1 History

While the historical development of the gas turbine is completely documented[1] and too lengthy to be presented here, a few significant developments, some of which have been patented, as described in literature, should be noted.

The basic principle underlying the gas turbine has been known since the time of the ancient Greeks[2], and the first cycle patent was given to John Barber in 1791 in England. This patent included all the elements of a modern simple gas turbine except that the compressor was of the reciprocating type and provision was made for cooling the hot gases by water injection.

Of much greater interest, however, is British patent No. 1328, awarded to W. F. Fernihough in 1850, for a mixed steam and gas turbine unit. It is typical of other patents that were based on the use of a combination of combustion gases and steam to drive a turbine. This one in particular consisted of a boiler, where high pressure air was added to the fuel and the mixture burned, in which the hot gases of combustion rose into a heat exchange matrix into which water was sprayed. The hot gases and the matrix would convert the water into steam by direct contact, and the mixture then travelled through a nozzle impinging on a turbine wheel.

Although serious attempts at obtaining a successful gas turbine were made in the late 1800's[3], it was not until 1905 that the first significant success was achieved. This was done by the Société Anonyme de Turbomoteurs in Paris, who built a gas turbine which did drive itself even though its efficiency was very low.[4,5] Again a combined cycle was used, that is, water was used to cool the combustion flame by use of a heat exchanger, after which the water was injected into the combustion chamber and made into steam in order to keep the temperature of the gases acting on the turbine wheel to about 1030°F.

From here further developments slowly took place until the outbreak of the Second World War which gave impetus to rapid developments in both materials used and component efficiencies, particularly in the jet propulsion field, from which the gas turbine benefited immensely.

It is interesting to note though, how the outlook on steam injection has varied. Initially steam was injected to keep the bucket or blade temperature to values dictated by the blade material strength under the adverse stress conditions as mentioned by Stodola[5] and Marks[6]. Even though Marks[6] does work out theoretical examples of steam injection, one with it doing useful work, another without, for some reason the compressor and turbine efficiencies were changed from one example to another, as well as the amount of steam per pound of gas flow injected and the temperatures obtained in the cycle, thus no theoretical conclusion can be drawn.

Coutant[7] states that tests were done with steam injection as far back as 1920, but the results obtained from such tests perhaps may have been inconclusive as no other sources are mentioned by Coutant, and none could be found.

The idea of steam injection remained dormant until 1945, when Sawyer[1] makes some "suggestions from the past". In summary, he says, "None of the foregoing suggestions, except that shown in figure 8 (the patent by W. F. Fernihough mentioned on page 1) has merit today."

The only difference between the patent by Fernihough and the thinking today is that the steam should be produced in a waste heat boiler, instead of injecting the water to produce steam directly into the combustion chamber.

Interest has again risen in recent years as evidenced by the number of papers written on this subject, although no experimental work could be found. All of these papers[7,8,9,10,11,12] do agree unanimously in that steam produced from a waste heat boiler and injected into the combustion chamber of a gas turbine should improve the turbine's thermal efficiency, the proof of which is the purpose of this experimental work.

1.2 Basic Types of Gas Turbine Cycles

The simple gas turbine or Brayton cycle operates on a continuous flow cycle. Air is compressed and fed into a combustion chamber where fuel is added and the mixture burned. The hot gases then accelerate in a nozzle ring which directs them onto a turbine wheel. The turbine wheel and the compressor (usually of a centrifugal or an axial flow type) are connected on a shaft. If the work of the turbine wheel exceeds that of the compressor, additional work can be produced by the machine. A flow diagram and a T-s diagram for a simple cycle are shown in figure 1-1.

The T-s diagram shows that due to less than 100% adiabatic efficiency of the components the temperature increases at the compressor outlet over the ideal

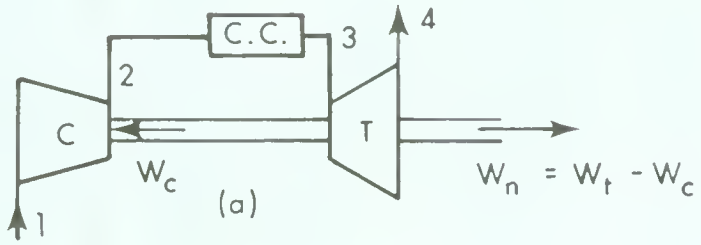

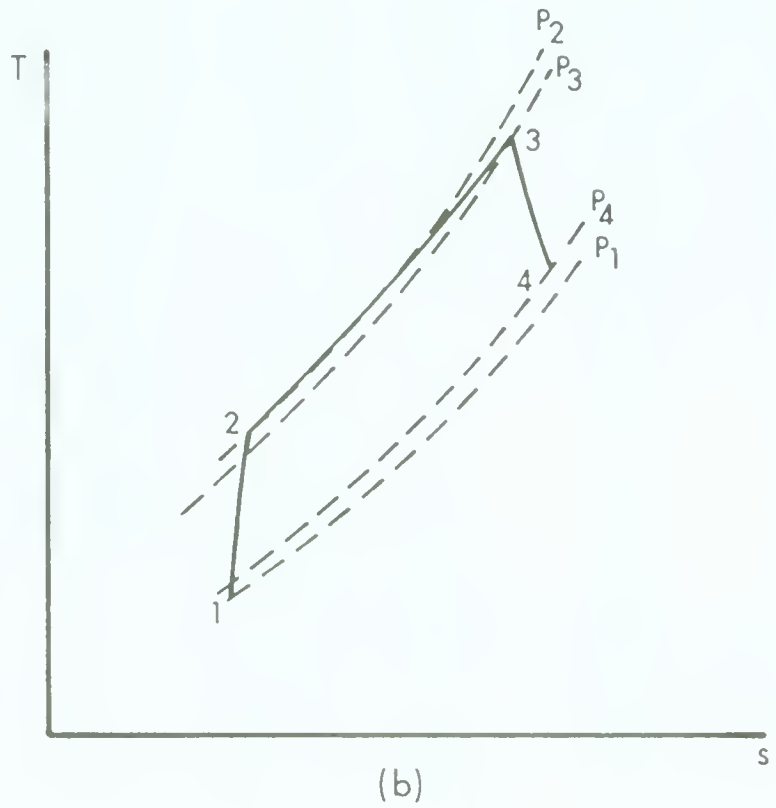

FIGURE 1-1 SIMPLE OPEN CYCLE

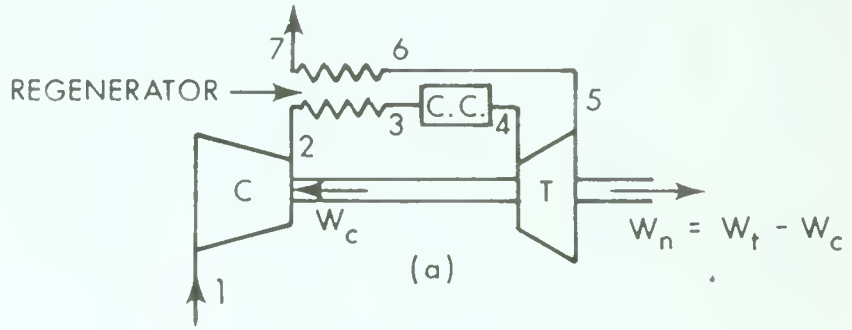

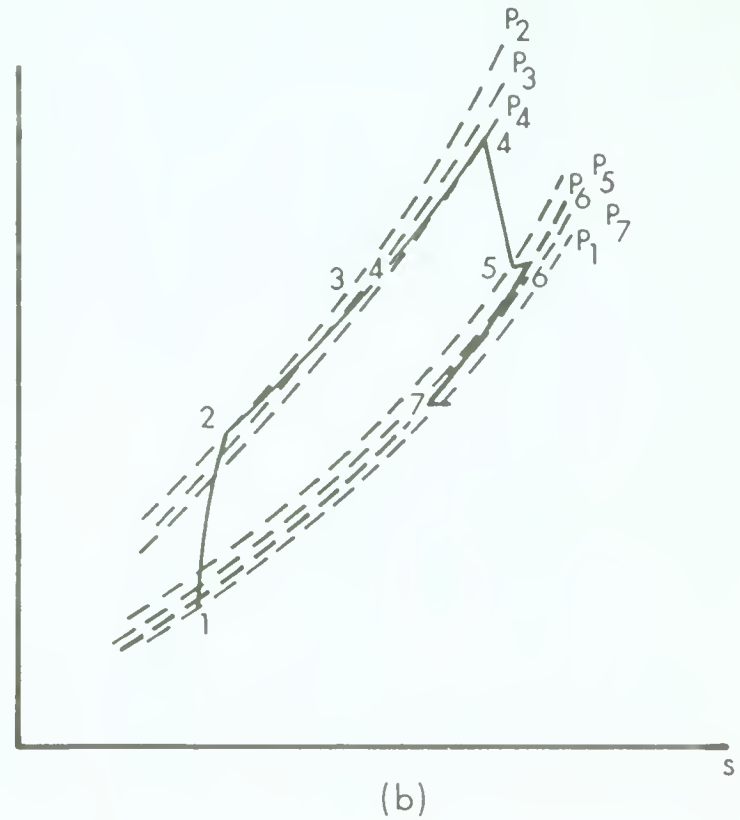

FIGURE 1-2 REGENERATIVE CYCLE

temperature rise, and similarly for the turbine, while a pressure drop exists through the combustion chamber. It is also evident that a great loss of heat from the cycle occurs when exhausting the hot gases to the atmosphere at T_4. To recover some of this energy variations of the simple open cycle have been developed.

The most obvious step is to use the hot exhaust gases to heat the compressed air before the combustion chamber, cutting down on the amount of fuel added to the cycle. Figure 1-2 shows a flow diagram and a T-s diagram of this cycle. By comparing the T-s diagram of figure 1-1 with that of figure 1-2, it is immediately evident that much less heat is lost to the atmosphere. By making more use of the heat available in the cycle, the overall thermal efficiency is consequently increased.

Another cycle variation is that of heating the hot exhaust gases at T_4 in figure 1-1 back to a temperature equal to that of T_3 and expanding them in another turbine. Naturally the pressure drop across each turbine must be less than that from P_3 to P_4, and the total pressure drop across the two turbines cannot exceed that of P_3 to atmospheric pressure. Figure 1-3 shows a flow diagram and a T-s diagram of this cycle.

The thermal efficiency of this cycle is actually less than that of a simple open cycle becuase there are two less-than-100%-efficient adiabatic expansions and additional pressure losses. But the mass of air/HP-HR required by the cycle is reduced greatly, thus reducing the size of the compressor.

It is also natural that the regenerate cycle be combined with the reheat cycle which increases the thermal efficiency above that of the simple regenerate cycle, besides reducing the mass of air/HP-HR required. Also, the use of multiple

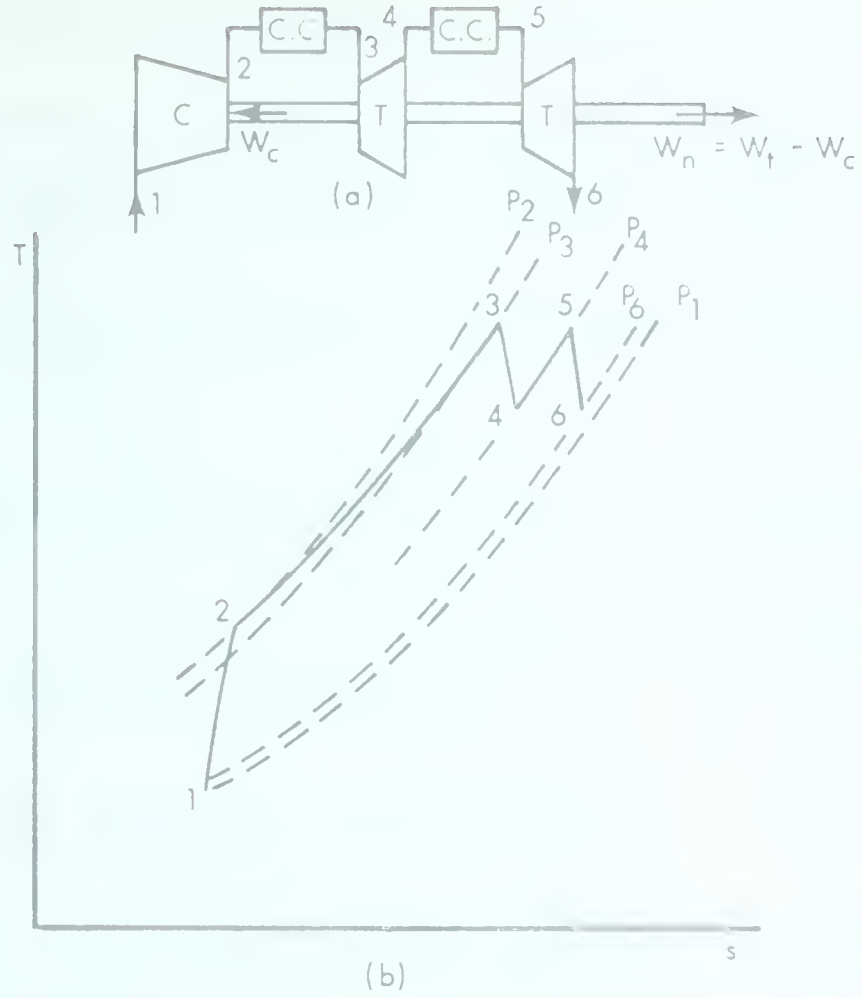

FIGURE 1-3 REHEAT CYCLE

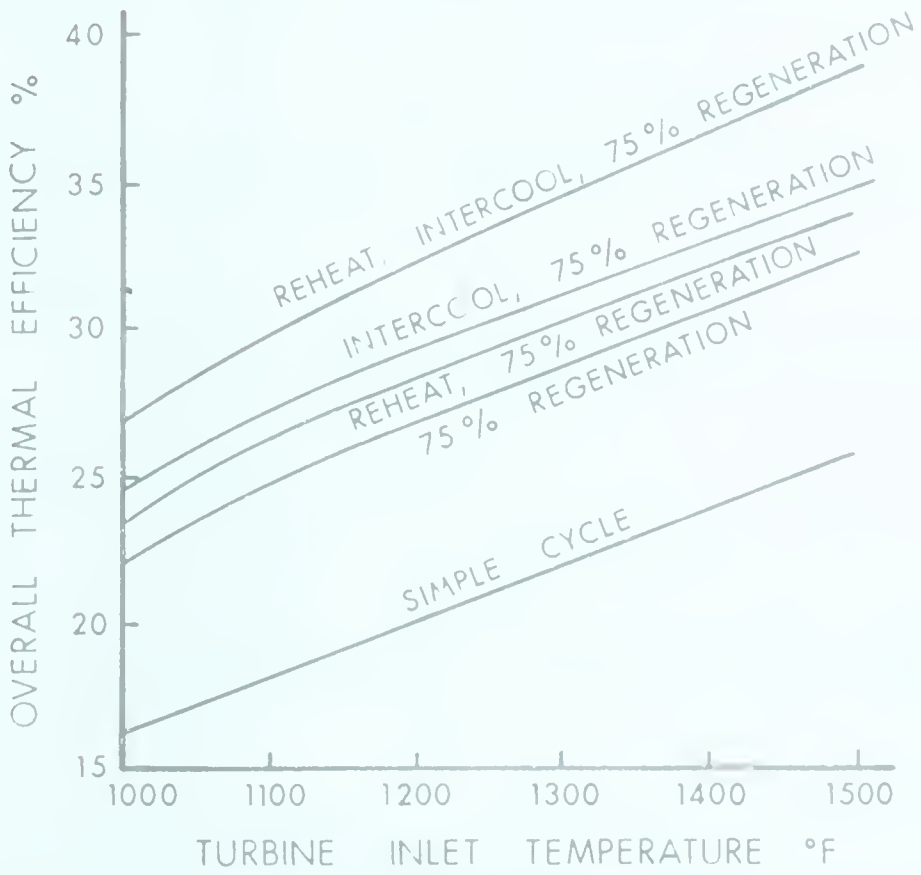

FIGURE 1-4 COMPARISON OF VARIOUS CYCLE SCHEMES

(85% TURBINE EFFICIENCY, 84% COMPRESSOR EFFICIENCY, 70°F AMBIENT, 5% REGENERATOR PRESSURE DROP)

stages of compression with intercooling can be used to reduce the HP required to drive the compressors, thus improving the overall thermal efficiency.

In addition to the above discussed cycles, there are multiple shaft units, closed-cycles and semiclosed-cycles, but these more involved cycles will not be included in this discussion.

Figure 1-4 shows a graph of overall thermal efficiency plotted against turbine inlet temperature for the various cycles discussed above. This graph is reproduced from page 427 of reference 13.

1.3 Theory of the Steam Injection Cycle

It is evident from the previous section that to improve the thermal efficiency of a gas turbine cycle, more effective use has to be made of the heat available or there must be a reduction of the horsepower required to compress the air used in the cycle, either by improving the compressor adiabatic efficiency or reducing the mass of air compressed. Steam injection can do both if the steam is produced in a waste heat boiler.

Consider the general energy equation for a flow process through a compressor. The equation is written as:

$$PE_1 + KE_1 + FE_1 + IE_1 + Q = PE_2 + KE_2 + FE_2 + IE_2 + W \qquad 1.1$$

Neglecting changes in PE, KE and any heat loss, the equation reduces to:

$$FE_1 + IE_1 = FE_2 + IE_2 + W \qquad 1.2$$

or by definition of FE and IE assuming perfect gases

$$p_1V_1 + U_1 = p_2V_2 + U_2 + W \qquad 1.3$$

or $$W = \Delta U + \Delta pV = \Delta(U + pV) \qquad 1.4$$

but by definition, $\Delta(U + pV) = \Delta h$,

therefore $$W = \Delta h \qquad 1.5$$

and for a given mass rate of flow $\dot{m}$,

$$W = \dot{m}\Delta h \text{ BTU's/Time} \qquad 1.6$$

which for perfect gases becomes

$$W = \dot{m}C_p\Delta T \qquad 1.7$$

The same result is obviously true for gases expanding in a turbine.

Now for several nonreactive gases flowing through the same system simultaneously, enthalpy being an extensive property, is cumulative, or, for a mixture n components,

$$h_{total} = h_1 + h_2 + \ldots h_n \qquad 1.8$$

or $$\Delta h_{total} = \Delta h_1 + \Delta h_2 + \ldots + \Delta h_n \qquad 1.9$$

and since mass is cumulative,

$$\dot{m}_{total}\Delta h_{total} = \dot{m}_1\Delta h_1 + \dot{m}_2\Delta h_2 + \dot{m}_3\Delta h_3 + \ldots \qquad 1.10$$

or by equation 1.6,

$$W_{total} = \dot{m}_1\Delta h_1 + \dot{m}_2\Delta h_2 + \dot{m}_3\Delta h_3 + \ldots \qquad 1.11$$

Therefore in this particular case of air being compressed and an air-superheated steam mixture being expanded in a turbine,

$$W_{comp} = \dot{m}_{air}\Delta h_{air} \qquad 1.12$$

and $$W_{turb} = \dot{m}_{air}\Delta h_{air} + \dot{m}_{st}\Delta h_{st} \qquad 1.13$$

or $$W_{turb} = \dot{m}_{air}C_p\Delta T_{air} + \dot{m}_{st}C_p\Delta T_{st} \qquad 1.14$$

for perfect gases.

Figures 1-5 and 1-6 show plots of pressure against volume at constant temperature and pressure against temperature at constant volume for air and superheated steam. It is evident that both air and superheated steam behave approximately as perfect gases thus showing justification for equation 1.14.

It is evident then, that adding steam to the cycle will increase the output of the turbine providing choking conditions do not exist in the nozzle ring. If choking does occur, the obvious solution is to lower the air mass flow reducing the compression horsepower. In either case, more power is available to do useful work.

The reason for the use of a waste heat boiler is to recover some of the energy from the hot exhaust gases which would otherwise be lost in exhausting to the atmosphere. The energy recovered by the boiler is available to the cycle by injecting the steam produced into the cycle after the compressor. This energy however is not obtained without slight charge to the cycle because a waste heat boiler increases the back pressure acting on the turbine, thereby reducing the turbine's pressure ratio and power output/mass flow. While more fuel has to be added to maintain the temperature at the inlet to the nozzle ring because the Cp of superheated steam is over twice that of air, equation 1.14 indicates more work should be obtained from the greater mass flow and higher Cp of superheated steam. But these restrictions caused by the steam injection are much less than if the increased mass flow were made up from an auxiliary air compressor driven by the turbine.

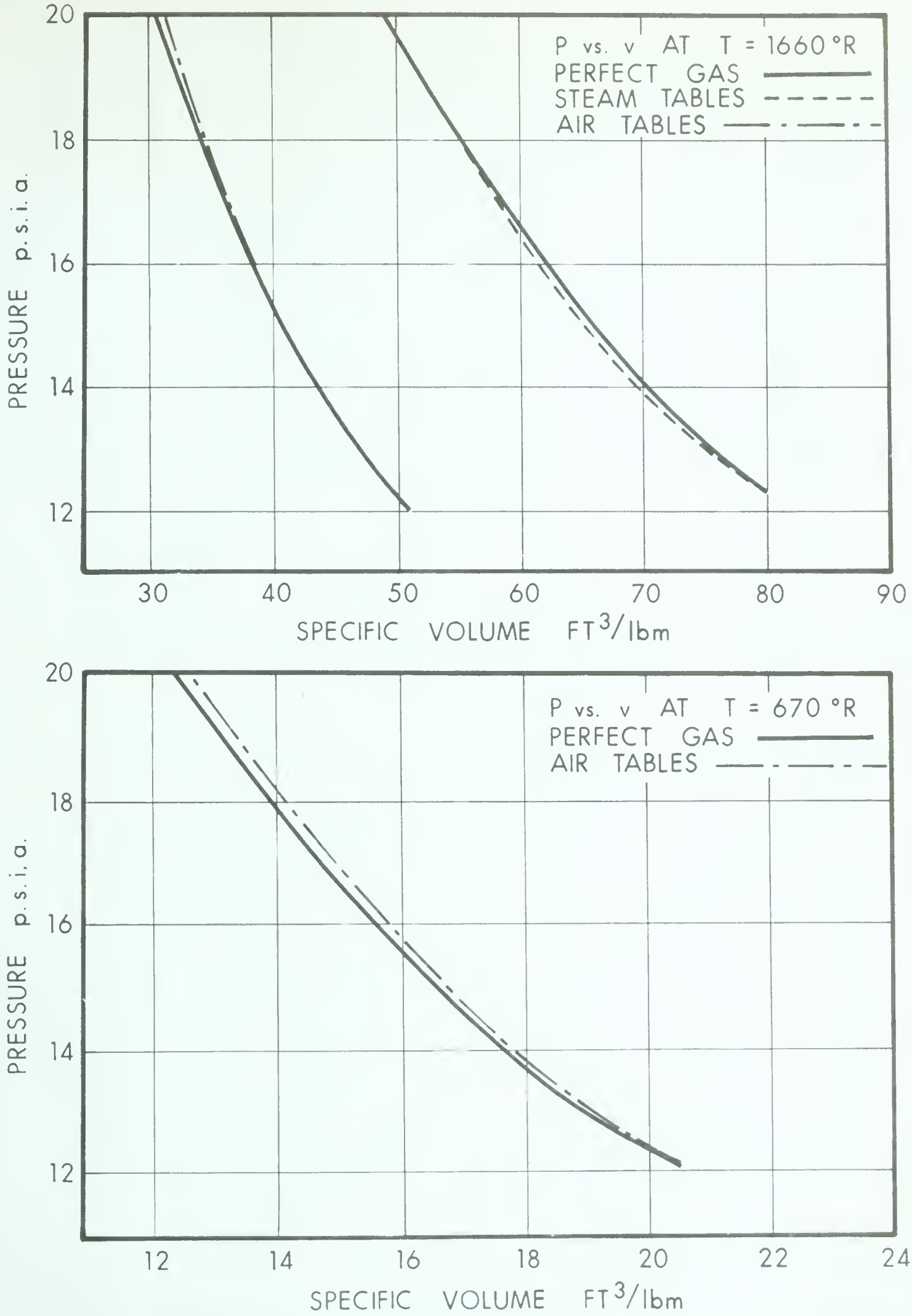

FIGURE 1 - 5 PRESSURE versus SPECIFIC VOLUME AT CONSTANT TEMPERATURE

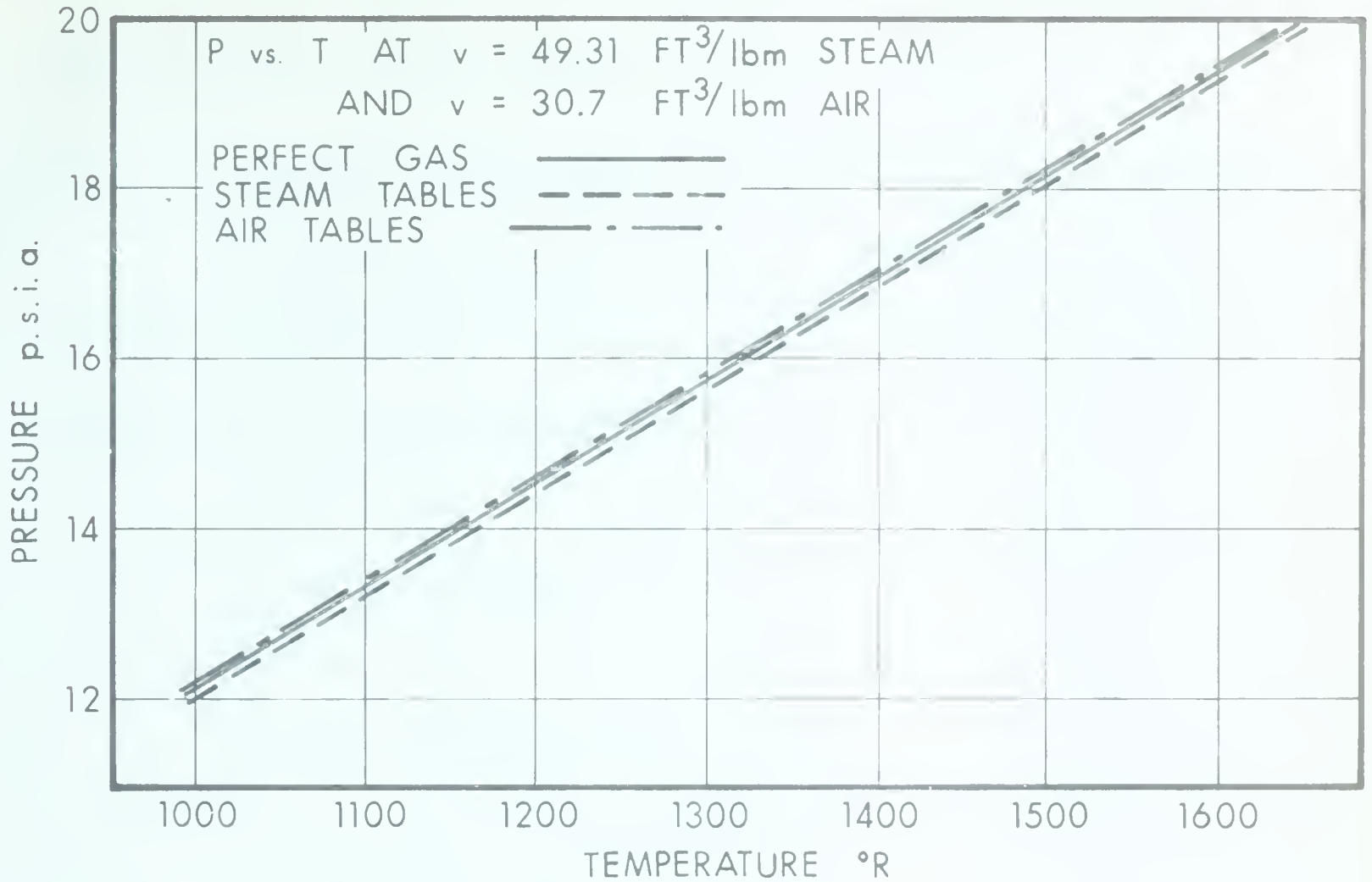

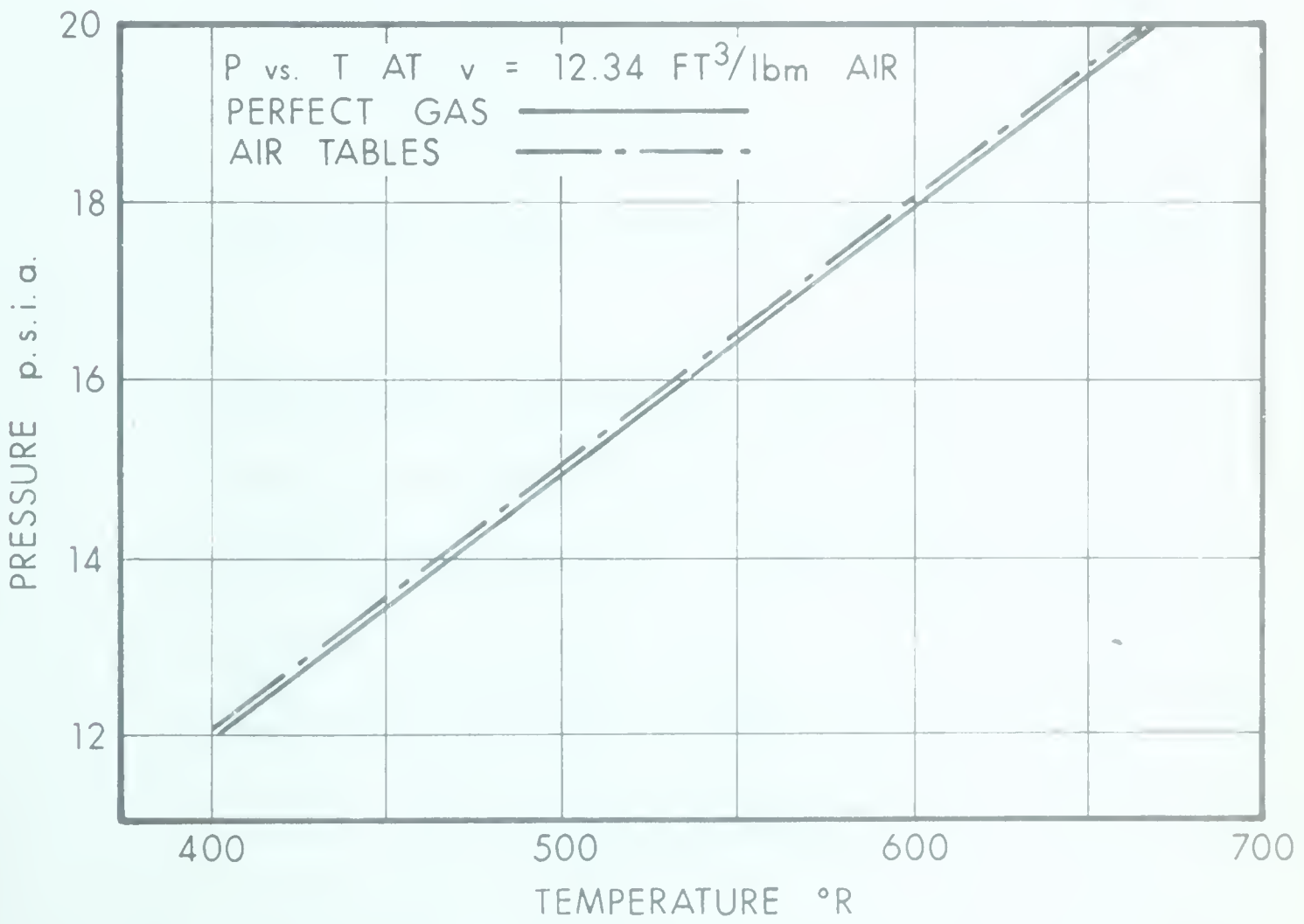

FIGURE 1 - 6 PRESSURE versus TEMPERATURE AT CONSTANT SPECIFIC VOLUME

A flow diagram of a simple open gas turbine with a waste heat boiler and steam injection is shown in figure 1-7.

1.4 Comparison of Gas Turbines with Steam Injection with the Basic Types

The following comparison was done by Schröder[11] who compared various cycles with and without steam injection for the same cycle conditions with varying pressure ratio. The cycles considered were:

1) Simple open
2) simple open-reheat
3) simple regenerate
4) simple regenerate reheat
5) simple open-steam injection
6) simple open-reheat-steam injection
7) simple regenerate-steam injection
8) simple regenerate-reheat-steam injection.

For these cycles, the following conditions and component efficiencies were stipulated:

1) Inlet conditions - 1 atmos., 15°C. (59°F.)
2) Compressor adiabatic efficiency 89%
3) Turbine adiabatic efficiency 87%
4) Pressure drop in compressor intake 2.5%
   Pressure drop in combustion chamber 1 3%
   in combustion chamber 2* 3%

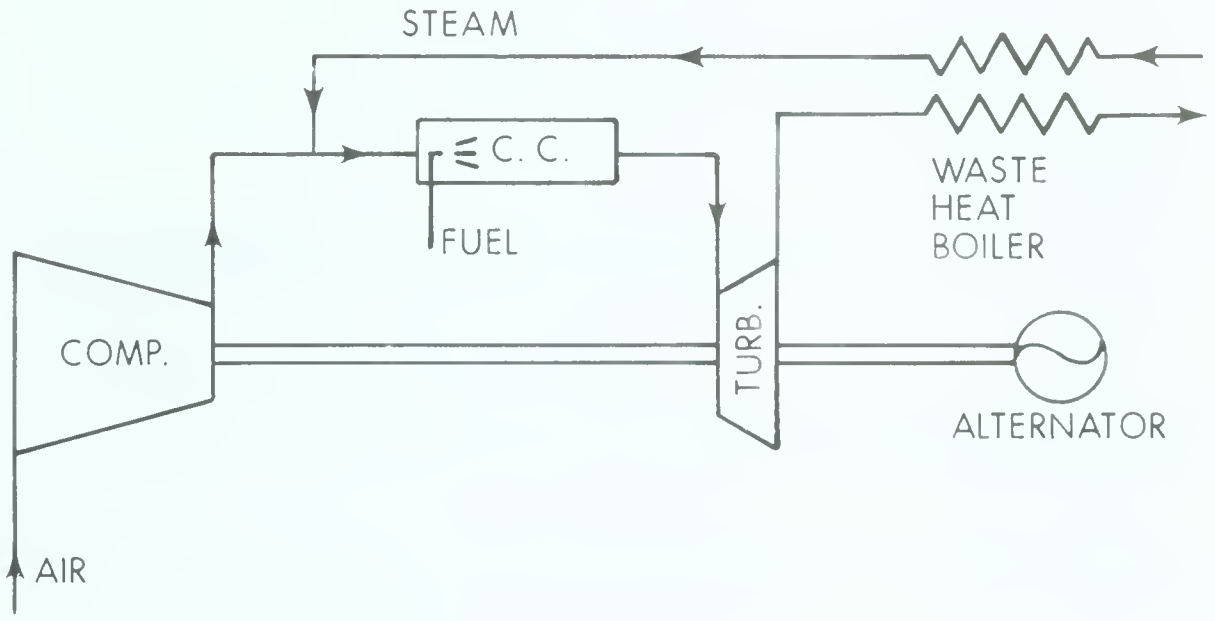

FIGURE 1 - 7 SIMPLE OPEN CYCLE WITH A WASTE HEAT BOILER

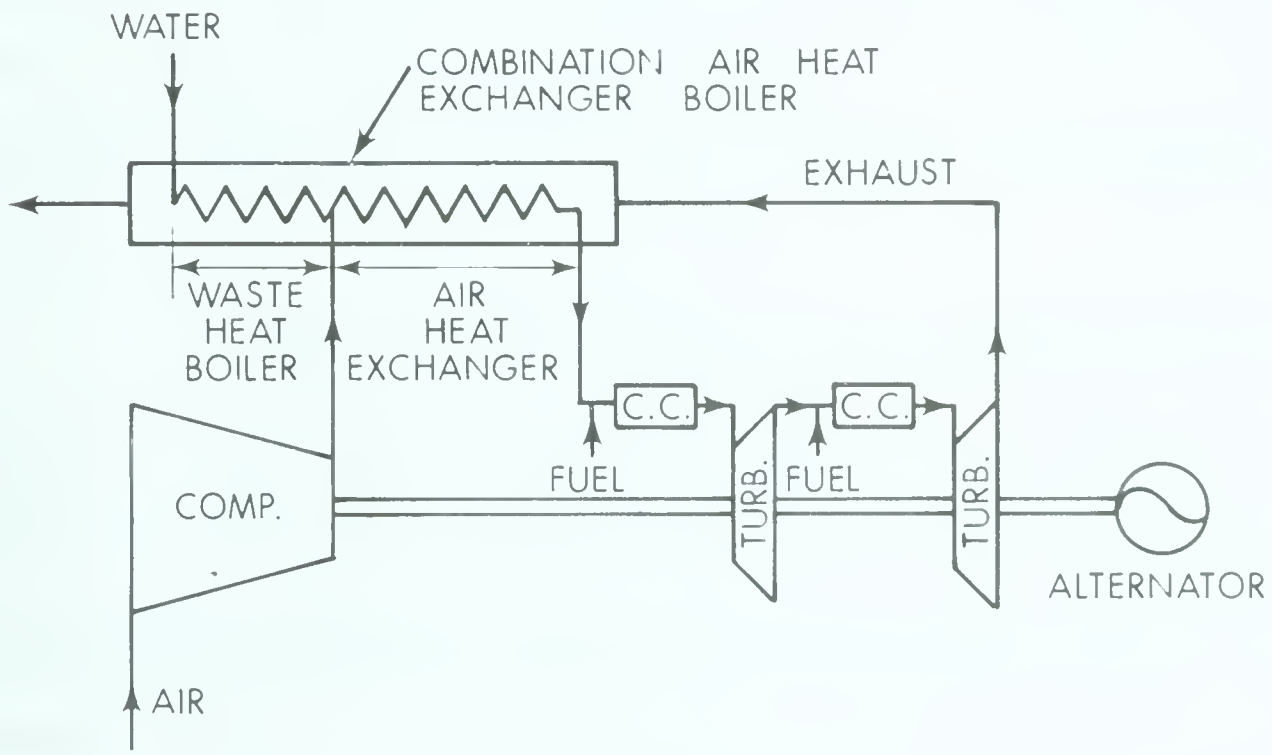

FIGURE 1 - 8 A THEORETICAL CYCLE BY SCHRÖDER

in waste heat boiler including the diffusers behind the turbine 6%

(also gas side of the combination air heat exchanger and waste heat boiler)* 3%

* if there is one

5) Cooling air bled off from the compressor 2%

6) Loss of combustion efficiency 2%

7) Lower heat value of fuel 10,200 kCal/Kg (18,350 BTU/lbm)

8) Loss of mechanical efficiency between the turbine and the compressor 1%

In all the above cases the maximum temperature at the turbine inlet was 777°C. (1430°F.). For the cycles with waste heat boilers, it was assumed that the steam temperature leaving the boiler is 100°C. (212°F.) less than the entering exhaust gases, and that the feed water entered the boiler at 50°C. (106°F.) below its boiling temperature for the given pressure. Figure 1-8 shows how this equipment was theoretically set up.

The resultant graphs from this accurate theoretical study are seen in figures 1-9, 1-10, 1-11, 1-12 and 1-13. These graphs show that for each particular case of steam injection versus basic cycle the thermal efficiency is increased, the specific fuel consumption is decreased, and the amount (mass) of air/HP-HR is reduced.

The increase in thermal efficiency obtained by Schröder[11] is supported closely by Chambadal[12]. In his paper, Chambadal produced the graph in figure

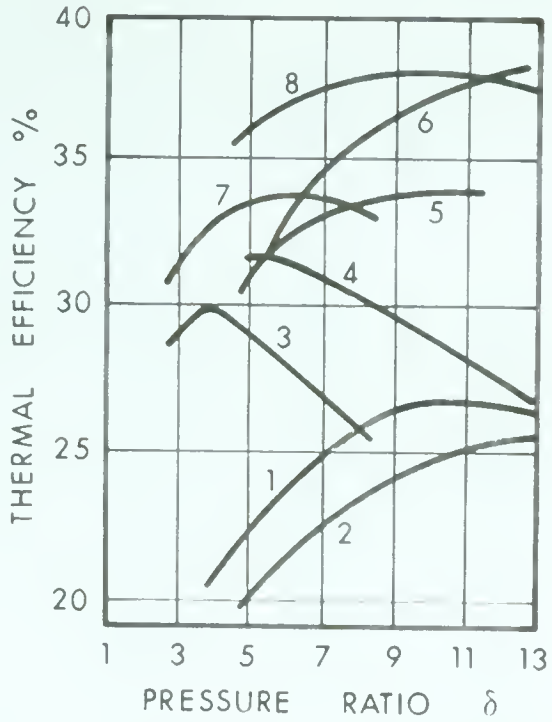

FIGURE 1-9 THERMAL EFFICIENCY

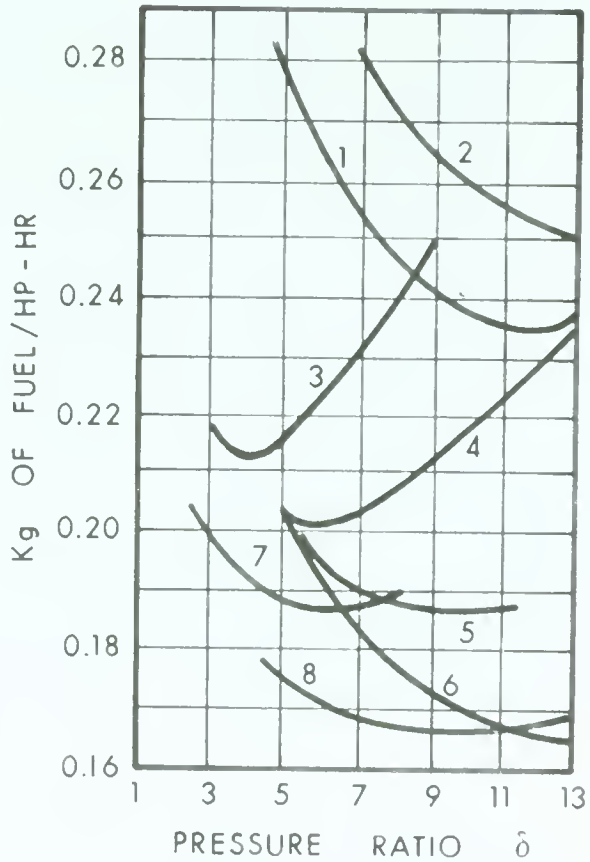

FIGURE 1-11 SPECIFIC FUEL CONSUMPTION

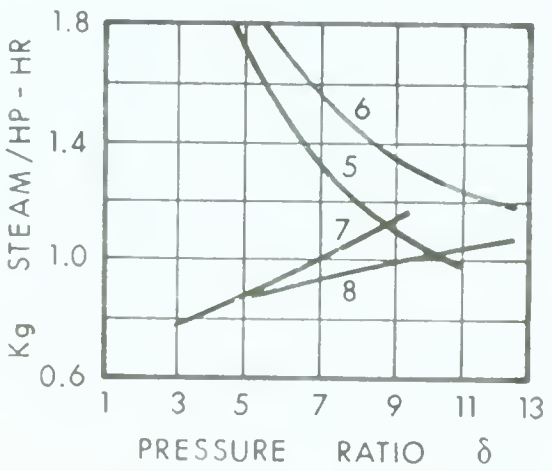

FIGURE 1-10 STEAM REQUIRED PER HP-HR

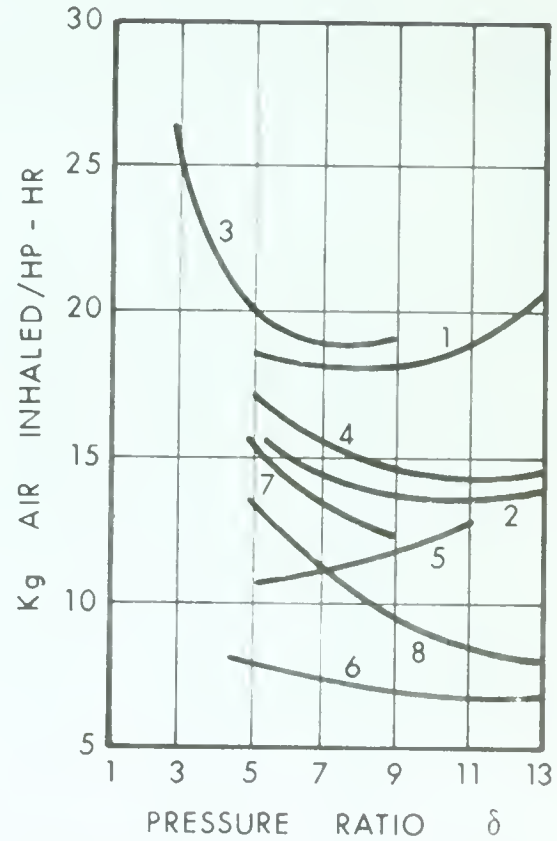

FIGURE 1-12 WEIGHT OF AIR INHALED PER HP-HR

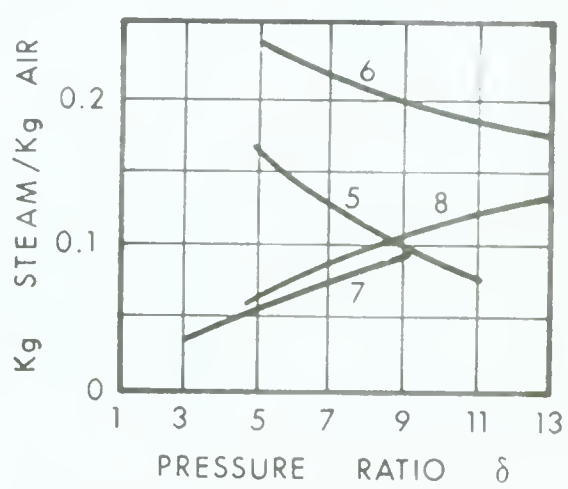

FIGURE 1-13 WEIGHT OF STEAM USED PER WEIGHT OF AIR INHALED

1-14 for a simple regenerate cycle with steam injection. The assumptions made for the turbine were:

1) Air intake at 1 atmosphere and 15°C. (59°F.)

2) Compressor adiabatic efficiency 85%

3) Turbine adiabatic efficiency 85%

4) Lower heating value of fuel 10,000 kCal/Kg (18,000 BTU/lbm)

5) Assumptions as to losses in pressure in the components were not stated.

A check of two operating points was made, one at a pressure ratio of 5 and the other at a pressure ratio of 8. The results are shown in table 1-1.

TABLE 1-1

COMPARISON OF THEORETICAL RESULTS BY SCHRÖDER AND CHAMBADAL

PRESS. RATIO	AUTHOR	$\frac{\text{lbm STEAM}}{\text{lbm AIR}}$	% INCREASE IN η_t AT 777 °C
5	SCHRÖDER	0.06	13.8
5	CHAMBADAL	0.06	10
8	SCHRÖDER	0.08	22.5
8	CHAMBADAL	0.08	20

It is evident that both Schröder and Chambadal agree in principle, Chambadal's results being a little lower due to the lower adiabatic efficiencies assumed for the compressor and the turbine (c.f. 85% versus 89% and 87%). Other points at the same pressure ratio could not be compared because Schröder chose only one mass of steam/mass of air ratio for each pressure ratio as seen in figure 1-13.

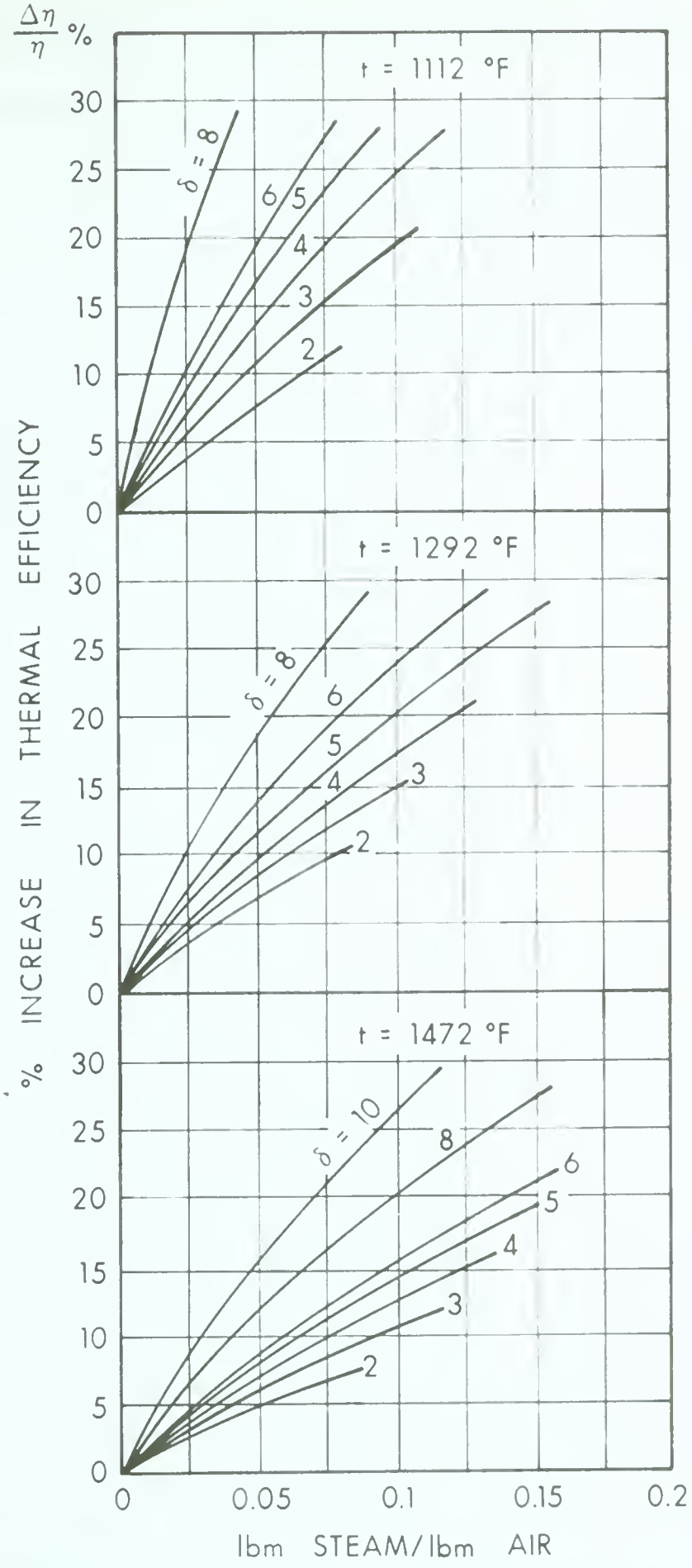

FIGURE 1 - 14 RELATIVE INCREASES IN THERMAL EFFICIENCY FOR SIMPLE REGENERATIVE CYCLE WITH STEAM INJECTION

The foregoing theoretical results supported by other authors[7,8,9,10] do indicate that experimental investigation of the effect of steam injection on a gas turbine cycle should be carried out.

CHAPTER 2

APPARATUS

A complete history of the development of the gas turbine used in these experiments is given in appendix A. But for convenience sake, a brief description of the apparatus and instrumentation will be presented here.

2.1 Basic Thermal Efficiency Test Runs

The gas turbine consists of a Brown Boveri Exhaust Turbo Charger Type 320 fitted with two combustion chambers complete with fuel nozzles and ignitors from a Derwent II aircraft jet engine. The general arrangement of this equipment can be seen in figures 2-1, 2-2, 2-3 and 2-4. It is to be seen that the combustion chambers were connected to the supply of compressed air by standard 8" pipe. The supply of compressed air was split at the upper chamber as shown in figure 2-2. The combustion chambers were joined by a flame jump tube, as shown in figures 2-4 and 2-7, while being held snugly against a 3/8" steel adaptor plate bolted to the turbine inlet casing by steel rods, as seen in figures 2-4 and 2-7.

The Turbo Charger itself was supported on a fabricated steel base, while all other equipment was bolted directly to the turbo charger's housing except for a support stand under the heavy 8" steel pipe and support stands under the air intake measuring system to insure the straightness of the duct.

A portion of the exhaust duct (16 gauge sheet steel) can be seen in figure 2-3. An inspection hole was cut into the right hand side of the duct so that the position

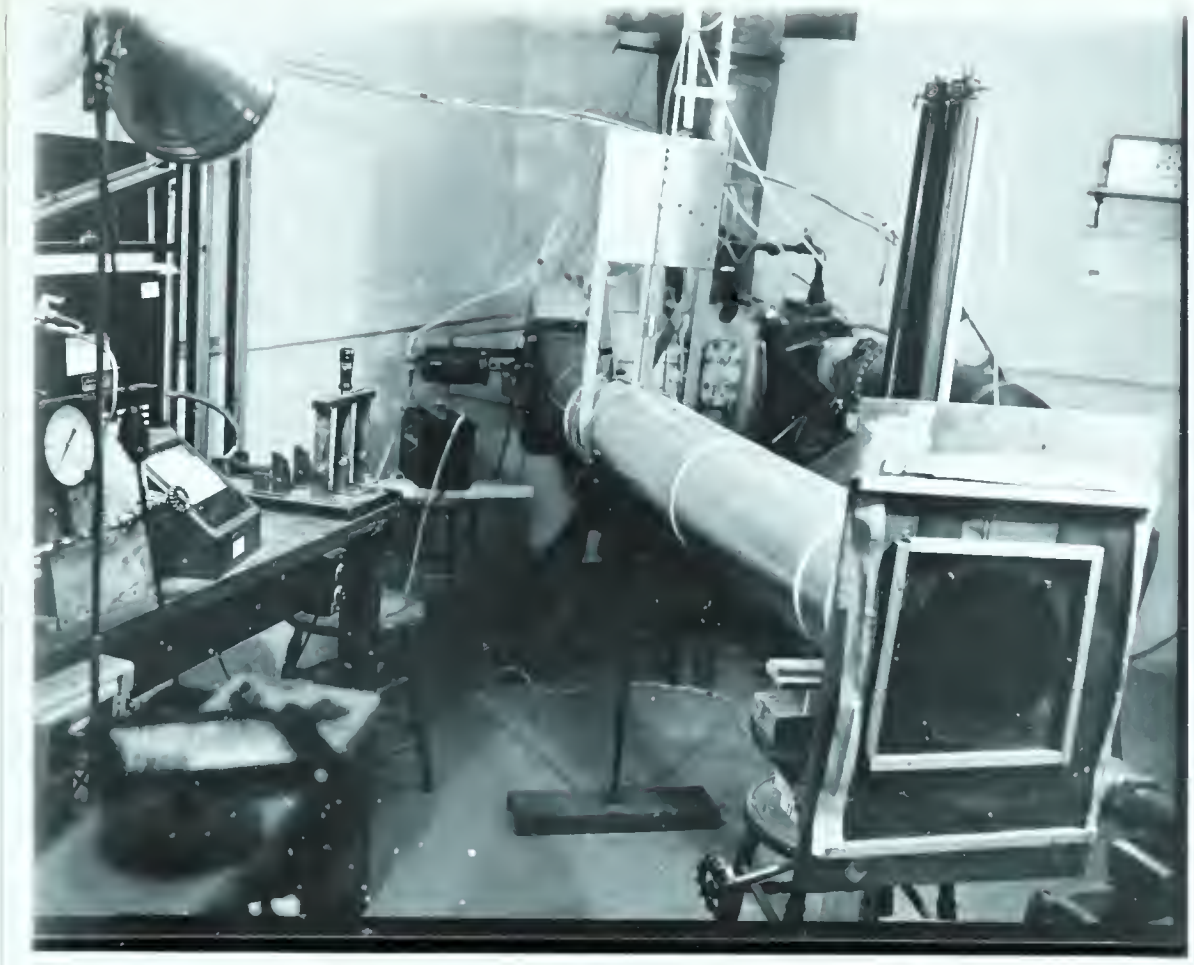

FIGURE 2-1 GENERAL VIEW OF TEST EQUIPMENT

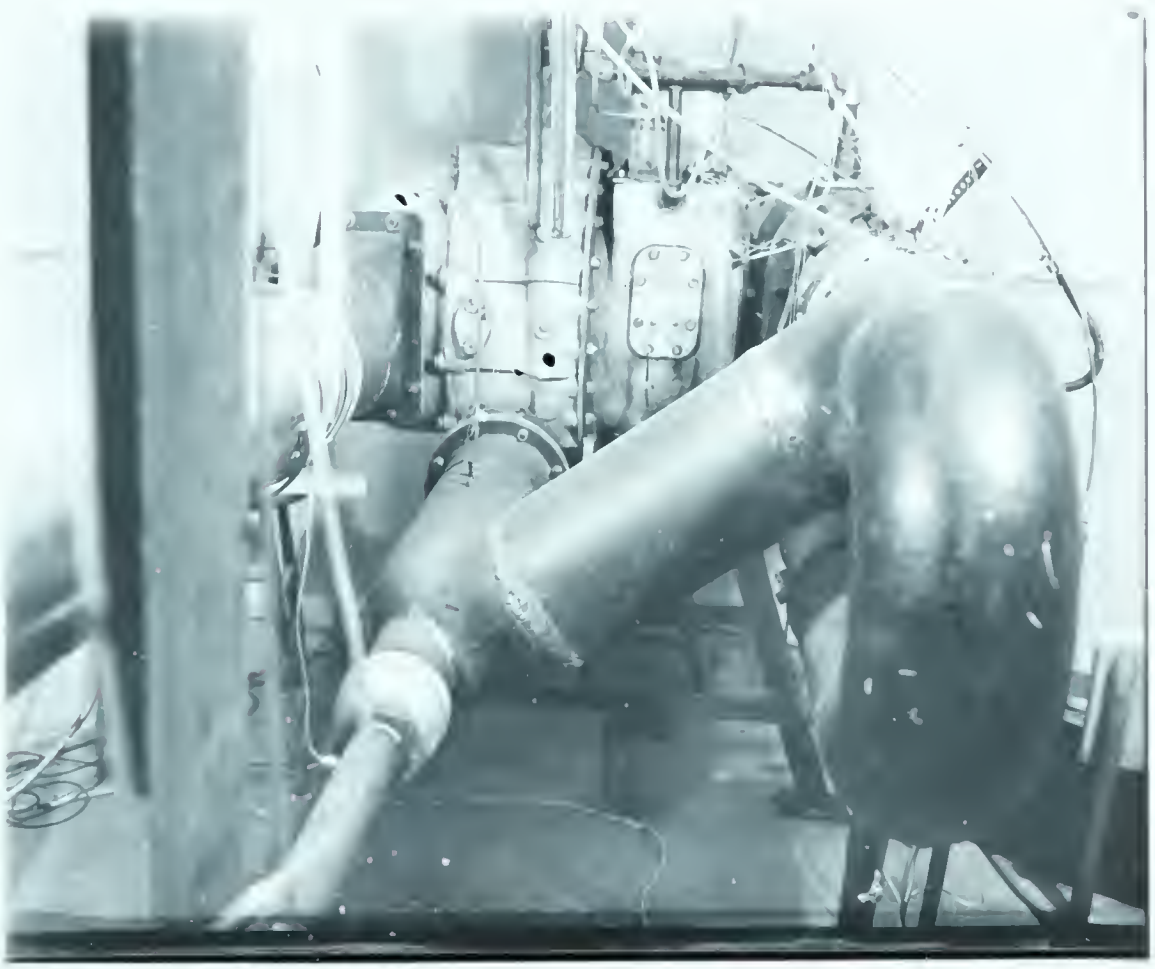

FIGURE 2-2 GENERAL VIEW OF TEST EQUIPMENT

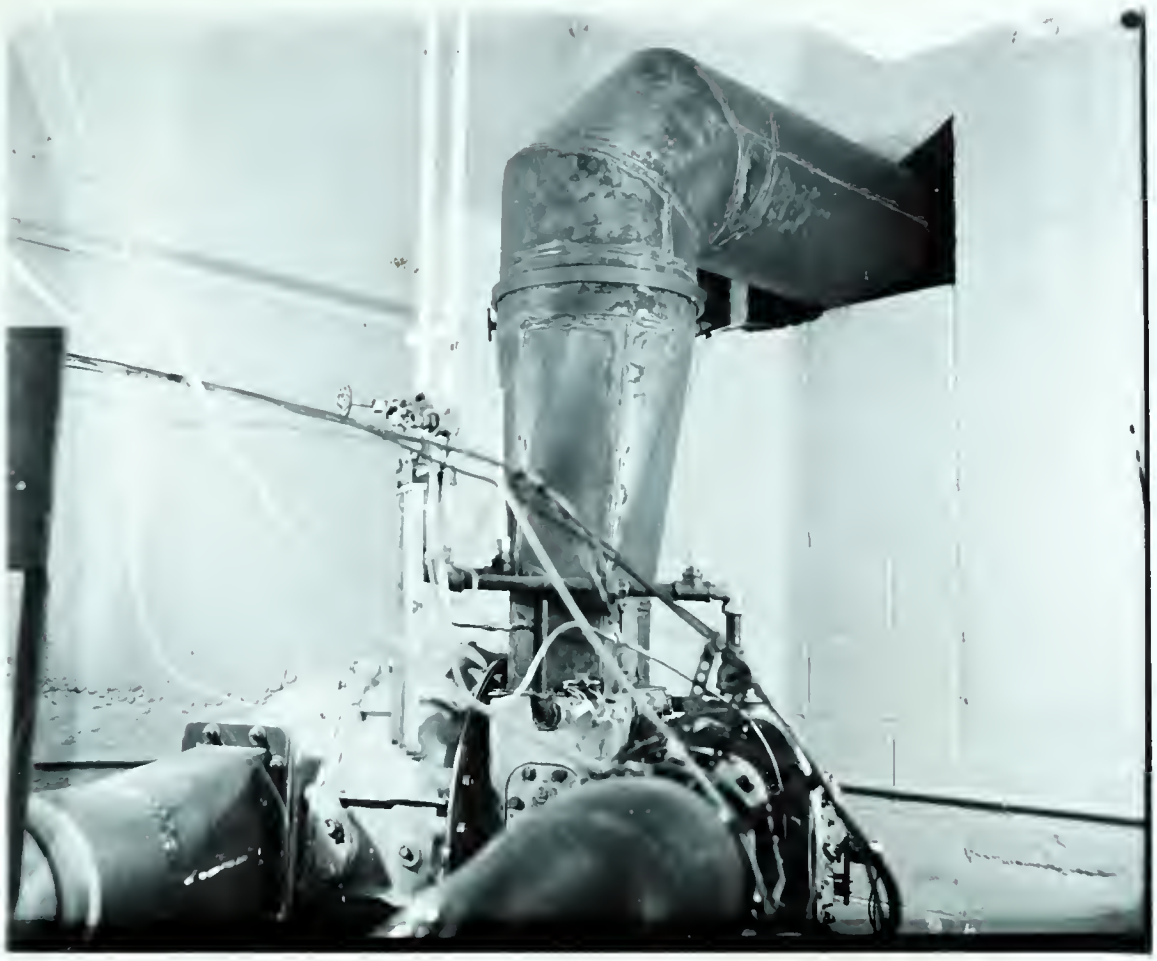

FIGURE 2-3 EXHAUST DUCT

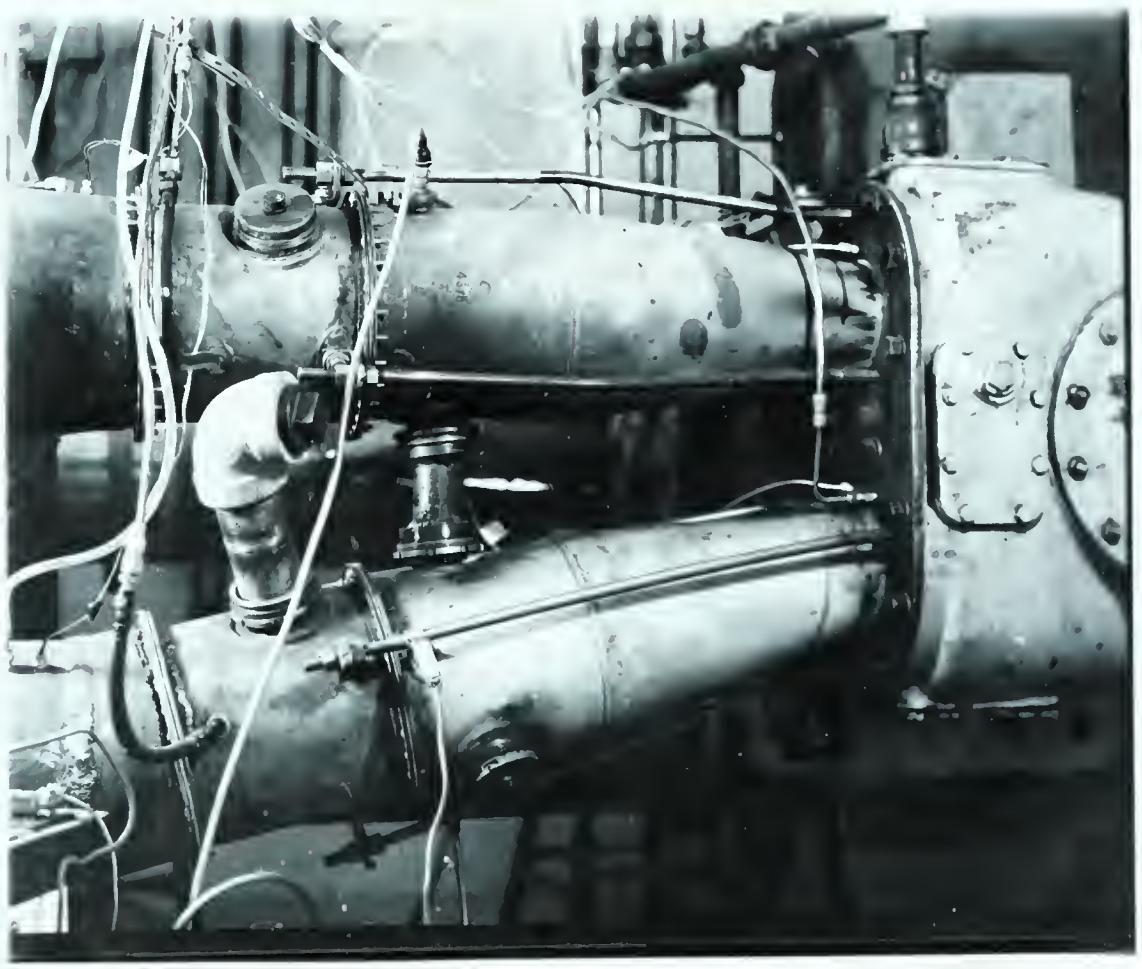

FIGURE 2-4 COMBUSTION CHAMBERS

of the thermocouples after the turbine wheel could be checked.

Positive cooling of the hot casing of the turbo charger was provided by running city tap water through it.

To start the turbine a Derwent II starter motor was fitted on the left hand end of the machine, as seen in figure 2-1. The starter motor was powered by a 12 volt storage battery and a 60 H.P. D.C. dynamometer driven by a 3-cylinder, 2 stroke G.M.C. diesel engine, which were used to run the turbine up to its self-sustaining speed of about 8000 R.P.M.

The spark for the ignitors was provided by a model "T" vibrating type induction coil.

The fuel, commercial kerosene with 1 per cent S.A.E. 20 oil added for pump lubrication, was pumped to the fuel nozzles by a seven-piston piston pump driven by a 1/4 H.P., 3 phase, 220 volt gear-in-head motor running at 220 R.P.M. A general view of the pump and motor, the fuel barrel and weighing scale is shown in figure 2-5. This system worked on a by-pass control, that is the fuel not used by the turbine was diverted back to the fuel barrel through a control valve. Additional control for each chamber was provided by use of throttling valves on the fuel lines to the chambers as seen in the upper right hand corner of figure 2-5.

2.1.1 Instrumentation for Basic Test Runs

In order to determine the thermal efficiency and check the operation of the turbine certain specific information was required. This included various temperatures and pressures, the amount of work produced and the amount of fuel added for a given

FIGURE 2-5 FUEL SUPPLY SYSTEM

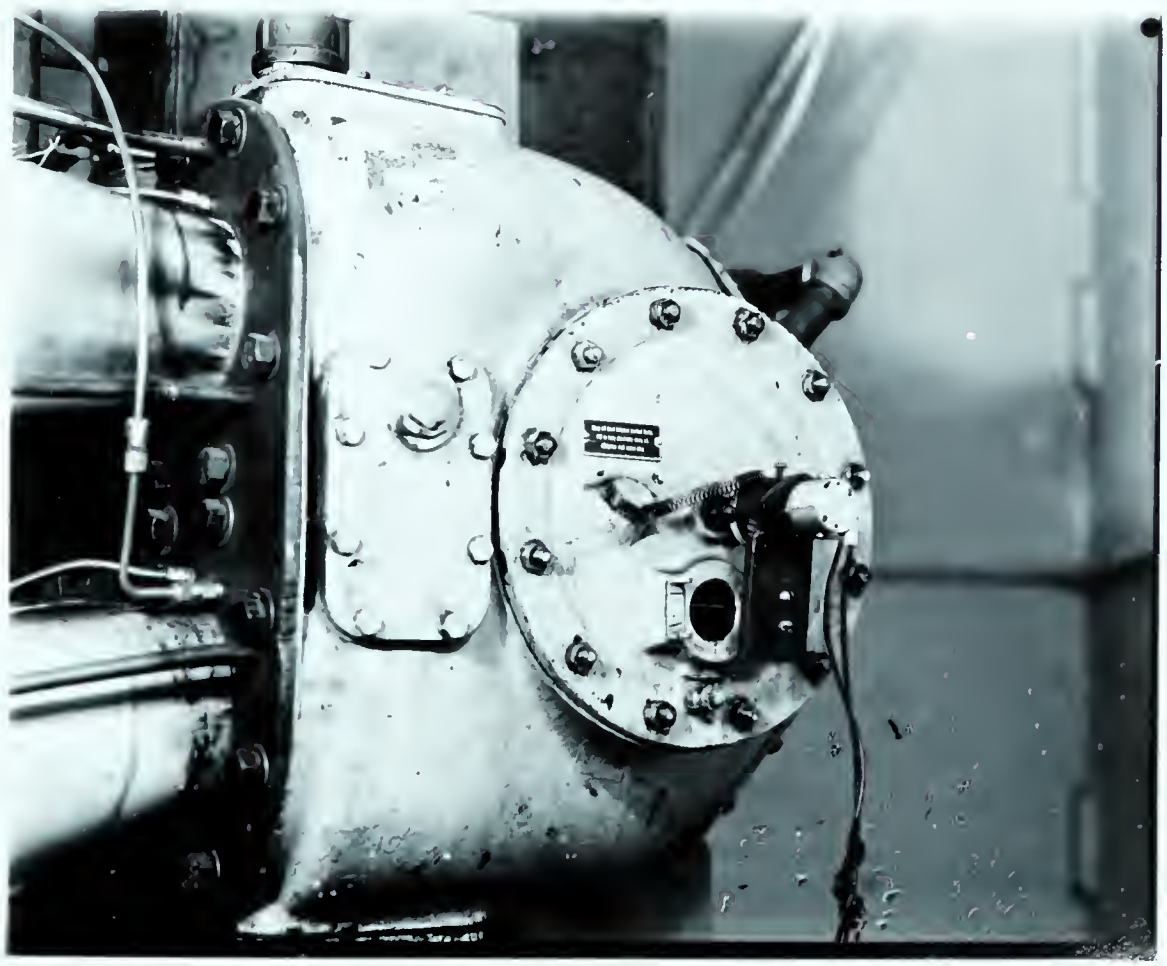

FIGURE 2-6 D.C. GENERATOR FOR R.P.M. RECORDING

time, plus the amount of air used per unit of time and the rotation speed of the turbine.

For temperature measurements, iron-constantan thermocouples were used for lower temperatures, while chromel-alumel thermocouples set inside a stainless steel casing were used for higher temperatures, all connected to a two range, 40 position, automatic balancing Honeywell potentiometer reading in °F. The iron-constantan thermocouples were placed at the compressor inlet, the compressor outlet, just before the top and bottom combustion chambers and between the inner "can" and the outer liner of the lower combustion chamber. The chromel-alumel thermocouples were placed before the nozzle ring on the top and bottom chambers and just after the turbine wheel, top and bottom. The location of the chromel-alumel thermocouples can be seen at the narrow end of the combustion chambers as in figures 2-4, 2-6 and 2-7. The vertical tube, seen in figures 2-4 and 2-6, was a static pressure tap to check the pressure drop across the lower combustion chamber.

Also seen in figure 2-7 was the method of connection of the dissimilar metal thermocouples to fine strand copper wire which runs to the potentiometer. That is, crimped electrical connections were used and joined by a bolt and nut to facilitate easy removal.

The pressure tappings consisted of a total-head tube at the compressor outlet connected to a U-tube manometer filled with mercury, static tappings before and after the lower combustion chamber to check the pressure drop through the chamber (figure 2-4) and a static pressure tapping on the exhaust duct (lower left of duct in figure 2-3) connected to a water filled U-tube manometer. A diagram of all the temperature and pressure tappings is shown in figure 2-9.

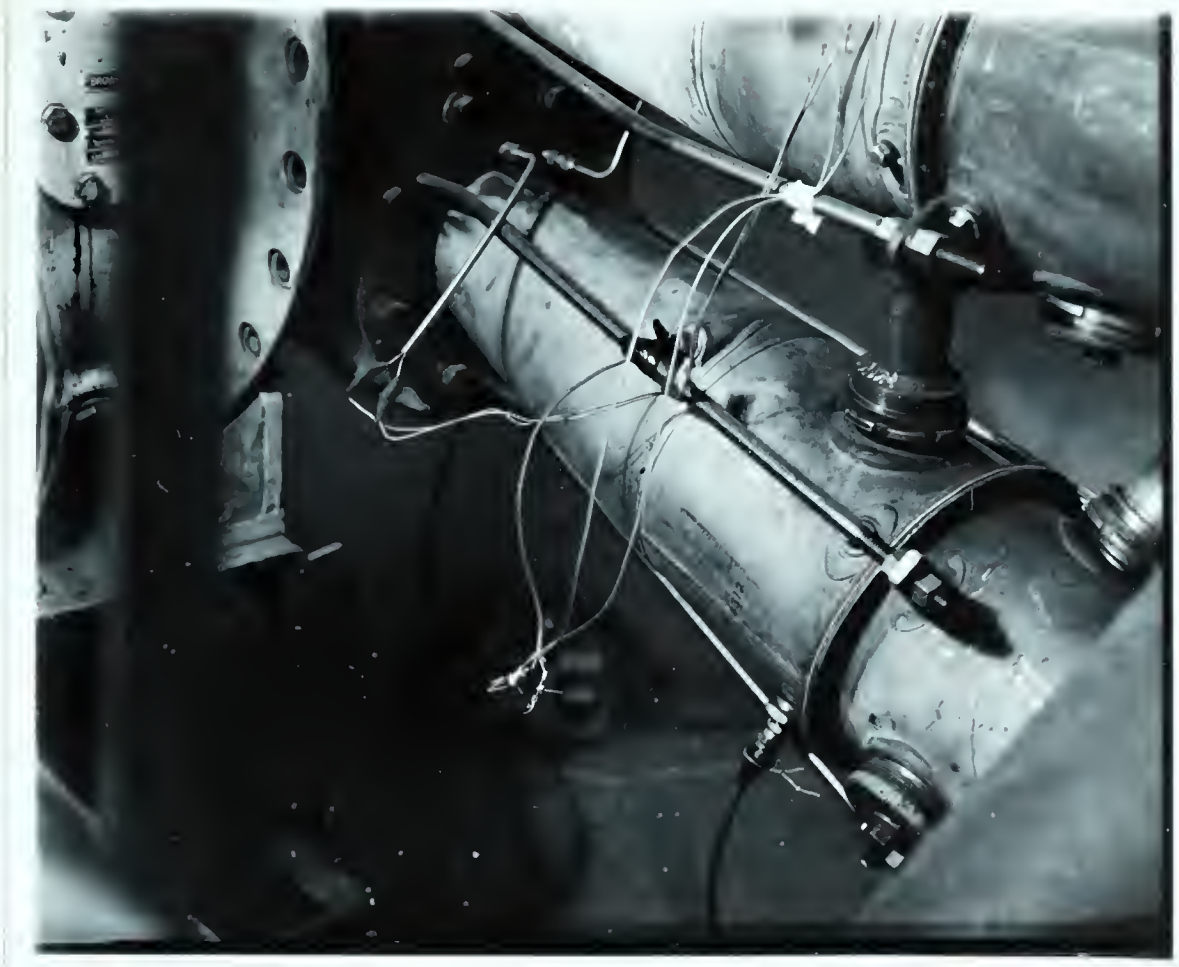

FIGURE 2-7 FLAME JUMP TUBE AND SECONDARY AIR TEMPERATURE THERMOCOUPLE LOCATION

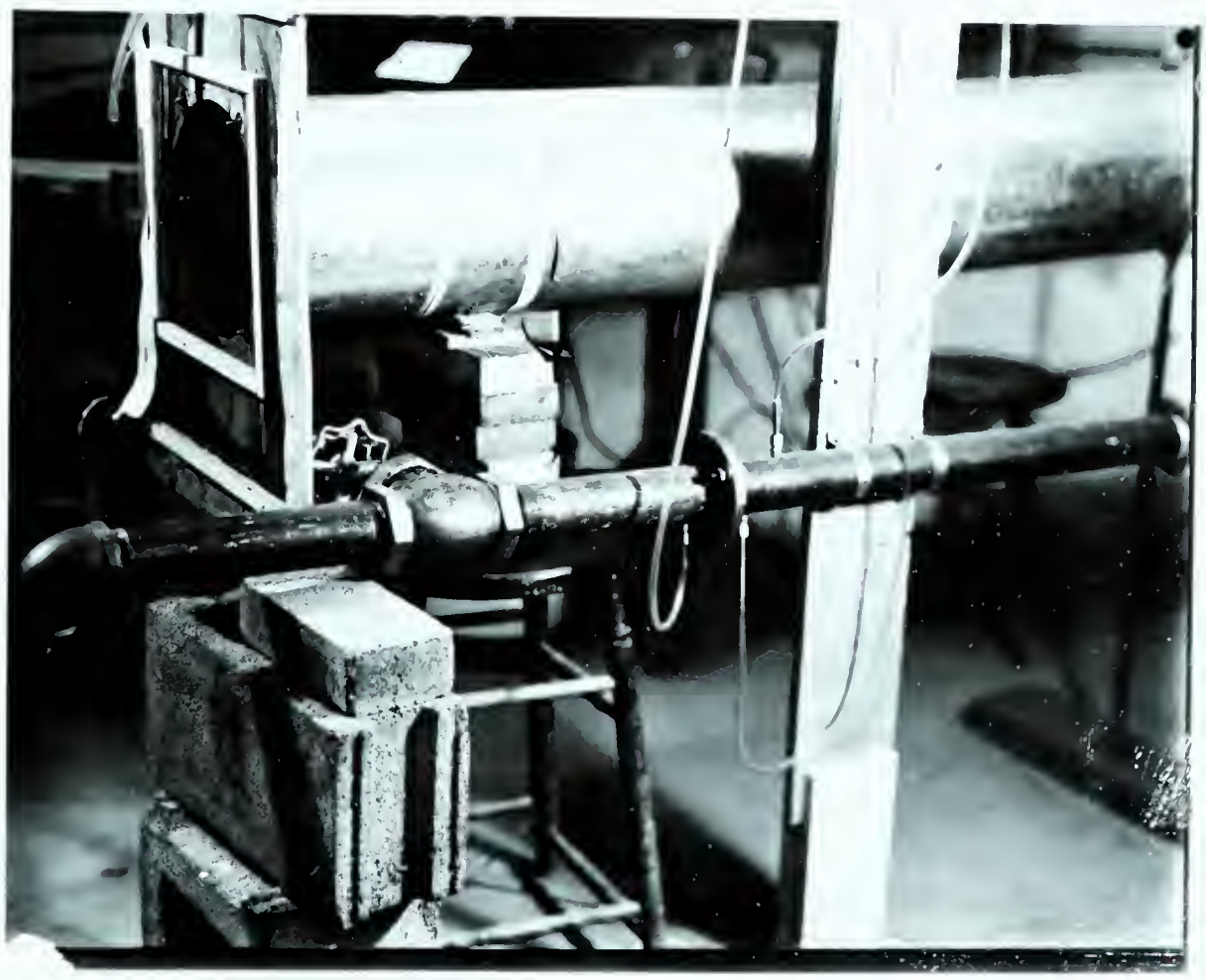

FIGURE 2-8 AIR-BLEED-OFF ORIFICE PLATE AND CONTROL VALVE

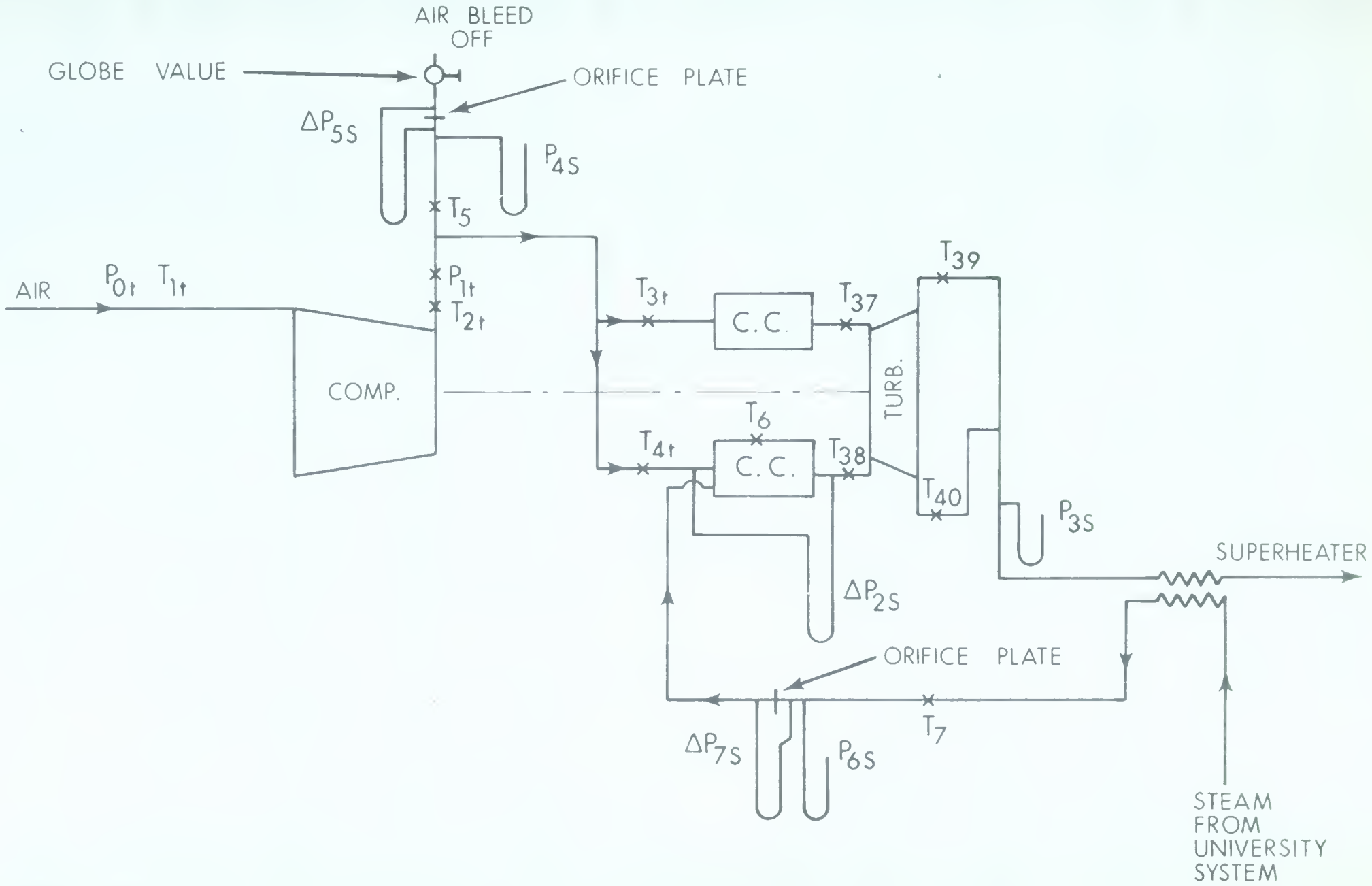

FIGURE 2 - 9 LOCATION OF TEMPERATURE AND PRESSURE TAPPINGS

In order to measure the actual work produced by the turbine, since no high speed dynamometer was available, air was bled off from the compressor through an orifice plate. The bleed-off itself can be seen in figures 2-2 and 2-8. Figure 2-2 shows the location of a 4" pipe welded into the 8" elbow at the compressor outlet and the pipe reduction to a standard 2" pipe. The iron-constantan thermocouple location for measuring air temperature is also to be seen in this figure 2-2. Figure 2-8 shows the orifice plate further down the 2" pipe complete with the "radius" pressure taps and globe control valve. Two U-tube manometers were hung on the other side of the vertical board near the orifice plate to measure the static pressure at the orifice plate and the static "radius" pressure drop across the orifice plate. These manometers can also be seen in figure 2-1.

To measure the weight of fuel used, the fuel barrel was set on a scale (figure 2-5). By fixing a commercial 110 volt micro-switch under the beam of the scale as shown in figure 2-10, it was possible to activate a fuel timing system. This system automatically started the clock, shown on the right of figure 2-11, mounted on the C.F.R. Engine control panel, when the micro-switch was closed. This also held a solenoid switch which keeps the clock running. By raising the balance arm on the scale and sliding the poise towards the micro-switch for a certain poundage, and reversing the solenoid action, the clock would remain in operation until the balance arm closed the switch again, thus the time for a given weight of fuel could easily be recorded.

Air flow into the compressor was measured by using a 10" metal duct with a pitot-tube traversing station mounted as seen in figure 2-1. The duct was originally

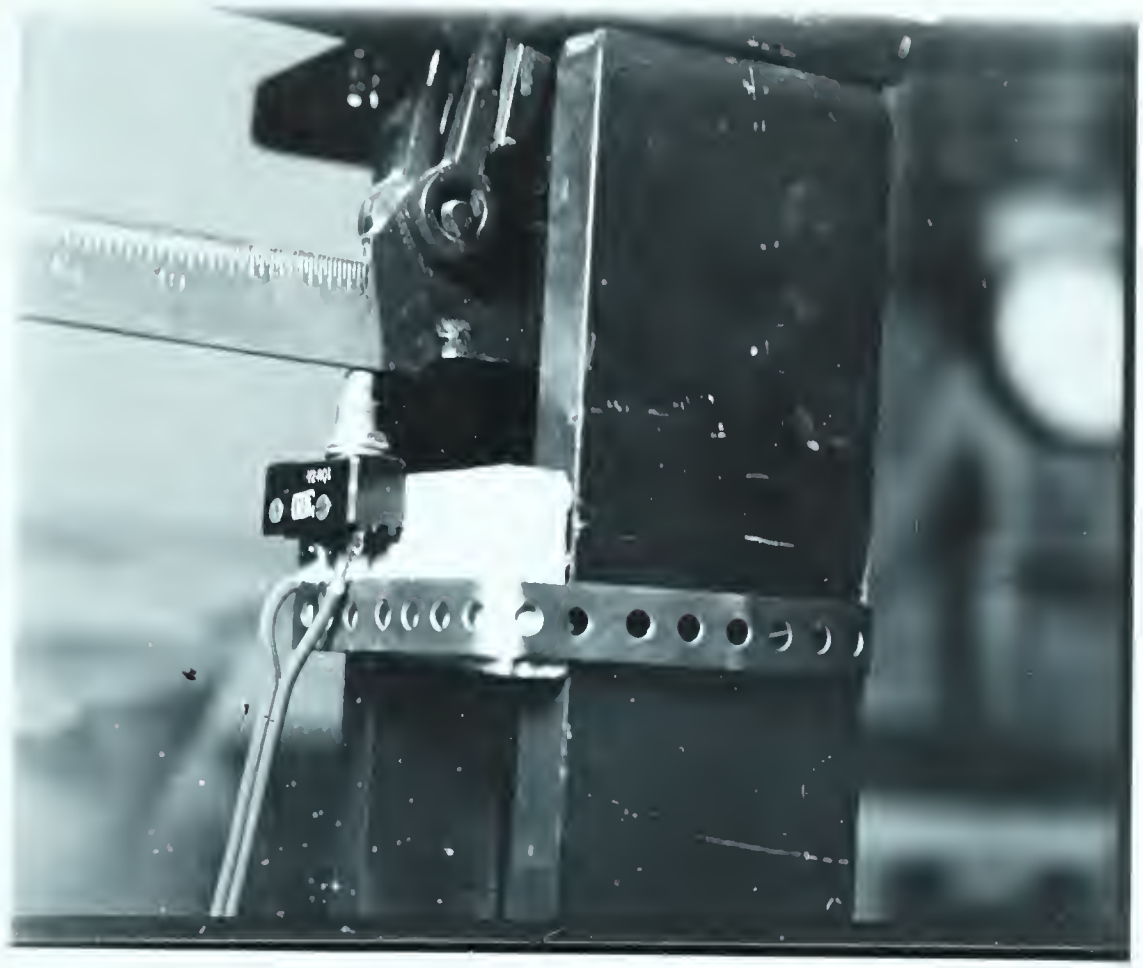

FIGURE 2-10 MICRO-SWITCH LOCATION FOR TRIPPING TIME CLOCK

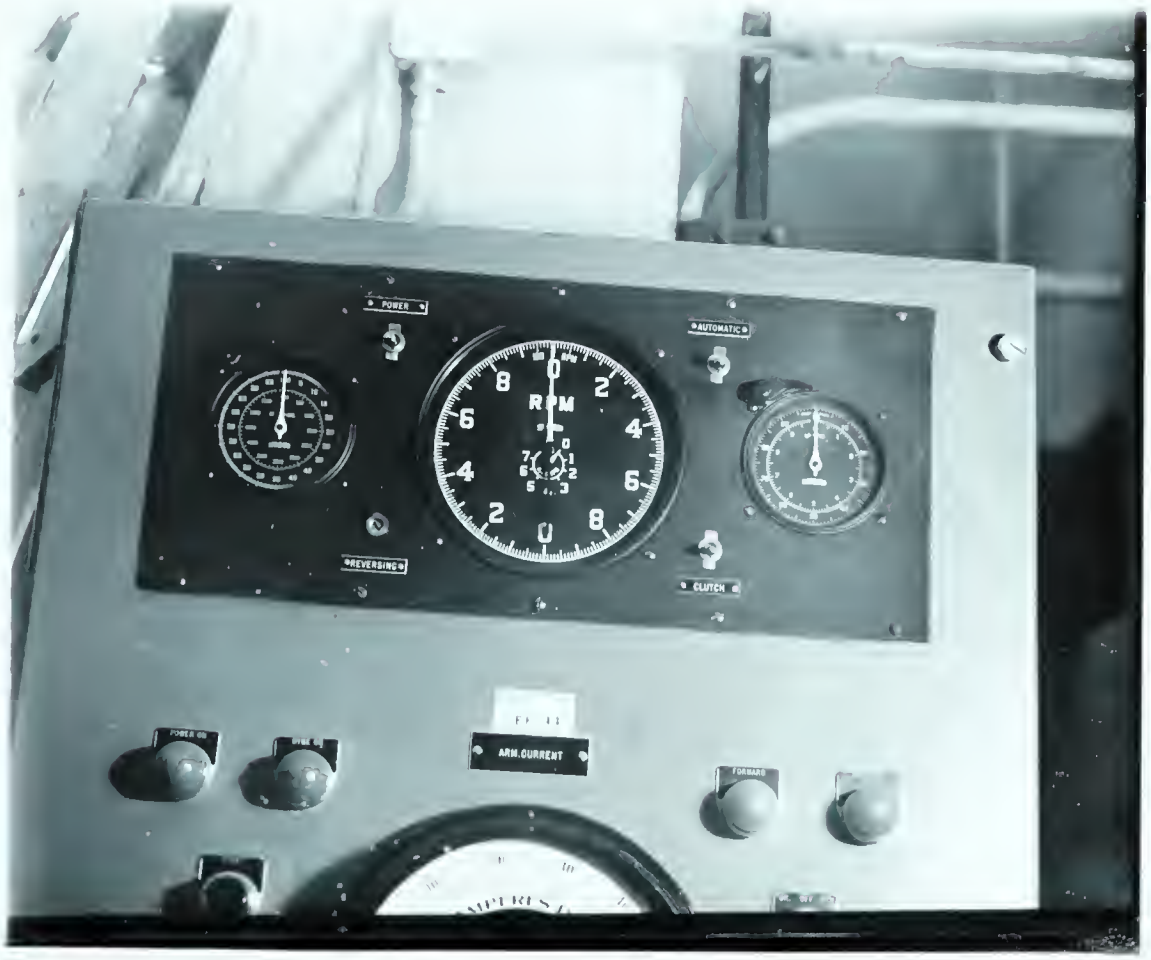

FIGURE 2-11 FUEL TIMING CLOCK

calibrated for average square root of the velocity head versus the velocity pressure at the centre line so only the centre line reading was necessary during the actual tests. The calibration curve is shown in figure 2-12.

The turbine's speed was measured by a small D.C. generator, running through a 5 to 1 reduction, mounted on the end of the turbine as shown in figure 2-6. The voltage change with speed was measured by a large voltmeter reading directly in R.P.M. as seen in front of the Honeywell potentiometer in figure 2-13.

Figure 2-13 is a general view of the control panel. It consisted of the pump on-off switch (lower left), total fuel pressure (large gauge 0-200 p.s.i.), fuel by-pass valve (to the right of the large pressure gauge), fuel throttling valves for each chamber (above and right of the large pressure gauge), the tachometer, the temperature indicator, an inclined manometer for air flow pitot-tube (on top of the potentiometer), starter motor control switches (on the right hand end of the table), and the ignitor spark push button switch. Most of these items can also be seen in figure 2-1.

2.2 Steam Injection Test Runs

For the steam injection runs, the only changes made were to add the necessary equipment for controlling the steam flow, superheating the steam, and measuring the steam flow. The supply of steam was obtained by adding an extension to a high pressure (185 p.s.i.g.) steam main and running it into the room. A 1" globe valve (on the left of figure 2-14) was put on the end of this line to throttle the steam down to a few inches of mercury above the turbine pressure. From here 1" pipe was run into the superheater set into the exhaust duct of the turbine as seen in figures 2-14

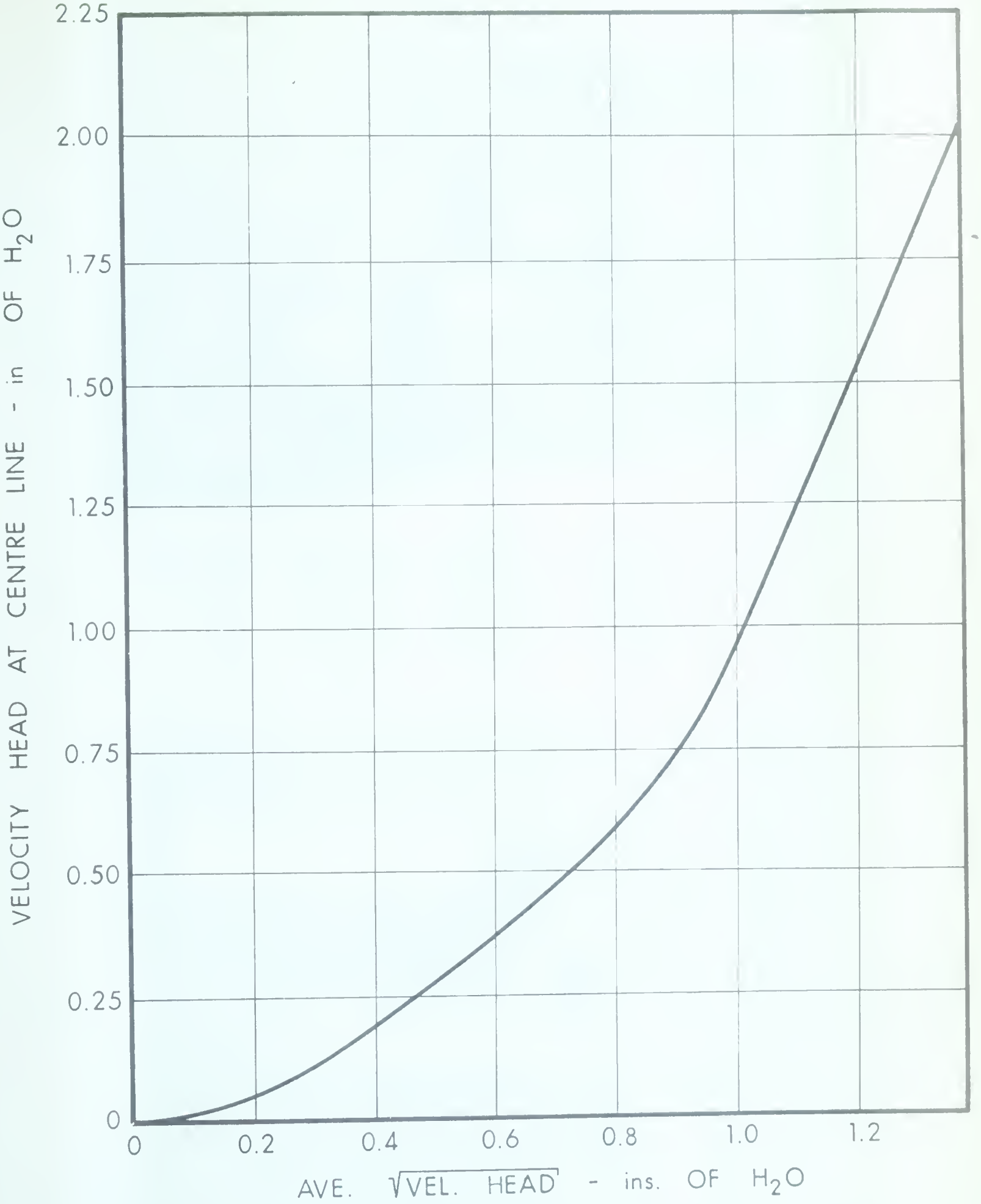

FIGURE 2 - 12 CALIBRATION CURVE FOR 10" AIR FLOW DUCT

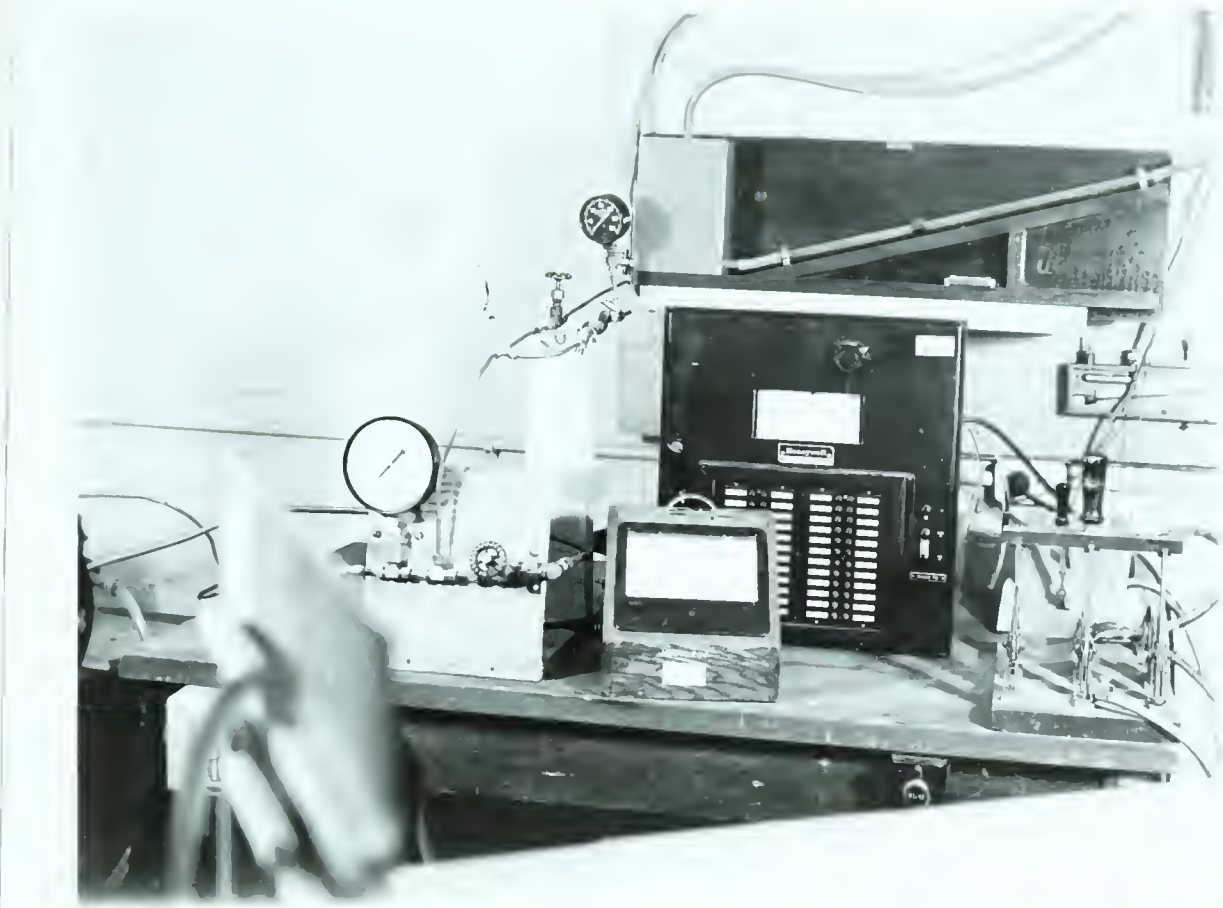

FIGURE 2-13 GENERAL VIEW OF TURBINE CONTROLS

FIGURE 2-14 STEAM PIPE TO SUPERHEATER

FIGURE 2-15 LOCATION OF SUPERHEATER IN EXHAUST DUCT

FIGURE 2-16 "T" CONECTION TO CONTROL STEAM FLOW

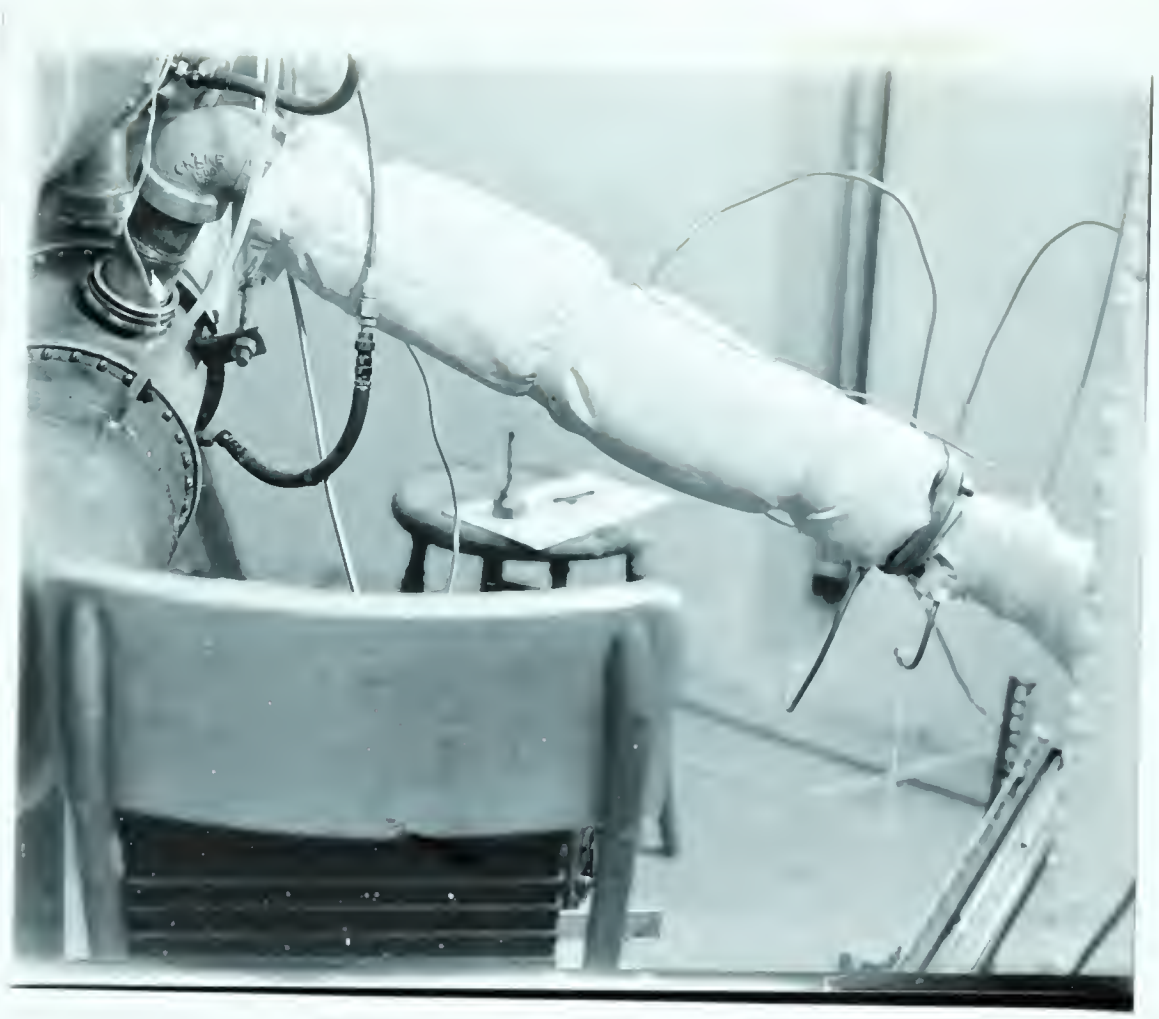

FIGURE 2-17 ORIFICE PLATE AND 2" PIPE INTO LOWER COMBUSTION CHAMBER

and 2-15, after which the steam ran into the "T" connection seen in figure 2-16.

This "T" formed a by-pass system in that during warm up all the steam could be run to drain. Normally the steam ran through the standard 2" pipe, which had an orifice plate placed in it, into the lower combustion chamber, as seen in figure 2-17.

2.2.1 Instrumentation for Steam Injection Runs

The instrumentation remained the same as described in section 2.1.1, only the necessary instruments were added to measure the steam flow through the orifice plate. That is, an iron-constantan thermocouple was used to measure the steam temperature, while the static pressure at and the "radius" pressure drop across the orifice plate were measured by the mercury filled U-tube manometers seen in figure 2-17.

2.3 Design of Orifice Plates and Superheater

2.3.1 Orifice Plates

Using the formulas provided and the method outlined in the A.S.M.E. Flow Measurements (1940) Part 5, Power Test Codes, the following two orifice plate designs, figures 2-18 and 2-19, one for the air bleed-off from the compressor and one for the steam injection pipe, were derived.

The assumptions made for the air bleed-off were a minimum mass flow of 0.1 lbm. per sec. at a temperature of 180°F. and a pressure of 19.6 p.s.i.a. and for the steam injection, a minimum mass flow of 0.1 lbm. per sec. at a temperature of 225°F. and at a pressure of 20 p.s.i.a.

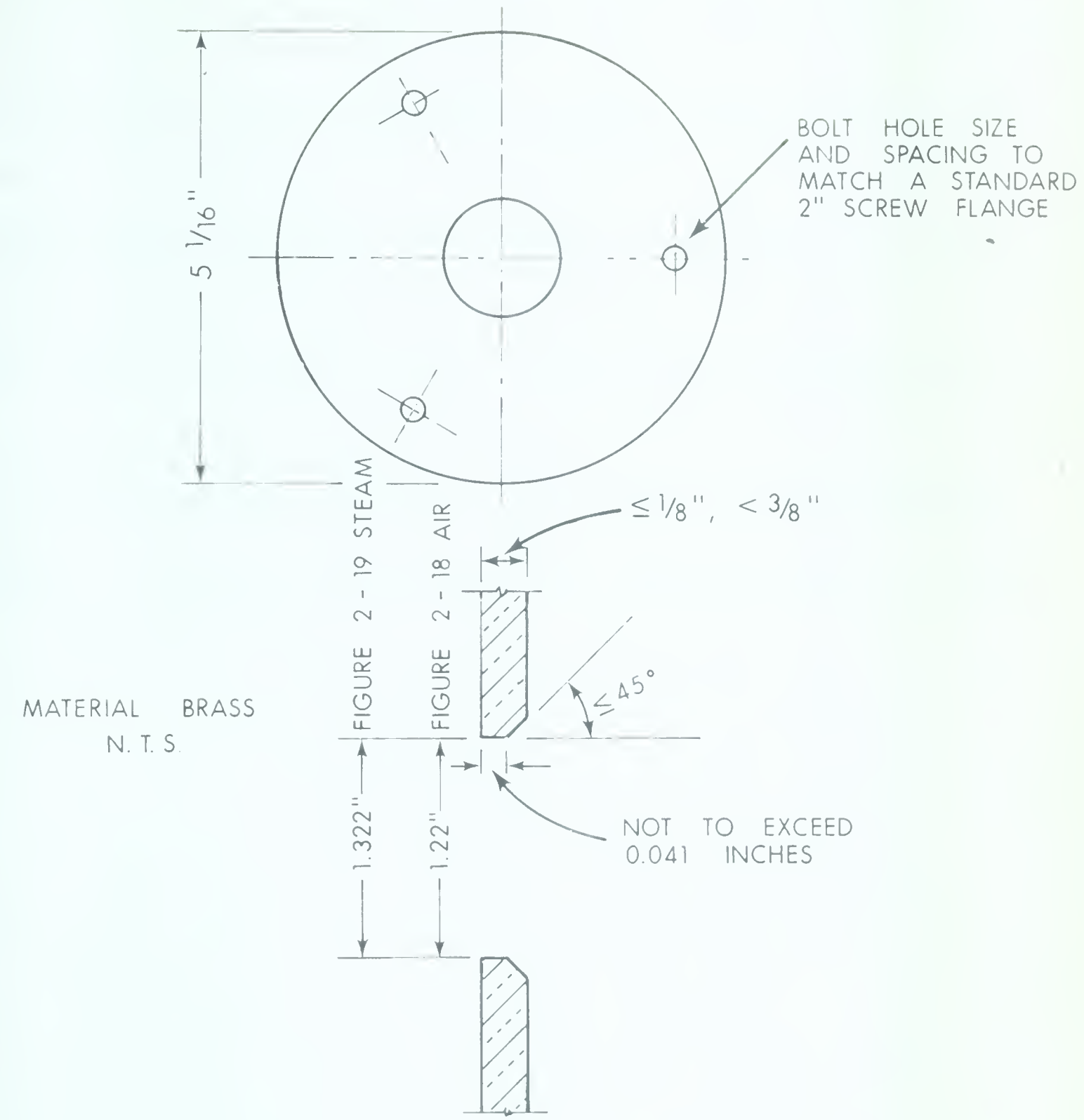

FIGURE 2 - 18 AIR BLEED OFF ORIFICE PLATE

FIGURE 2 - 19 STEAM INJECTION ORIFICE PLATE

2.3.2 Superheater

The superheater was designed to be of a simple, one-pass type providing superheat to the steam eliminating the possibility of water being injected into the turbine. By assuming minimum and maximum steam flows of 0.1 lbm./sec. and 0.8 lbm./sec. respectively at 20 p.s.i.a. and 225°F. entering the superheater and an exhaust gas temperature of 800°F. at 13.5 p.s.i.a. (atmospheric pressure) for a steady flow of exhaust gases of 2.5 lbm./sec., and using formulas VIII-3 and VIII-4 on pages 140 and 141 of reference 14, it was possible to calculate an estimate of the h(B.T.U./HR Ft^2°F.) values for the inside of standard 1" pipe at minimum and maximum steam flow conditions and for the outside at a film temperature of 500°F. This allowed the calculation of the required area (or length of 1" pipe) necessary to insure the superheated condition. A drawing of the resulting superheater showing its position in the exhaust duct is seen in figure 2-20.

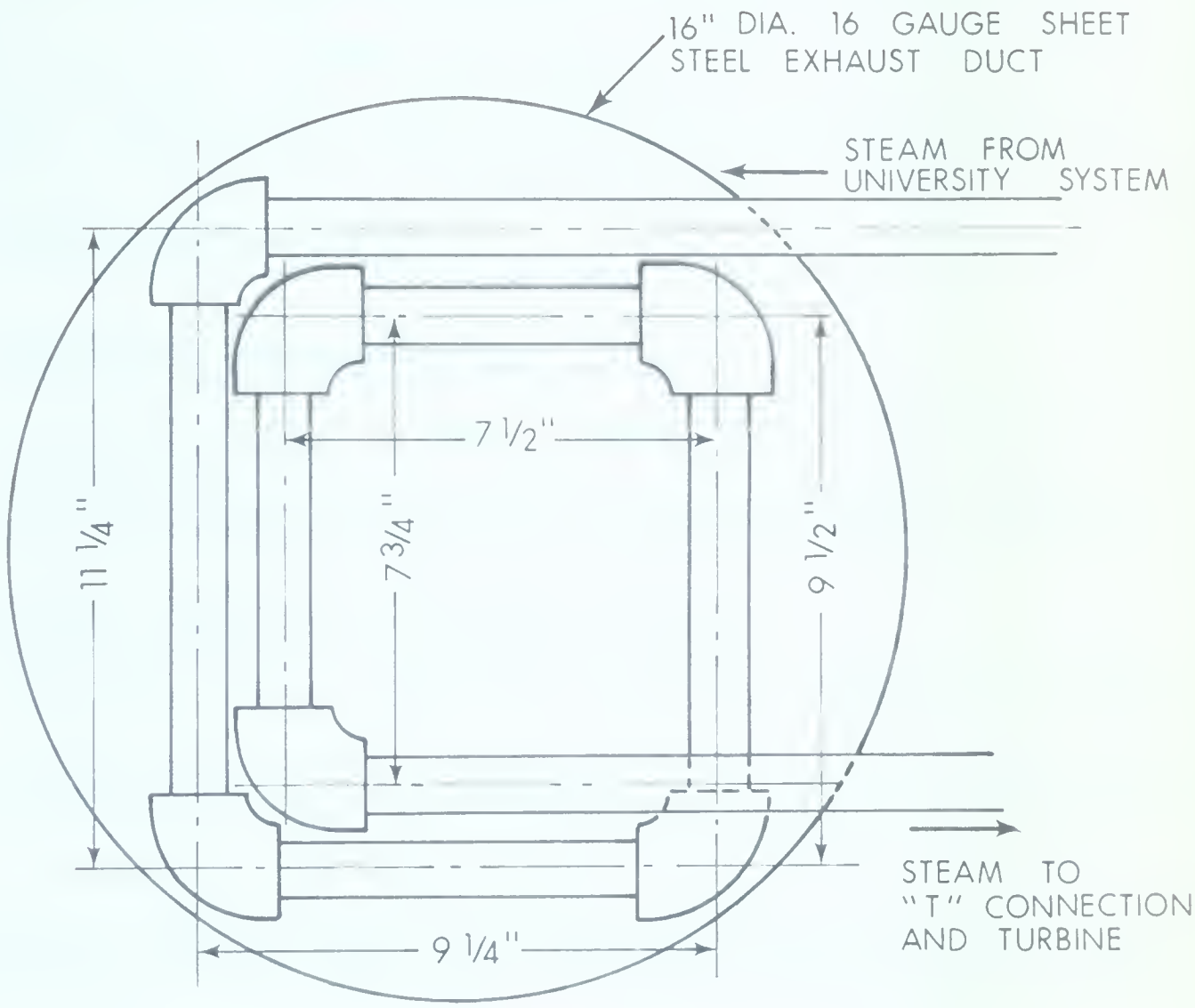

ALL PIPE STD. 1" AND THREADED 90° ELBOWS

FIGURE 2 - 20 EXHAUST DUCT SUPERHEATER

CHAPTER 3

EXPERIMENTAL PROCEDURE

All tests were carried out at a pressure ratio of approximately 1.5 to 1 (about 15,000 R.P.M.) and at maximum cycle temperatures (inlet to the nozzle ring) as close to 1200°F. as was possible. The fuel used was commercial kerosene with 1% S.A.E. 20 oil added for pump lubrication.

3.1 Basic Thermal Efficiency Test Runs

Before each test began, a turbine check list (figure 3-1) was used to insure proper start up and running of the test. Also, information required, as seen on the top of a data sheet, figure 3-2, was recorded at this time.

The turbine was then rotated by the starter motor. Running on low voltage the turbine would reach 2000 R.P.M., at which point the fuel pump was started and the combustion chambers ignited. High voltage was then quickly applied to the starter motor accelerating the turbine to 5000 R.P.M. Keeping the combustion chamber outlet temperatures near 1200°F., the turbine would slowly accelerate to its self-sustaining speed of 8000 R.P.M. The starter motor's electrical circuit was then broken and the motor disengaged from the turbine.

The turbine was accelerated to 14000 R.P.M. by keeping the combustion chamber outlet temperatures near 1200°F. (reading positions 37 and 28 on the potentiometer), then reducing them to 1050°F. to maintain a steady speed of 14000 R.P.M. With the turbine running at this speed, all the temperatures, pressures and the air flow

Gas Turbine Check List

Open main steam valve

Diesel fuel

Kerosene

Inspection hole closed

Duct block removed

Steam valve to turbine closed

Steam drain valve open

Crank valve to superheater

Balances are up

Micro-switch clear

C.F.R. clock on

Auto power on

Start switch on

Micro-switch plug in

Fuel drain closed

Air bleed valve closed

Pump valve open

L.H. valve open

R.H. valve open 1 turn

Starter switches open

Starter engaged

Starter hold clamp

Pump power on

Potentiometer on

Ignition and plugs

Ventilation fan on

Cooling water on

Cables plugged together

Diesel exhaust fan

Diesel started

Field, oil

Diesel at 800 R.P.M.

Dyno excitation on

Water can under turbine

FIGURE 3-1 GAS TURBINE CHECK LIST

GAS TURBINE TEST DATA

DATE _____ BAROMETER _____ in. of Hg.

ROOM TEMP. START _____ °F OBSERVERS _____
FINISH _____ °F _____

FUEL WT. USED _____ LBS. SPEED APPROX. _____ R.P.M.
TIME _____ MINS.

TIME START TEST EQUIPMENT _____ AIR FLOW _____ in. of H_2O
TIME START TURBINE _____ TOTAL FUEL PRESS. _____ PSIG.
TIME STOP TURBINE _____ LOWER C.C. FUEL PRESS. _____ PSIG.

TEMPERATURES - °F

1	2	3	4	5	6	7

37	38	39	40

MANOMETERS:

1	2	3	4	5

6	7	8	9	10

NOTES:

FIGURE 3-2 GAS TURBINE DATA SHEET

readings were quickly checked. The speed was then increased to produce a compressor pressure ratio of 1.5 to 1.

When at this condition, the air-bleed-off valve was slowly opened until the combustion chamber outlet temperatures had to be increased to near 1200°F. to maintain a steady running speed. After allowing several minutes for the turbine to stabilize itself at this speed and temperature (compressor inlet and outlet remain constant), the test proper began.

First, the balance arm on the fuel weighing scale was set to trip the micro-switch starting the clock. Then, once the clock had started and the fuel weight set, the clock stop circuit was set and data recorded.

The data recorded were:

Potentiometer Position	Temperature	Manometer No.	Pressure
1	Compressor inlet	1	Total at compressor outlet
2	Compressor outlet	2	Static drop across lower combustion chamber
3	Before top combustion chamber	3	Static exhaust
4	Before lower combustion chamber	4	Static at air bleed off orfice plate
5	Air bleed off	5	"Radius" differential across air bleed off orfice plate
6	Secondary air		
37	Before nozzle ring top		
38	Before nozzle ring bottom		

39 After turbine wheel top

40 After turbine wheel bottom

In addition to the above, the turbine speed and the air flow reading at the compressor inlet (usually surging up and down slowly) were noted. All of these readings were taken several times during a test until the fuel clock stopped. The time shown by the clock was then recorded.

The stopping procedure for the turbine was first to close the air bleed-off valve and then to reduce the fuel supply slowing the turbine to 10,000 R.P.M. to allow it to cool under reduced temperatures. After a few minutes the fuel pump was shut off, stopping the turbine.

After the turbine had stopped, the auxiliary equipment was shut off and the fuel drain valve opened. After the water jacket temperature reduced to 80°F. or less, the cooling water flow was stopped.

3.2 Initial Inspection

Before the steam injection runs were begun, the turbine was partially dismantled exposing the inside of the combustion chambers, the nozzle ring, and the turbine blades. This was done to check the general condition of the turbine as high temperature measurements can be considerably inaccurate.

The turbine blades (figure 3-3) were found to be in satisfactory condition, but the nozzle ring showed definite heat warping (figures 3-4 and 3-5) where the top combustion chamber discharged into it. It can also be seen in figure 3-4 that the deposits left by the diesel engine (previous service of the turbo charger) were completely

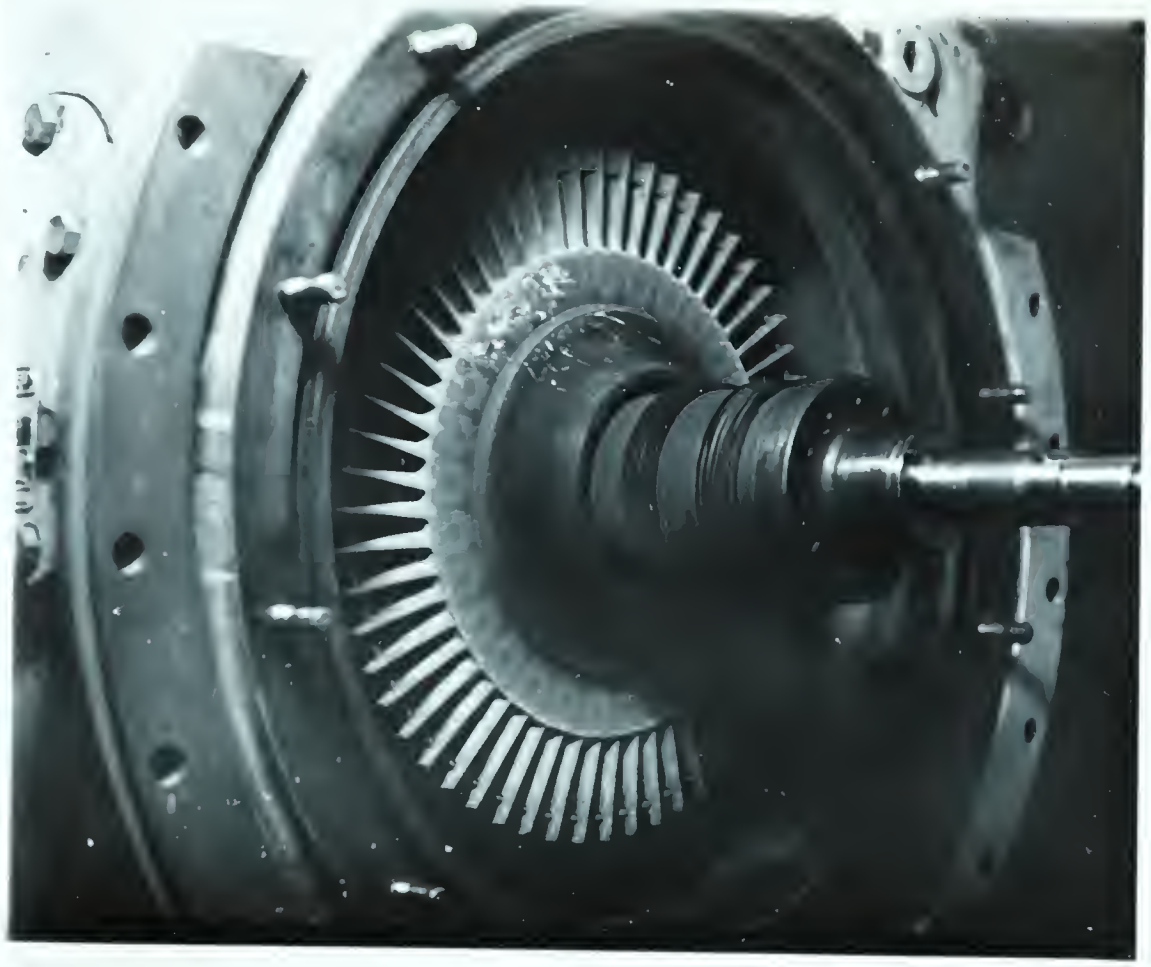

FIGURE 3-3 TURBINE BLADES

FIGURE 3-4 NOZZLE RING

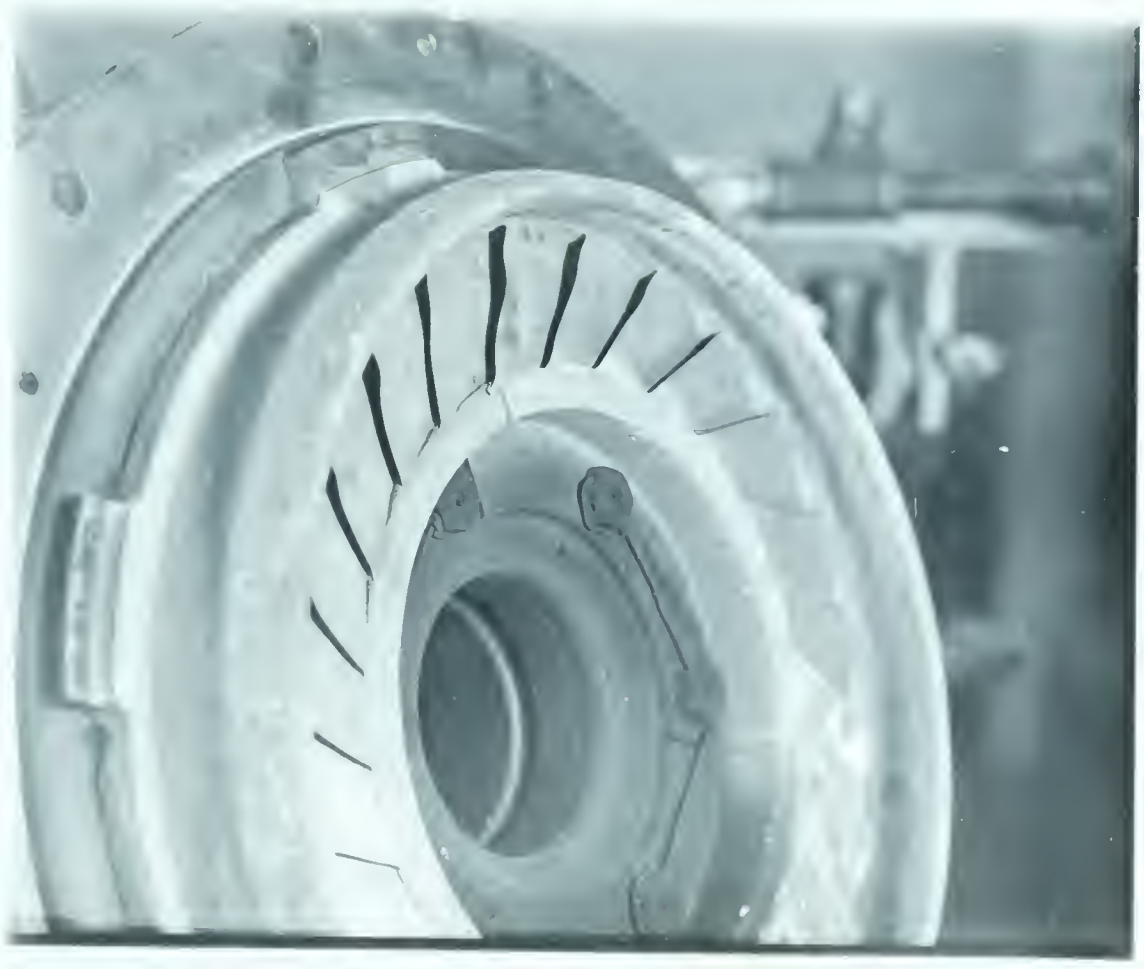

FIGURE 3-5 EXTENT OF NOZZLE RING WARPING

FIGURE 3-6 FLAME ENDS OF COMBUSTION CHAMBERS

burnt off where the top chamber exhausted, but partially remained where the lower chamber exhausted. Figure 3-5 clearly shows the extent of the nozzle warping on the upper chamber while none existed for the lower chamber, all indicating that the top combustion chamber was definitely too hot.

Examination of the combustion chambers' ends indicated that the top combustion chamber was burning very cleanly, while the lower chamber shows an extremely sooty condition, as if incomplete combustion was taking place (figure 3-6).

Inside the combustion chambers however, the reverse existed. The lower combustion chamber, figure 3-7, was very clean while the top chamber, figure 3-8, had a very curious inner deposit, extremely thick (1") in places. This deposit is difficult to see in figure 3-8, but was located in the dark area just behind the large mixing holes seen in the chamber. It looked and felt like pure carbon (i.e. similar to the carbon given off by an oxy-acetylene welder burning acetylene only). No attempt was made to analyze the deposit or fuel used at this time in an effort to determine why the deposit occured, as it was felt to be beyond the scope of this experimental study.

After carefully straightening out the warped nozzle ring, the turbine was reassembled and a check of its operation made.

3.3 Steam Injection Test Runs

The procedure followed during the steam injection runs was the same as that for the basic thermal efficiency runs except that two persons were needed to operate all the necessary controls.

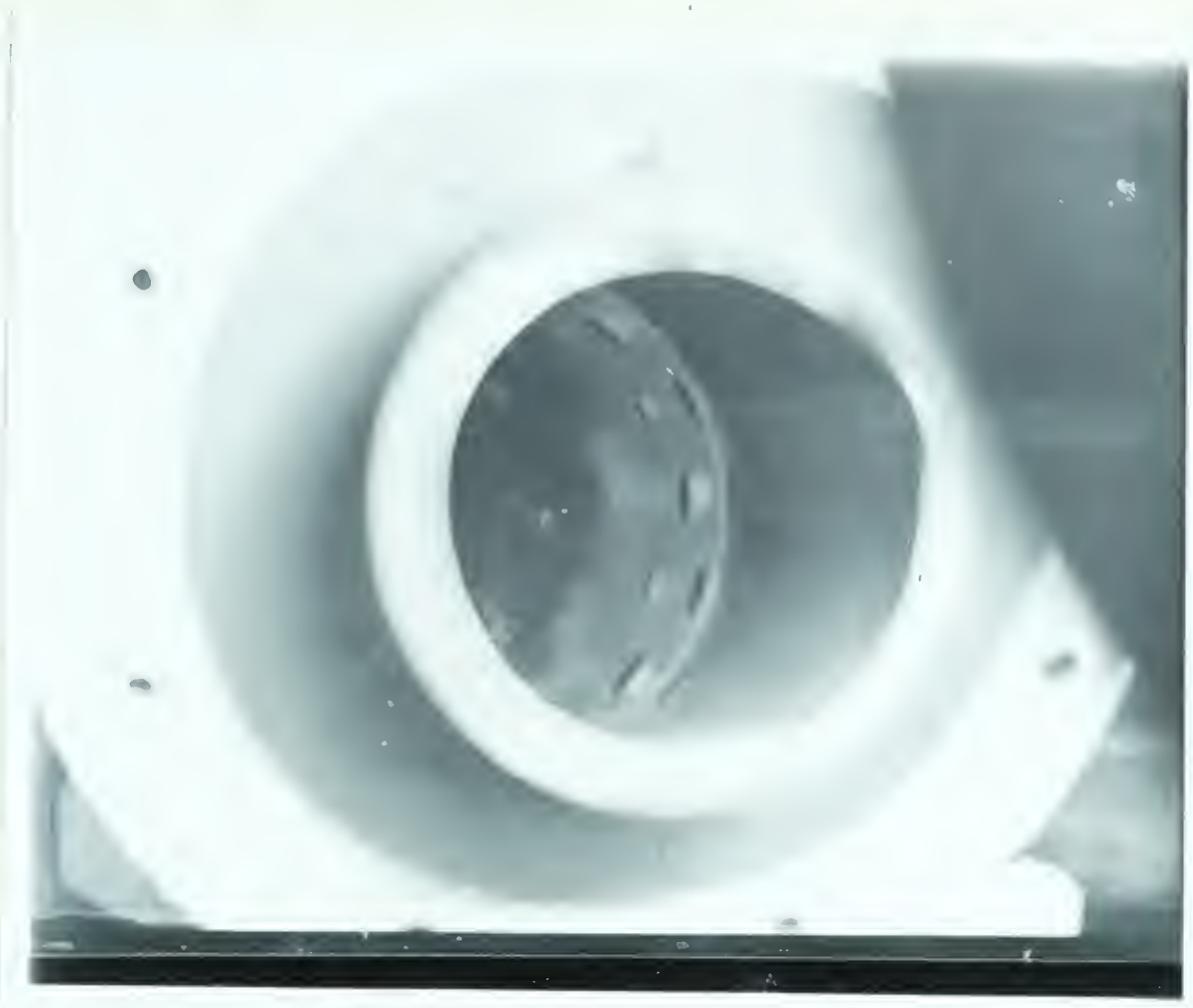

FIGURE 3-7 INSIDE LOWER COMBUSTION CHAMBER

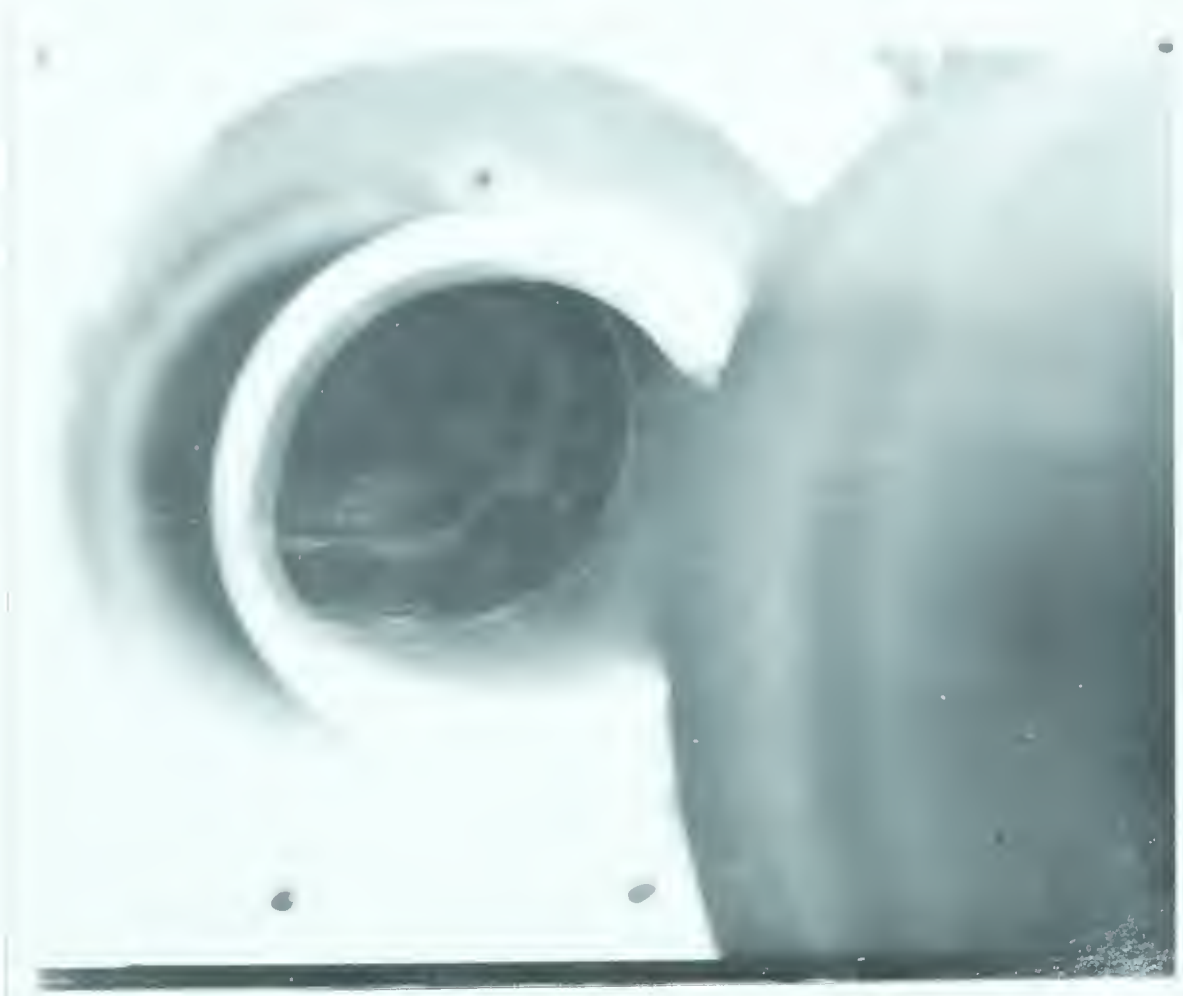

FIGURE 3-8 INSIDE TOP COMBUSTION CHAMBER

The main steam valve was opened first to force the water out of the superheater pipes before starting the turbine. After the steam condition was as good as possible without superheating, the turbine was started, as described in section 3.1.

Following a thermal efficiency run, two more runs with added steam were done. The actual rate of change of injection proceded very slowly because both persons, one operating the turbine and air bleed off, the other controlling the steam injection, had to closely co-ordinate their actions, otherwise flame-out (due to excessive steam) would occur.

To accomplish the actual injection, the drain valve was slowly closed as the valve to the orifice plate was opened fully, directing the flow of superheated steam into the turbine until a predetermined pressure differential existed across the steam orifice plate "radius" taps. While the superheated steam was being injected, the turbine operator tried to keep the pressure ratio constant and the temperatures of the combustion chambers near 1200°F. by adjusting the fuel to each chamber. Once equilibrium was achieved, the fuel clock was set and, once started, the data were recorded. Additional data required were the temperature of the steam through the orifice plate (position 7), the static pressure at and the "radius" differential pressure across the steam orifice plate (manometers 6 and 7).

After the two steam runs were completed, the turbine was stopped in the described manner after the steam had been turned to drain. The steam was left on after stopping the turbine in order to cool the superheater pipes.

CHAPTER 4

METHOD OF ANALYSIS

The order of the analysis presented below is in the same order in which the results in Cahpter 5 are presented. In all cases, the temperatures and manometer readings used herein (see tables 5-3 and 5-4) were mean values, the manometer readings being corrected for changes in density of their respective fluids with temperature.

4.1 Compressor Efficiency

The compressor adiabatic efficiency was calculated in two manners; using the compressor curves (figure 4-1) supplied by Brown Boveri (Canada) Ltd., and by total temperature rise method.

To use the compressor curves, the pressure rise (ratio) through the compressor and the amount (meter^3/sec.) of air handled by the compressor had to be known. The pressure rise (ratio) was found from the total-head tube reading and the atmospheric pressure, while the amount of air drawn in at 59°F. was calculated from the air flow reading using the calibration curve (figure 2-12) to obtain the average square root of the velocity head.

The total temperature rise can readily be used since the adiabatic efficiency of a compressor is defined as[15]

$$\eta_c = \frac{\text{adiabatic work of compression}}{\text{actual work of compression}} \qquad 4.1$$

or

$$\eta_c = \frac{\Delta h \text{ adb}}{\Delta h \text{ act}} \qquad 4.2$$

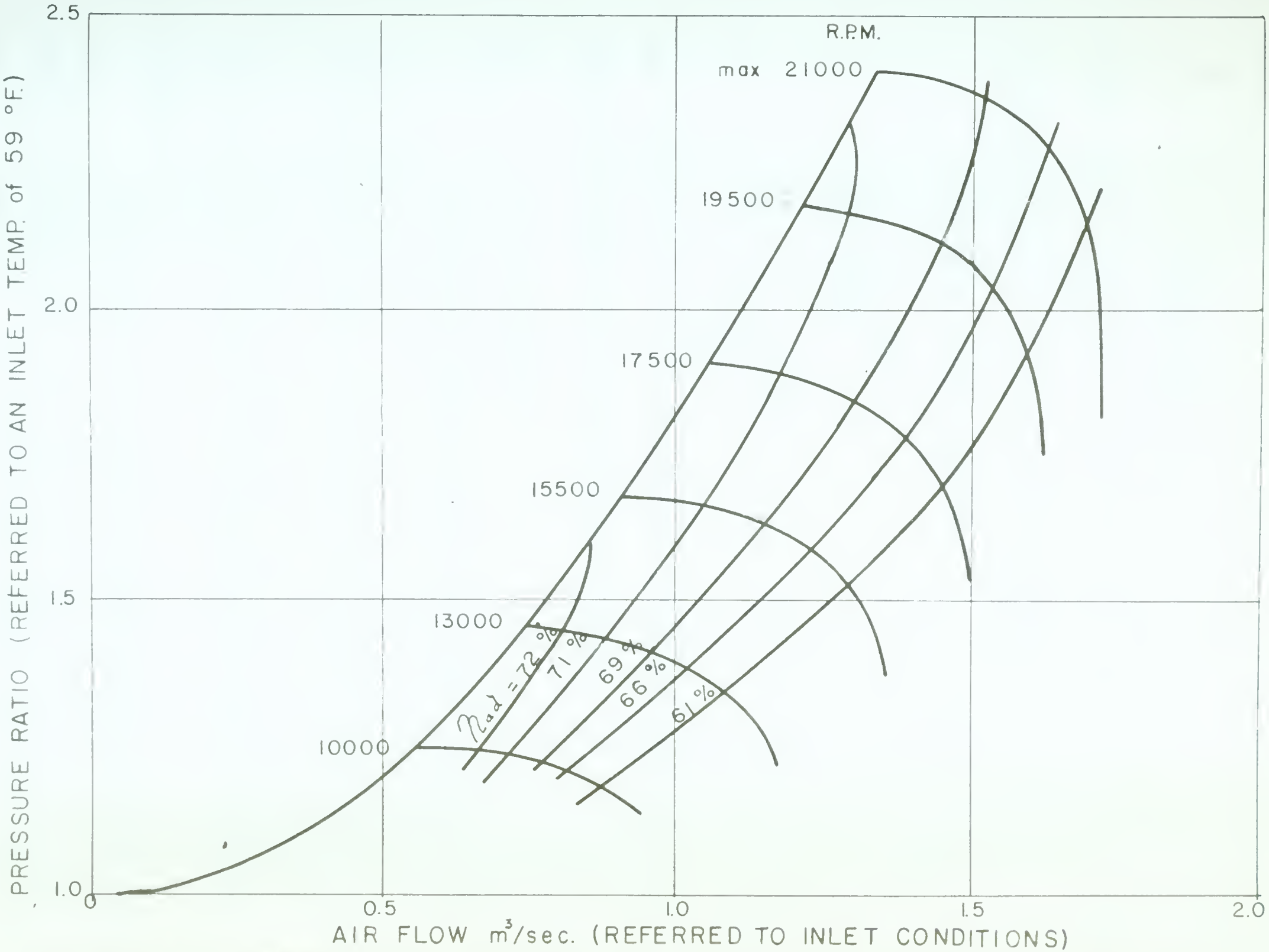

FIGURE 4-1 COMPRESSOR CURVES (BY PERMISSION OF BROWN BOVERI CANADA LTD.)

which for perfect gases is

$$\eta_c = \frac{Cp(Tt_2' - Tt_1)}{Cp(Tt_2 - Tt_1)} \qquad 4.3$$

or simply $$\eta_c = \frac{Tt_2' - Tt_1}{Tt_2 - Tt_1} \qquad 4.4$$

if Cp remains constant as it does for air at low temperatures.

Now if the compressor is adiabatic,

$$\frac{Pt_2}{Pt_1} = \left(\frac{Tt_2'}{Tt_1}\right)^{\frac{k}{k-1}}$$

or $$Tt_2' = Tt_1\left(\frac{Pt_2}{Pt_1}\right)^{\frac{k-1}{k}} \qquad 4.5$$

then it was possible to calculate the theoretical total temperature after compression, and using the measured value, find the compressor efficiency.

4.2 Combustion Efficiency

To compute the combustion efficiency, air tables[16] and tables of combustion products of 400% air[16] (see section 5.1 for validity of use) were used to find the enthalpy of the air before the combustion chambers and the enthalpy of the air-fuel products after combustion, using the measured temperatures. The enthalpy difference (BTU's/sec.) was then divided by the heat added (BTU's/sec.) giving the efficiency (x 100%).

The heat added to the combustion chambers was found from the fuel rate (lbm/sec.) multiplied by the lower heating value (since it was assumed that the H_2O would not condense out) of the fuel (BTU's/lbm). The L.H.V. of the fuel was found

to be 18,600 BTU's/lbm by taking an °A.P.I. gravity and using figure 72 on page 118 of reference 17.

For the cases where superheated steam was injected, the mixture was considered to be nonreactive, allowing the enthalpy rise of the superheated steam to be obtained from steam tables[18] using the measured temperatures and pressures. The sum of the enthalpy rise of the air and the superheated steam (BTU's/sec.) was divided by the heat added (BTU's/sec.) to give the combustion efficiency in these cases.

4.3 Turbine Efficiency

The turbine isentropic efficiency was found by use of figure 4-2 which was drawn from information supplied by Brown Boveri (Canada) Ltd. The isentropic heat drop for the air-fuel products was obtained from the tables of combustion products of 400% air[16] using the measured temperature into the nozzle ring and the pressure drop (ratio) incurred by the air-fuel products expanding in the turbine wheel. The pressure ratio was found from the pressure after compression minus the pressure drop through the combustion chambers, and this difference was divided by the exhaust pressure, all in absolute units. The isentropic heat drop (BTU's/lbm) was then converted to Joules/kilogram giving the H value for figure 4-2.

The circumferential speed (U) of the turbine at the medium turbine diameter was obtained by multiplying the turbine speed, radians/sec., (average value of observed reading and compressor curve point) times the diameter of the turbine wheel at the mean diameter (measured as 5.73" or 0.1457 meters). Thus the isentropic efficiency of the turbine was found directly.

$$\mu = \frac{H}{U^2}$$

WHERE H= ISENTROPIC HEAT DROP IN THE TURBINE (J/Kg.)

AND U= CIRCUMFERENTIAL SPEED OF THE TURBINE AT MEDIUM DIAMETER (m/sec.)

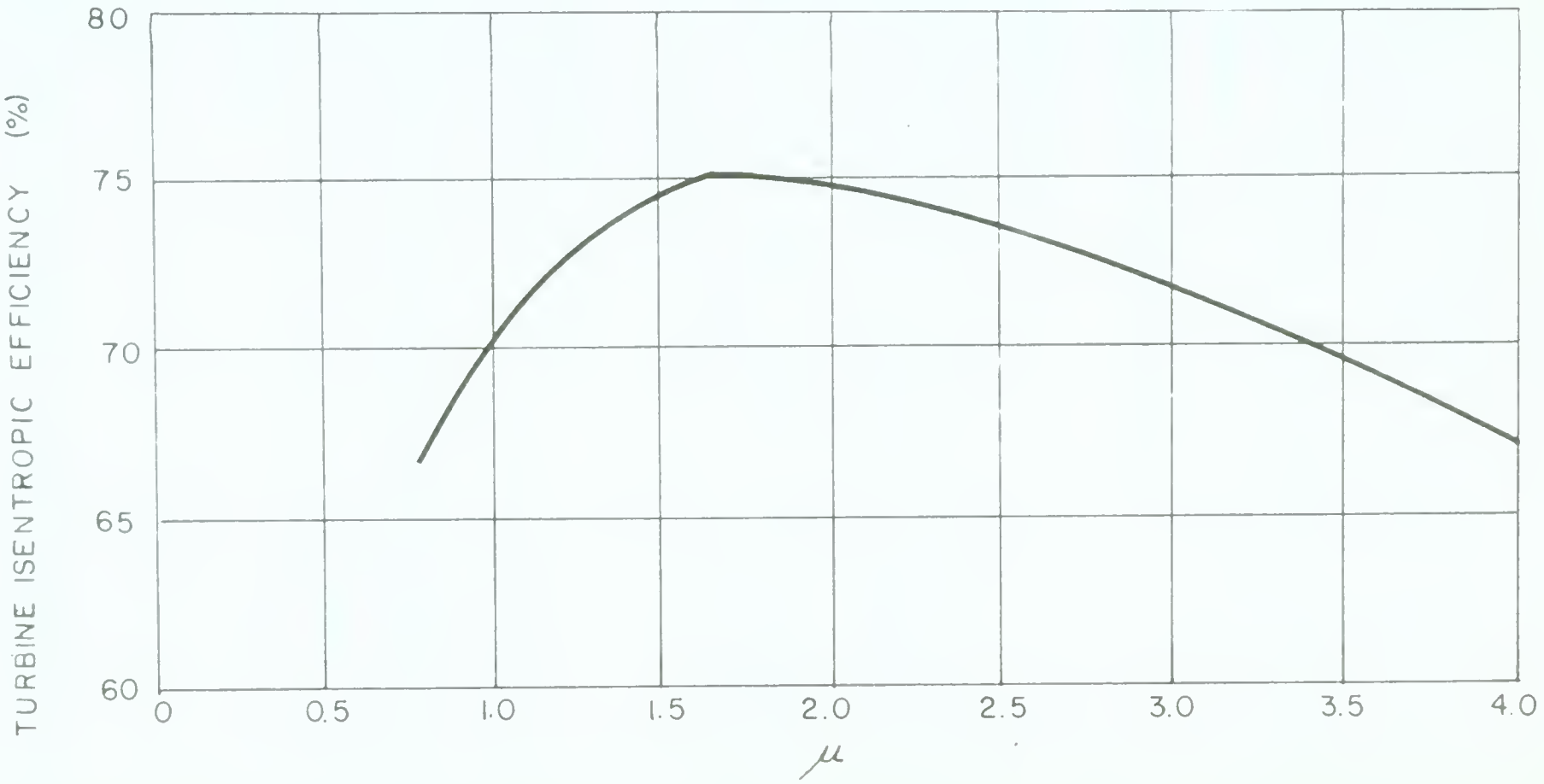

FIGURE 4-2 TURBINE ISENTROPIC EFFICIENCY

(BY PERMISSION OF BROWN BOVERI CANADA LTD.)

4.4 Fuel to Air Ratio

The lbm of air for each lbm of fuel used was found simply by dividing the mass rate of air through the combustion chambers, that is,the total mass rate flowing through the compressor minus the mass rate of air bleed off, by the mass rate of fuel added. The mass rate of air bled off from the compressor was calculated from the readings taken at the bleed-off orifice plate using the method outlined in the A.S.M.E. Flow Measurements (1940) Part 5, Power Test Codes.

4.5 Fuel to Mixture Ratio

The lbm of mixture for each lbm of fuel used was computed by dividing the mass rate of air plus the mass rate of superheated steam travelling through the combustion chambers by the mass rate of fuel added. The mass rate of superheated steam added to the cycle was found by the same method as the mass rate of air bled off from the compressor.

4.6 Superheated Steam to Air Ratio

This was simply computed by dividing the mass rate of air through the combustion chambers by the mass rate of superheated steam added to the cycle. Note that although superheated steam was only added to one chamber, the air mass that was computed flows through both.

4.7 Work Output

The work output by the cycle was the work required to compress the air bled off from the compressor. This was found by multiplying the mass rate of air bled off times the actual enthalpy increase imparted by the compressor to it. The enthalpy

increase was obtained from air tables[16] using the measured temperatures at the compressor inlet and outlet.

4.8 Heat Added

The amount of heat added to the cycle by the fuel was computed as described in section 4.2.

4.9 Thermal Efficiency

Thermal efficiency for a thermodynamic cycle is defined[19] as net work output divided by the heat added to the working substance. Thus dividing the work output (section 4.7) by the heat added (section 4.2) gives the thermal efficiency. But since the work to pump the fuel and to pump the water for steam production were considered negligible, the thermal efficiencies obtained from these calculations might be classed as "gross" thermal efficiency.

4.10 Compressor Horsepower

The horsepower required by the compressor to compress all the air supplied was calculated by multiplying the total mass rate of air by the enthalpy increase imparted by the compressor to this air and converting it to horsepower.

4.11 Turbine Horsepower

The horsepower produced by the turbine was calculated by finding the enthalpy drop through the turbine from the measured temperatures, multiplied by the mass flow of air-fuel mixture and converting this to horsepower. For cases with added superheated steam, the horsepower produced by the steam was added to that of the air-fuel mixture.

4.12 Theoretical Turbine Horsepower

The theoretical horsepower produced by the turbine was calculated by obtaining the isentropic heat drop (BTU/lbm) in the turbine, multiplied by the turbine isentropic efficiency and converted to horsepower.

CHAPTER 5

EXPERIMENTAL RESULTS AND DISCUSSION

The experimental results are shown in tables 5-1, 5-2, 5-3 and 5-4. Tables 5-1 and 5-2 list the results of all the experimental tests as discussed in Chapter 4, while tables 5-3 and 5-4 show the mean value of the readings taken during these tests. Table 5-5 is a comparison of experimental and theoretical results.

5.1 Discussion of Errors in the Trial Runs and Methods of Analysis

Before discussing the experimental results, certain errors noted during the course of the trials should be noted.

At the beginning of trial 9, it was found that the thermocouple at the top combustion chamber outlet was not recording the maximum temperature of the hot gases and was therefore adjusted to do so. This meant that the temperatures recorded at this position for all the previous runs were in error as evidenced by the warping of the nozzle ring (section 3.2). During trial 5, however, this thermocouple did record continuously in the 1280°F. to 1290°F. range (table 5-3), producing a combustion efficiency of 97.2% (table 5-1) which is probably close to its true value and considerably higher than any other value calculated.

One of the reasons for not detecting this erroneous thermocouple earlier is also seen in table 5-3. That is, the thermocouple after the turbine wheel top always recorded a lower temperature than at the turbine wheel bottom. These readings differed from 40°F. to 140°F. and it was felt at the time that the thermocouples after the turbine wheel would have been more accurate than those before the nozzle ring. This

low reading at the top of the turbine wheel outlet may have been caused by poor location of the thermocouple. It should also be noted that no attempt was made to use radiation shields on the chromel-alumel thermocouples, or to correct the readings for radiation losses.

Another source of error that may exist in the calculations of combustion efficiency, turbine efficiency and turbine horsepower, is that the percent theoretical air varied from 400% to 443%, while tables of combustion products of 400% air were used. The effect of using the 400% air tables instead of ones for higher percentage values (tables were not available for higher percentage values although charts are, but undue error is introduced reading charts) is to increase the combustion efficiency, since the enthalpy per lb mole at any given temperature is higher for 400% air than for percentages greater than 400%. Thus the enthalpy difference obtained by the air is greater than would actually be the case. But for a temperature of 1660°R. (1200°F.), the difference between the enthalpy per lbm of 200% and 400% air is less than 1.7%, thus for 443% air compared with 400% air, the error involved is about 0.36%.

Also to be noted is that the products of combustion of 400% air tables were tabulated for olefin series fuels, $((CH_2)_n)$, while kerosene is a paraffin series fuel (C_nH_{2n+2}). Again for any value of n, a paraffin series fuel has a higher enthalpy of combustion[20], but the effect in the enthalpy per lbm at any temperature is almost nil as the lbm of products per lb mole changes very little[21].

5.2 Compressor Efficiency

In table 5-1, the results of the compressor efficiency as calculated from the Brown Boveri compressor curves and by the total temperature rise method, and also

TABLE 5-1

SUMMARY OF EXPERIMENTAL RESULTS

Trial No.	Comp. Ratio	Compressor EFF%			Combus-tion EFF%	Turbine EFF by Brown Boveri %	Fuel to Air	Fuel to Mix	Steam to Air	Work Output BTU/sec.	Heat Input BTU/sec.	Gross Thermal Efficiency %
		Brown Boveri	Total Temp. Rise	Ave.								
1	1.52	66	63.3	64.6	87.75	74.9	1/61.8	--	--	3.415	837.5	0.407
2	1.523	64.5	64.2	64.35	92.5	74.7	1/66.0	--	--	3.48	849	0.408
3	1.54	64	65	64.5	88.3	75	1/62.4	--	--	3.91	884	0.4425
4	1.527	63.5	63.6	63.55	90.1	74.8	1/63.5	--	--	3.62	859	0.421
5	1.50	63	64	63.5	97.2	74	1/65.7	--	--	3.78	822	0.459
6	1.513	65.5	65.8	65.65	92.4	74.9	1/65	--	--	3.84	809	0.469
7	1.52	67	63.25	65.1	89.7	75	1/62.6	1/64.36	1/36.4	6.41	813	0.795
8	1.522	67.5	62.5	65	88.4	74.8	1/60.3	1/62.62	1/25.9	8.195	824	0.939
9	1.512	62.75	65.6	64.2	94.4	74.4	1/66.5	--	--	2.88	807	0.344
10	1.51	66.25	65.9	66.1	91.6	74.9	1/61.8	1/64.1	1/22.4	5.58	793	0.705
11	1.51	66.75	65.6	66.2	94.75	74.8	1/60.0	1/64.05	1/14.83	6.60	795	0.814

the average values are shown. The results show good agreement between the methods of calculation with the efficiencies varying from 62.5% to 67.5%. The maximum disagreement between the two methods is less than 8%.

5.3 Combustion Efficiency

The combustion efficiency is seen to vary from a minimum of 87.75% to a maximum of 97.2%, the average value of all the runs being 91.55%. The effect of the erroneous thermocouple is clearly seen by comparing the combustion efficiency of trials 6, 7 and 8, with trials 9, 10 and 11 respectively.

5.4 Turbine Efficiency

The turbine efficiencies shown in table 5-1 are almost all the same, varying from 74.0% to 75%. It was assumed in all cases that the temperatures measured at the turbine inlet were correct (neglecting radiation losses) but this is obviously in error except perhaps for trials 5, 9, 10 and 11. If the temperature were 100°F. higher than indicated at top combustion chamber outlet, the average temperature inlet would be raised only 50°F.

Assuming this, a recalculation of the turbine efficiency shows that for trial 3, the turbine isentropic efficiency would be 74.8%. Thus the error involved is very small.

Since the correlation between the methods of calculating the compressor efficiency was good, it is felt that the turbine efficiencies obtained from the data published by Brown Boveri (Canada) Ltd. are equally as accurate. This is verified when one compares the horsepower required by the compressor (allowing for a 98% drive efficiency and windage losses) with the theoretical horsepower produced by the

turbine (table 5-2 and section 4.12).

5.5 Fuel to Air Ratio

The fuel to air ratios vary between 1/60 (400% theoretical air) and 1/66.5 (443% theoretical air), which for the fuel used and the maximum temperatures reached are normal as evidenced by the combustion efficiencies.

5.6 Fuel to Mixture Ratio

The fuel to mixture ratios show a smaller variation than the fuel to air ratios. This is because the superheated steam replaced some of the air flowing through the combustion chambers, reducing the fuel to air ratio, producing a wider difference in the fuel to air ratios.

5.7 Steam to Air Ratio

In the first steam injection trials, trial 7 had only 2.75% added superheated steam, while in trial 8, it was increased to 3.86%. The higher value (3.86%) was restricted in these first trials because the air-bleed-off valve was fully opened, and a further increase in the steam injection rate would only have necessitated the temperatures before the nozzle ring to be reduced to maintain a constant pressure ratio of 1.5 to 1.

To overcome this, a larger orifice plate was installed (the design was exactly the same, only the hole was 1.44" in diameter) in the air-bleed-off line. This allowed the steam injection rate to be increased to 4.46% for trial 10, and to 6.75% for trial 11. The value of 6.75% superheated steam (actually about 13.5% superheated steam for the lower combustion chamber) was found to be very near the limit for flame out in the lower combustion chamber. This limit was most likely due to the location

TABLE 5-2

SUMMARY OF EXPERIMENTAL RESULTS

Trial No.	Total Air Flow lbm/sec.	Air Bled off lbm/sec.	Steam Injected lbm/sec.	Fuel Rate lbm/sec.	Comp. H.P.	Turb. H.P. Measured Temp. Drop	Theo. Turb. H.P. Theo. Temp. Drop
1	2.91	0.1323	-	0.0450	106	141	-
2	3.15	0.1327	-	0.0456	112.5	149.5	-
3	3.11	0.1448	-	0.0475	118.8	181.5	124.5
4	3.07	0.1380	-	0.0462	112	182	120
5	3.05	0.1480	-	0.04425	110	218	114.3
6	2.98	0.1502	-	0.0435	106	162.5	112
7	2.98	0.2425	0.0752	0.0437	112.3	162.2	116
8	2.96	0.289	0.103	0.044	113	145.3	116.6
9	2.995	0.108	-	0.0434	110	204	114
10	2.845	0.2175	0.1168	0.0426	103	188	109
11	2.82	0.258	0.1725	0.0427	102	258	109

where the superheated steam entered the combustion chamber. That is, the superheated steam was injected directly onto the primary mixing holes on the end of the inner "can", causing momentary quenching of the flame in the combustion chamber. If the superheated steam could have been easily injected further upstream from the inner "can", better distribution of the superheated steam could probably have been achieved, allowing more superheated steam to be injected. With the 6.75% superheated steam, and the new air-bleed-off orifice plate, the control valve on the air-bleed-off was not fully opened.

5.8 Work Output

For the first 6 trials, table 5-1, the net work output is seen to be about the same, but after correcting the thermocouple on the top combustion chamber (trial 9), a decided decrease is noted. This would obviously be the case, as more air is required to cool the flame, reducing the amount of air that could be bled off (table 5-2). It is also obvious that if the superheated steam was used to replace some of the air passing through the lower combustion chamber, more air could be bled off from the compressor, producing more work output. This is also verified by the net work output (table 5-1) and the amount of air bled off (table 5-2).

5.9 Heat Input

The heat input (BTU's/sec.) is seen to vary quite widely for the trials. This perhaps can be expected as an error of 1/4 lbm on the weighing scale can produce a difference up to 11 BTU/sec. in the heat added. The amount of fuel added to the cycle is also dependent upon the mass flow of air through the combustion chambers, and the maximum temperature before the nozzle ring. Further the mass flow itself is affected

TABLE 5-3

EXPERIMENTAL READINGS

Trial No.	Average Temperatures °F.										RPM
	Air Intake	Comp. Outlet	Comb. Chamber In	Comb. Chamber Out Top	Comb. Chamber Out Lower	Turb. Out Top	Turb. Out Lower	Air Bleed	Steam In	Comb. Chamber Secondary Air	
1	81.0	188.5	185.8	1177.5	1185	1010	1070	171.4	--	204.5	14,700
2	90.7	200.4	197.5	1187	1170	1005	1100	183.0	--	210.7	14,900
3	97.0	209.5	205.3	1195	1192.5	995	1105	201.8	--	220.8	15,400
4	92.0	201.3	198.3	1182.5	1197.5	990	1075	193.8	--	211.0	15,000
5	93.0	199.3	195.4	1283.3	1170	1000	1068.8	184.3	--	204.0	14,900
6	88.0	194.3	191.9	1200	1175	1020	1060	178.3	--	202.0	14,800
7	92.0	203.5	201.6	1140	1188	965	1080	190.5	369.0	272.0	14,800
8	95.7	208.0	204.7	1180	1170	992.5	1100	193.6	390.0	260.0	14,800
9	96.0	202.8	200.0	1195.6	1190.7	949.2	1091.7	196.2	--	210.4	14,900
10	101.3	208.0	205.9	1180	1175.5	943	1067.6	204.0	377.3	280	14,900
11	104.5	211.0	208.1	1190.8	1200	945	990	208.8	374.0	276	14,900

TABLE 5-4

EXPERIMENTAL READINGS

Trial No.	Average Pressures - in. of Hg *in. of H_2O								Air Intake Ave*
	After Comp. Total	Before Comb. Chamber Static	Δp Lower Chamber	Exhaust Static*	Air Bleed Static	Δp Air Bleed	Steam Injection Static	Δp Steam Injection	
1	14.4	14.3	-	>0.1	14.0	21.6*	-	-	1.30
2	14.4	14.2	-	0.2	14.1	21.8*	-	-	1.45
3	15.3	15.1	3.0	>0.1	14.9	26.8*	-	-	1.55
4	14.7	14.6	2.9	>0.1	14.6	24.6*	-	-	1.50
5	14.0	13.8	2.9	>0.1	14.0	29.0*	-	-	1.55
6	14.25	-	2.95	0.30	14.0	1.615	-	-	1.40
7	14.35	-	3.0	0.40	14.0	5.96	15.17	0.719	1.40
8	14.45	-	3.0	0.40	14.0	9.16	15.17	1.40	1.40
9	14.05	-	2.95	0.30	14.0	1.0	-	-	1.45
10	13.95	-	3.0	0.35	13.6	3.1	14.51	5.35	1.25
11	14.0	-	3.05	0.35	13.45	6.23	15.56	11.8	1.25

by the air intake temperature. That is, as the air intake temperature increases, the air density (lbm/FT^3) is reduced, reducing the mass flow drawn in by the compressor.

For the trials with steam injection, the amount of heat added is also dependent upon the amount of superheated steam added and the temperature rise imparted to the superheated steam (average Cp of superheated steam between 300°F. and 1200°F. is 0.494 BTU/lbm°F.)[22]. This effect is clearly shown in trials 6, 7 and 8, where the mass of air handled by the compressor remained fairly constant (table 5-2). The effect, however, is not quite as pronounced here as it should be because the maximum temperatures were not kept constant (table 5-3). On the next set of trials, that is, 9, 10 and 11, the reverse almost seems to be true. But closer examination reveals that the air intake temperature (table 5-3) increased from 96°F. to 104.5 °F. for these trials reducing the mass flow of air (table 5-2), while the compressor efficiency increased from 64.2% average to 66.2% average, reducing the work to drive the compressor (table 5-2), allowing for a reduction in the heat added.

It is correct though, that if the conditions remained the same, that is, the compressor efficiency, speed, and the air intake temperature, more heat would have to be added to the cycle if superheated steam was injected because of the higher Cp value of superheated steam compared with air or air-fuel mixture.

5.10 Thermal Efficiency

The computed "gross" thermal efficiencies shown in table 5-1 are seen to be very low. This is to be expected, particularly, with the apparatus used for the trials. That is, a gas turbine operating with maximum temperatures of 1200°F., a pressure ratio of 1.5, a compressor efficiency of 65%, a turbine efficiency of 75%,

high intake temperature (91°F. average), with 100% combustion efficiency and no pressure losses, has a theoretical thermal efficiency of only 3.19%. Thus with the losses encountered in the experimental apparatus the results obtained are considered to be reasonable (see section 5.14).

The efficiencies are seen to be fairly consistent for the first 6 trials without the added superheated steam, but for trial 9, after the high temperature thermocouple was corrected, a decided drop in thermal efficiency was obtained. With the steam injection, however, significant gains in the work output and thermal efficiency were obtained. These trials show that if the mass rate of superheated steam injected was increased, the thermal efficiency increased.

Because identical operating conditions were not obtained for the two series of steam injection runs (that is, the combustion chamber outlet temperatures varied considerably, as did the mass rates of air flow), it is difficult to conclude the effect of increased cycle temperature (that is, assuming the top combustion chamber outlet temperature was higher than that actually recorded) on the increase in efficiency to be obtained.

The experimental error in these trials was found to be 12% assuming that the mass rate of air-bleed-off was correct. That is, the orifice plates were not calibrated against a known discharge, as this equipment was not available.

5.11 Compressor Horsepower

The horsepower required to compress all the air drawn in by the compressor for each trial is seen in table 5-2. The values obtained are highly dependent upon the air intake temperature (changes in the density of the air) and the compressor adiabatic

efficiency. The adiabatic efficiency of the compressor affects the air delivery temperature directly, that is, the enthalpy of the air at discharge, and the enthalpy difference induced by the compressor.

The maximum difference in horsepower is seen to occur during the last series of trials (that is, trials 9, 10 and 11), accounting for the obvious drop in the heat added, even though steam injection took place.

5.12 Turbine Horsepower

A comparison of the horsepower produced by the turbine (table 5-2) with the horsepower required by the compressor for any given trial shows definite disagreement between them. The reason for this is that the turbine horsepower was calculated on the average measured temperature drop through the turbine wheel. While the temperatures into the nozzle ring were kept about equal (neglecting the effect of the erroneous thermocouple), the temperatures after the turbine wheel differed as mentioned in section 5.7.

A check of table 5-5, however, shows that the theoretical temperature after the turbine wheel, assuming that the temperature in was correct, is considerably higher than the average of the measured temperatures. It should be noted, however, that the temperature measured at the bottom after the turbine wheel, matches the theoretical values computed in table 5-5 for trials 9 and 10 closely (that is, $1091.7_{exp.}$ versus $1093_{theo.}$, and $1067.6_{exp.}$ versus $1075_{theo.}$). For trial 11, however, the measured temperature is about 100°F. below the theoretical value.

5.13 Theoretical Turbine Horsepower

The results obtained from the theoretical horsepower calculations are in close agreement (table 5-2) with the horsepower required by the compressor. This will further substantiate the erroneous temperature after the turbine wheel.

5.14 Comparison of Theoretical and Experimental Results

Table 5-5 shows a comparison of theoretical and experimental results for trials 9, 10 and 11. The theoretical values were arrived at by using the temperature and pressure readings taken during the actual tests. That is, the air intake temperatures were the same in each case as well as the compressor adiabatic efficiency. The temperature after compression was calculated from air tables using the measured pressure ratio. The results are very close.

The turbine inlet temperature was also assumed equal in both cases, as well as the steam temperature into the nozzle ring. The turbine pressure ratio was found as described in section 4.3, and using tables of combustion products of 400% air, and steam tables where necessary, the isentropic heat drop was computed. Assuming the turbine efficiency to be the same, the actual enthalpy drop and temperatures were obtained.

The question arises at this point as to whether the turbine has the same efficiency for superheated steam as for the air-fuel products of combustion. It is perhaps a reasonable assumption as is evidenced in section 1.3, superheated steam behaves approximately as a perfect gas, as would the products of combustion of 400% air for the range considered (that is, about 100°F. drop and 6 p.s.i. drop). If the turbine efficiency were lower than the assumed value, say 70%, the theoretical efficiency for trial 11

TABLE 5-5

COMPARISON OF THEORETICAL AND EXPERIMENTAL RESULTS

Trial No.		Air Intake Temp °F.	Comp. Eff. %	Air Temp. After Comp. °F.	Turb. Inlet Temp. °F. Ave.	Steam Temp. At Turb.	Turb. Outlet Temp. °F.	Steam Temp. Turb. Outlet	Work Comp. BTU/ Sec.	Work Turb. BTU/ Sec.	Comp. Turb Eff. %	Heat Added BTU/ Sec.	Thermal Eff. %
9	Exp.	96.0	64.2	202.8	1193	--	1021	--	--	--	--	807	0.344
	Theo.	96.0	64.2	204.0	1193	--	1093	--	74.9	80.8	98	807	0.545
10	Exp.	101.3	65.9	208.0	1177	1175.5	1005	--	--	--	--	793	0.705
	Theo.	101.3	65.9	207.6	1177	1175.5	1075	1090	67.2	77.15	98	793	1.093
11	Exp.	104.5	66.2	211.0	1195	1200	967	--	--	--	--	795	0.814
	Theo.	104.5	66.2	211.2	1195	1200	1096	1116	65.6	77.18	98	795	1.29

would be 1.225%, or if it were 80%, the efficiency would be 1.353%. In either case, the agreement is good.

The heat added to the cycle was assumed to be the same in both cases, and a turbine-compressor drive efficiency of 98% was assumed for the theoretical calculations.

The compressor work calculated was only that necessary to compress the air supplied to the combustion chambers, and the difference between the turbine work and the compressor work divided by the drive efficiency was considered as the gross work left over by the cycle. Thus dividing the gross work by the heat added gave an efficiency comparable to the "gross" thermal efficiency defined in section 4.9.

The compressor work and the turbine work were computed as described in sections 4.10 and 4.12 respectively.

CHAPTER 6

CONCLUSIONS AND RECOMMENDATIONS

6.1 Conclusions

The effect on the thermal efficiency of a simple open gas turbine by injecting superheated steam into a combustion chamber has been studied. Although the pump works to supply the fuel and the water to their required pressures were neglected, and the turbine did not produce the steam used in a waste heat boiler, only superheating it, it is concluded that injection of superheated steam into a simple open gas turbine cycle will improve the thermal efficiency of the cycle. This was substantiated experimentally, and when checked against theoretical calculations for the same cycle operating conditions and component efficiencies, close agreement was obtained.

It is felt that while large gains in thermal efficiency were obtained for the particular apparatus used, the effects in commercial units would not be as large, and could be predicted closely by careful calculations as in the cases of Schröder[11] and Chambadal[12].

Except for the limit of flame stability reached in the lower combustion chamber, the detrimental effects, if any, of injecting superheated steam into the gas turbine cycle were not obvious as the running time was very short.

Also verified is the fact that if the ratio of steam mass to air mass is increased, the thermal efficiency will be increased, but in decreasing amounts, until, as in these experiments, a limit of flame stability is reached.

6.2 Recommendations

Although the effect of steam injection upon a simple open gas turbine has been studied, it is felt that a more thorough investigation should be made. If possible these tests should be done on a gas turbine which has a much higher basic thermal efficiency. This would result in more typical results, particularly if the pressure ratio and the temperature into the nozzle ring can be varied easily. Naturally the turbine should produce all the steam used and the pump works should be considered.

If another turbine is not available and the one used in these experiments is used again, it is suggested that a high speed dynanometer be obtained for the machine, and better methods for measuring the temperatures before and after the turbine wheel be employed. Also the position of injection of the superheated steam should be relocated further up stream from the combustion chamber to avoid the flame quenching situation encountered.

In addition, analysis of the exhaust gases should be carried out to check the validity of the non-reactive gases assumption.

BIBLIOGRAPHY

1. R. Tom Sawyer, "The Modern Gas Turbine", Prentice-Hall, Inc., 1945, Chapters 1 and 3.

2. Ibid., p. 1.

3. Ibid., chapter 3.

4. Ibid., pp. 29-31.

5. A. Stadola, "Steam and Gas Turbines", McGraw-Hill Book Co. Inc., 1927, pp. 1235-1236.

6. L. S. Marks and M. Danilov, "Gas Turbines", Trans. A.S.M.E., vol. 46, 1924, pp. 1116-1120.

7. J. G. Coutant, "Water or Steam Injection in Gas Turbine Cycle Provides Unique Performance", Power Engineer, vol. 63, June 1959, p. 95.

8. B. Miller, "Will Added Steam Give Economical Power Boost to Gas Turbines", Gas, vol. 30, December 1954, pp. 93-96.

9. B. Miller, "Gas Turbines for Process Use - I", Chem. Eng., vol. 62, January 1955, pp. 175-180.

10. W. D. Marsh and C. M. Wright, "Gas Turbines for Peak Load Generation on a Large Utility System", Presented to the 1956 American Power Conference.

11. H. J. Schroder, "Die Gasturbine mit Zusatzdampt aus Eigner Abwarme", Motortechnische Zeit (MTZ), vol. 19, February 1958, pp. 56-59.

12. P. Chambadal, "Interet de l'injection d'eau ou de vapeur dans la chambre de combustion d'une turbine a gaz", Chaleur et Industrie, vol. 38, July 1957, pp. 173-186.

13. S. L. Soo, "Thermodynamics of Engineering Science", Prentice-Hall, Inc., 1959, p. 427.

14. M. Jakob and G. A. Hawkins, "Elements of Heat Transfer", John Wiley and Sons, Inc., 1959.

15. V. M. Faires, "Thermodynamics", The Macmillan Co., 1957, page 168.

16. J. H. Keenan and J. Kaye, "Gas Tables", John Wiley and Sons, Inc., 1960.

17. L. C. Lichty, "Internal Combustion Engines", McGraw-Hill Book Co. Inc., 1951, p. 118.

18. J. H. Keenan and F. G. Keyes, "Thermodynamic Properties of Steam", John Wiley and Sons, Inc., 1958.

19. V. M. Faires, op. cit., p. 92.

20. J. H. Keenan and J. Kaye, op. cit., table 10.

21. Ibid., table 9.

22. J. H. Keenan and F. G. Keyes, op. cit., p. 80.

23. P. H. Wilkinson, "Aircraft Engines of the World, 1957", P. H. Wilkinson, 1957.

24. Ibid., "Aircraft Engines of the World, 1959/60", P. H. Wilkinson, 1960.

25. J. D. Pearson, "The Rolls-Royce Derwent Gas Turbine, Jet Propulsion, Aero Engine", Commercial Aviation, October, 1945, p. 27.

APPENDIX A

THE DEVELOPMENT OF THE GAS TURBINE USED IN THIS EXPERIMENTAL STUDY

A.1 Introduction

The actual development of the turbine started as a laboratory assignment in MECH. E. 521. The Mechanical Engineering Department was donated a Brown Boveri Turbo Charger Type VTR 320 by Trans Mountain Oil Pipe Line Co., and it was decided to convert it into a gas turbine.

Correspondence with Brown Boveri (Canada) Ltd., gave specific information on the turbo charger. This included a compressor curve (figure 4-1) and a method of calculating the turbine efficiency (figure 4-2). Brown Boveri also indicated that the turbo charger could be converted into a gas turbine if certain steps were taken.

A.2 Basic Theory of the Gas Turbine

The gas turbine or Brayton cycle operates on a simple continuous flow cycle. Air is compressed and fed into a combustion chamber where fuel is added and the mixture burned. The hot gases then expand in a turbine wheel, driving the air compressor (usually of a centrifugal or an axial flow type). The excess energy in the exhaust gases is then used to produce useful work of some nature; i.e. electrical power generation, jet propulsion, supplying compressed air, etc. A diagram of a simple open cycle is shown in figure A-1.

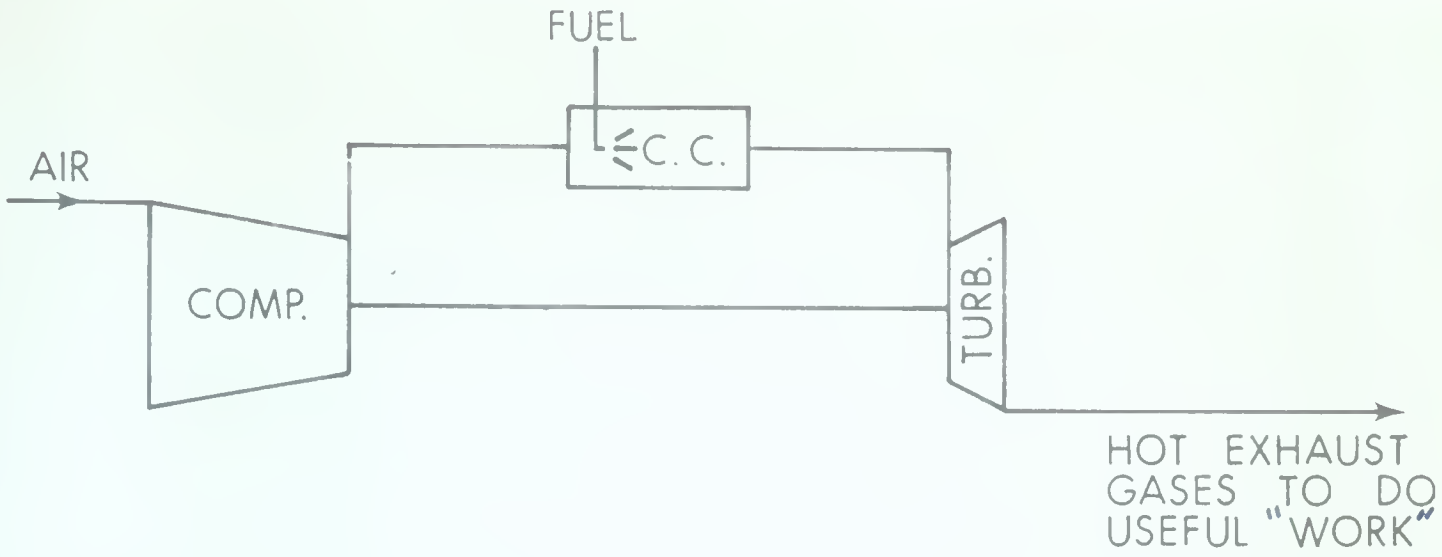

FIGURE A-1 SIMPLE OPEN CYCLE

From figure A-1 it is evident that a turbo charger contains two of the three basic elements of a simple open gas turbine. That is, a compressor (centrifugal type in this case) and a turbine wheel connected on a shaft. Thus, all that is necessary to complete the machine is to install a combustion chamber capable of handling the air flow induced by the compressor.

A.3 Selection of a Combustion Chamber

From the compressor curves supplied by Brown Boveri (figure 4-1) it was possible to calculate the maximum quantity of air induced by the compressor of the turbo charger, this being approximately 57 FT^3/sec. at the stated inlet conditions to the compressor (i.e. atmospheric pressure and 15°C. or 59°F.).

The Mechanical Engineering Department had available two jet aircraft engines, a Derwent II and an Oranda 8. Since the Derwent II had about one-third the thrust of the Oranda, and 10 combustion chambers compared with the Oranda's 6, it was thought that the Derwent chamber(s) would be more suitable.

Since specific information as to the air mass flow rate of the Derwent was not available, a rough check was obtained from Wilkinson[23,24] by plotting the mass flow in pounds of air per second at inlet against thrust output for numerous engines given in the reference. Figure A-2 shows the resultant curve with the range of the Derwent II clearly marked. This range was obtained from Pearson[25]. This figure shows then, that the capacity of the Derwent is approximately 40 pounds mass of air per second at inlet conditions. Since there are 10 combustion chambers, each chamber is capable of handling about 4 pounds mass of air per second.

Converting 4 pounds mass of air per second to feet cubed per second at the compressor inlet conditions of 13.5 p.s.i.a. (for Edmonton) and 59°F., assuming perfect gas laws,

$$Pv = RT \qquad A.1$$

or

$$v = \frac{RT}{P}$$

$$v = \frac{53.3 \times 519}{13.5 \times 144} = 14.22 \text{ FT}^3/\text{lbm}$$

Therefore one Derwent chamber can handle

$$4 \text{ lbm/sec.} \times 14.22 \text{ FT}^3/\text{lbm} = 56.88 \text{ FT}^3/\text{sec.}$$

Comparing this value with the maximum of the turbo charger, i.e. 57 FT^3/sec., it is seen that one chamber should ideally fit the requirements since maximum speeds and mass flow were not intended to be used in the actual running of tests.

It should also be noted that the Derwent engine is designed to operate in the range of 4 atmospheres pressure, which is well above the capabilities of the Brown Boveri unit. Whether or not this will have any effect on the combustion characteristics

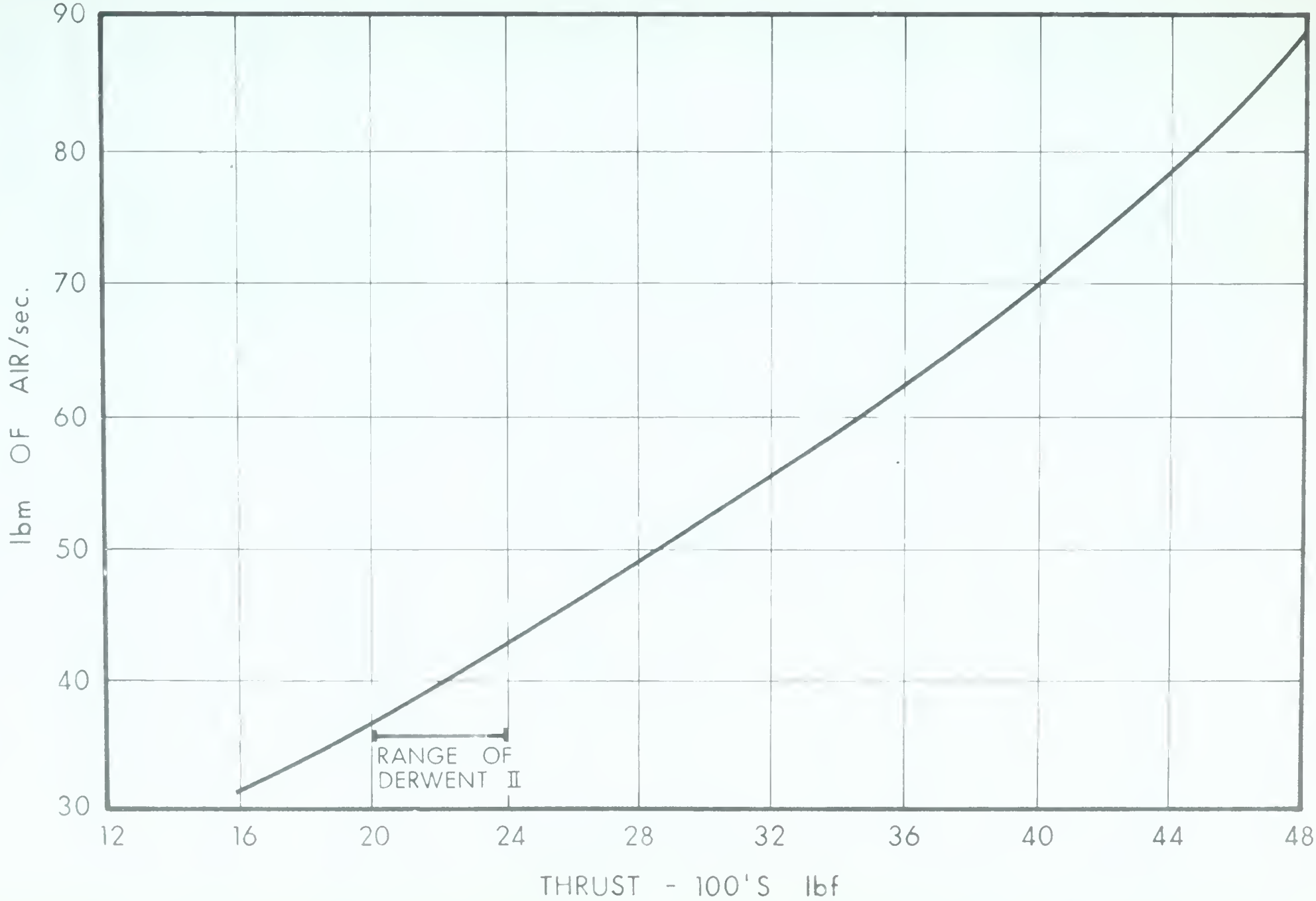

FIGURE A - 2 MASS AIR FLOW versus THRUST FOR JET AIRCRAFT ENGINES

of the chamber is hard to determine (i.e. combustion efficiency and film cooling of the inner "can").

A.4 Fuel Spray Characteristics

Once the decision to use a Derwent combustion chamber was made it seemed desirable to make a study of the spray characteristics and fuel flow rates of a Derwent fuel nozzle or burner.

The actual testing of the burner was done by using a 1/4 H.P., 110 volt electric motor to drive a gear pump pumping varsol through the burner. Since the gear pump is of the positive displacement type, a by-pass system was used as shown in figure A-3.

The burner was supported independently of the container with a transparent lid permitting observations. The valve controlled the pressure (i.e. flow) at the burner since the flow through the burner orifice depends upon the pressure of the fluid at the orifice. When the valve was fully open, the flow through the burner was nil.

The characteristics shown in figure A-4 were obtained by visual observation (a haze would form over the container if the lid was left off) and by the replacement weight method for the mass flow.

It should be noted that the burner was designed to use the compressed air entering the inner "can" to help impart additional swirl to the fuel. Thus, these observations could conceivably be in error, but do give good indications of the actual characteristics.

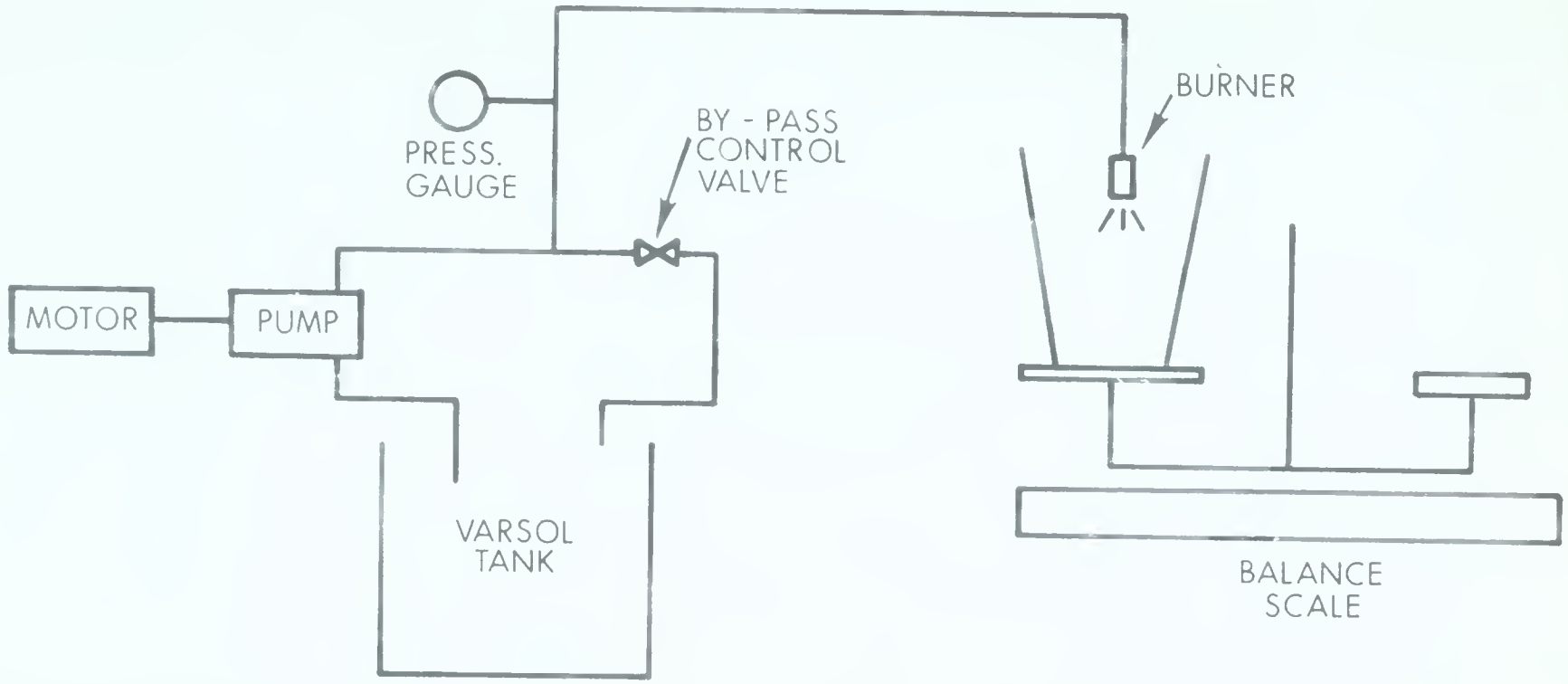

FIGURE A - 3 METHOD OF TESTING DERWENT BURNER

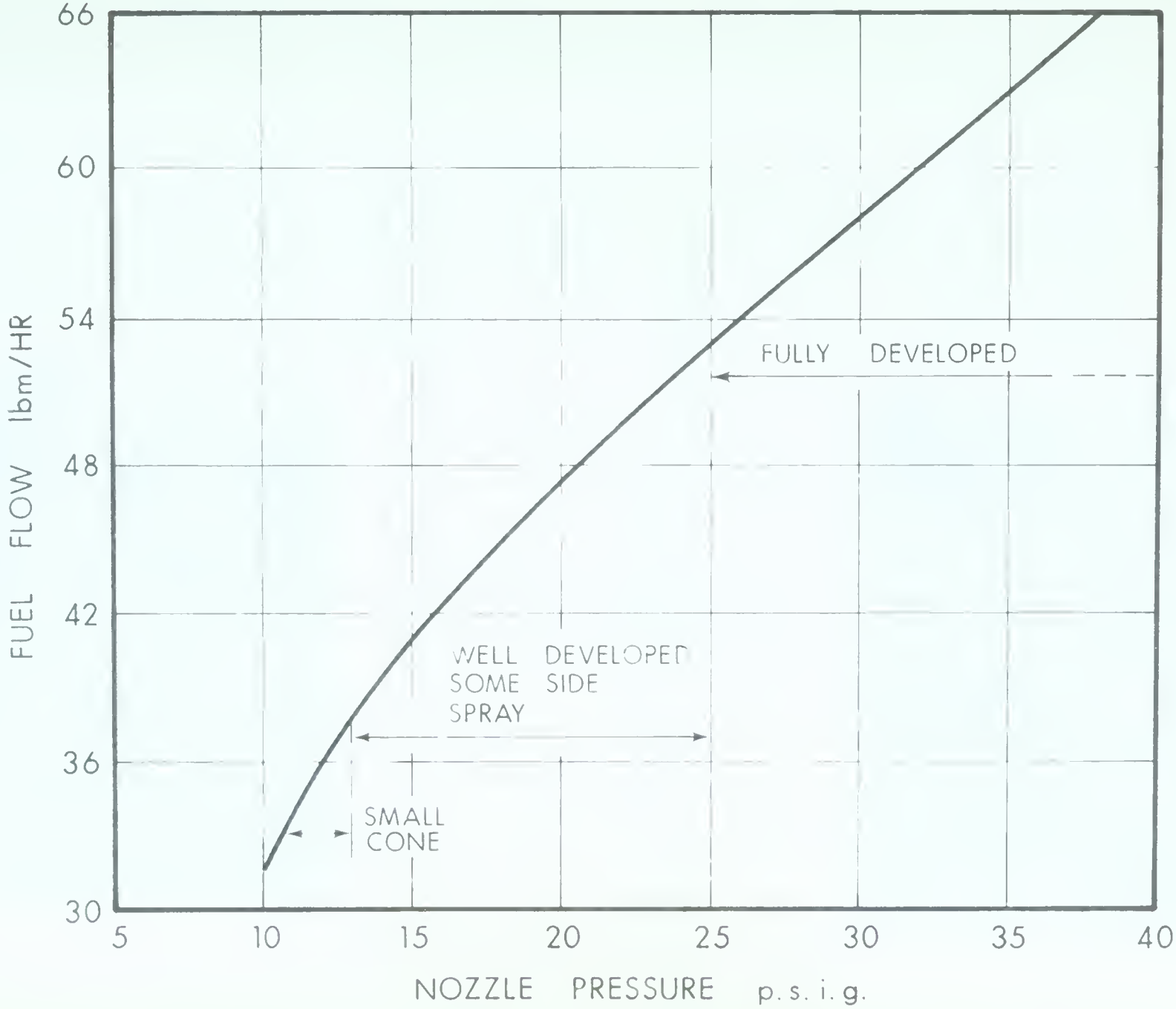

FIGURE A-4 SPRAY CHARACTERISTICS OF A DERWENT BURNER

FIGURE A-5 EQUIPMENT FOR COMBUSTION CHAMBER IGNITION TESTS

FIGURE A-6 COMBUSTION CHAMBER SHOWING THE OUTER LINER AND THE INNER "CAN"

A.5 Flame Testing of the Combustion Chamber

After choosing the combustion chamber and checking the characteristics of the burner, the next obvious step was to see if it was possible to obtain a stable flame in the combustion chamber at atmospheric pressure. To do this the combustion chamber was set up in the same jet room as shown in figure A-5. Initially, compressed air from the University Power Plant and the Mech. E. 340 laboratory was used.

The compressed air entered the pipe shown on the left of figure A-5, and then ran through tin duct work around to the end of the combustion chamber as would be the case when set up in the turbine. (See figure A-12.)

In order to facilitate this, certain modifications were made to the outer liner of the combustion chamber. Initially the chambers in the aircraft engine looked as shown in figure A-6, with 2 holes in the outer chamber to allow the flame to jump from one chamber to the next on light up. One of the holes can be seen on the left side of the chamber in figure A-6. These holes were plugged, as shown in figure A-7. With the plugs installed, the outside of the chamber looks as in figure A-5 or A-9.

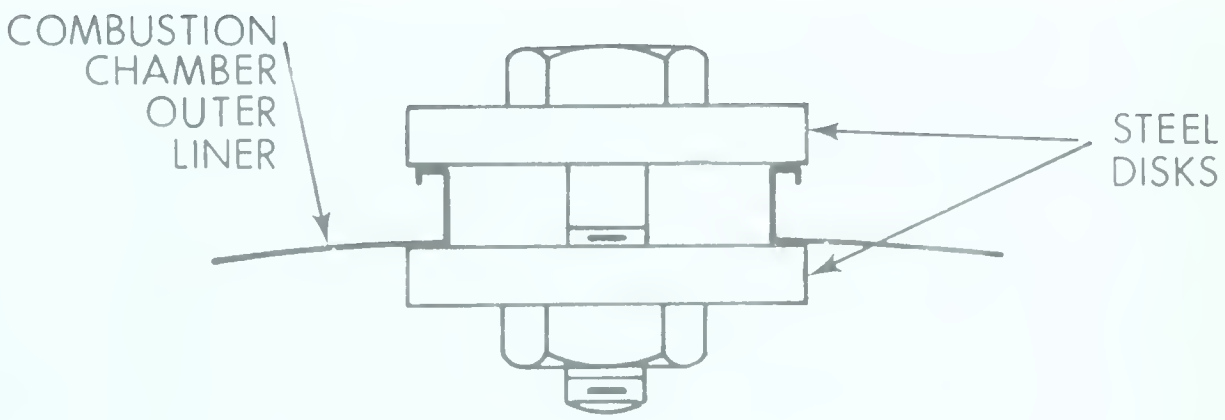

FIGURE A - 7 METHOD USED TO BLOCK EXTRA FLAME JUMP HOLES

In addition to this, the straight portion of the outer chamber was cut from another chamber, the flame holes plugged, and mounted back to back to the original chamber as shown in figure A-8. This can also be seen in figure A-9. This allowed an 8" circular metal duct to be fitted snugly over the end to complete the air flow circuit as shown in figures A-5 and A-9.

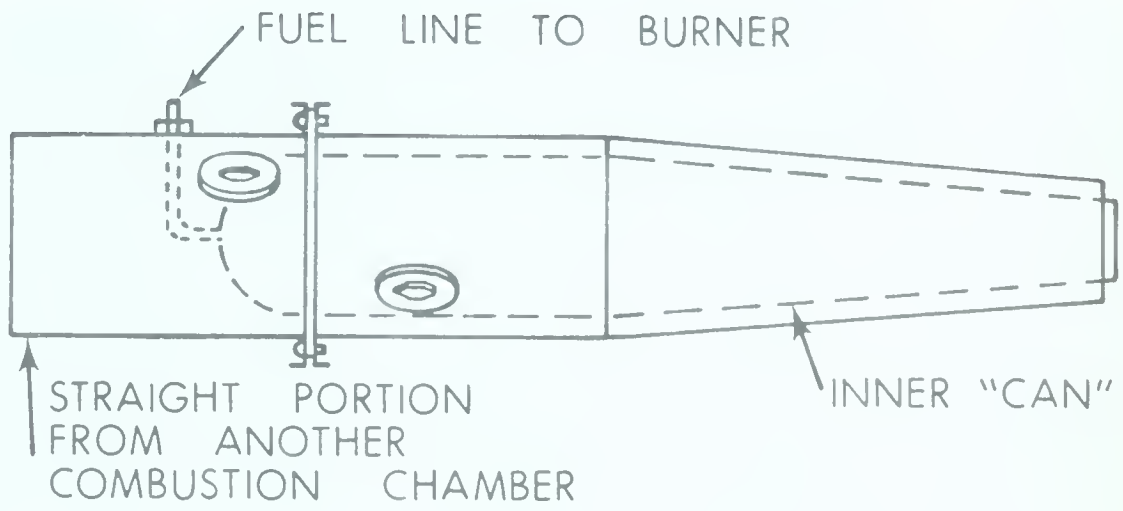

FIGURE A - 8 METHOD OF MODIFYING COMBUSTION CHAMBER

The combustion chamber was then mounted in the ram jet room as shown in figure A-5. For safety sake, the controls were mounted outside the ram jet room on a bench allowing the operator to observe the operation of the tests through a hole in the wall (see figure A-10).

In the initial tests, to insure positive ignition, a lighted propane torch was used in place of the Derwent ignitor plug. These tests showed that a flame could be obtained using diesel fuel or kerosene pumped in from outside the room. They also showed that a much greater supply of air was required to maintain a flame for any

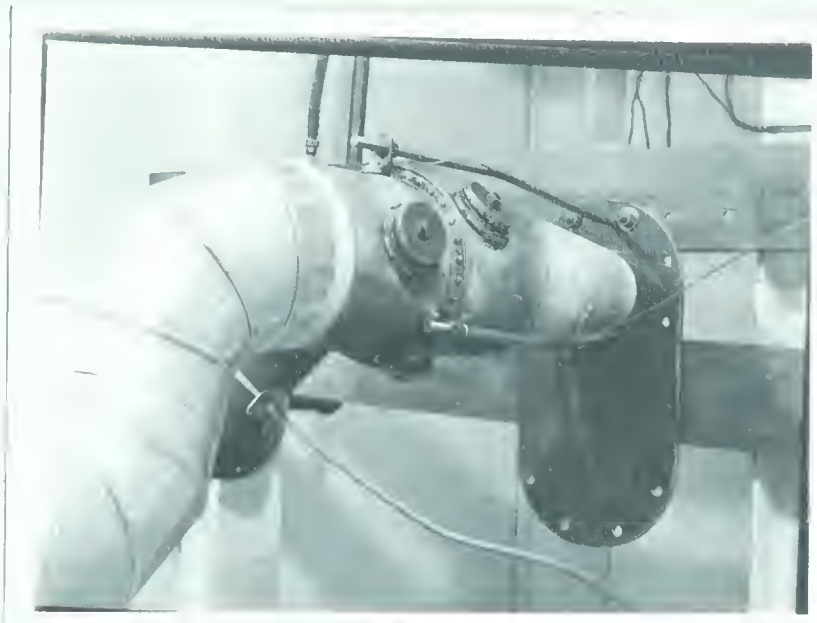

FIGURE A-9 CLOSE-UP OF THE COMBUSTION CHAMBER DURING FLAME TESTS

FIGURE A-10 VIEW OF OBSERVATION PORT AND TURBO CHARGER BEFORE CONVERSION

length of time.

A larger and steady supply of air was obtained from the "nozzle" air gun shown in figure A-5. Controlling the air supply by fan speed variation by use of a variac, flames were obtained using diesel fuel or kerosene, still using the propane torch as the source of ignition. As a matter of interest, the propane torch was still lit at the conclusion of each test.

The next step was to obtain a more normal means of ignition, that is spark ignition. To do this, the spark transformer and an ignitor from the Oranda engine were used. Since the Oranda transformer would not spark the Derwent plug, the Oranda plug was modified to fit the Derwent chamber and to accept the Derwent fuel catcher.

With this ignitor and the "nozzle" gun, flames were obtained using both kerosene and methyl alcohol within 20 - 30 seconds of pump on.

When diesel fuel or kerosene was ignited, a "whump" was always heard, while with the methyl alcohol, no noise accompanied ignition. The methyl alcohol burned very quietly with a blue flame, while both diesel fuel and kerosene, having about twice the heating value per pound mass, burned bright yellow even with minimum pump pressure and maximum air flow.

Because of the rather low temperature restriction in the turbo charger, 1200°F., it was necessary to check the flame temperature leaving the combustion chamber to see if it was acceptable.

To do this, 5 iron-constantan thermocouples were connected to an automatic balancing, 40 position, 2 range, Honeywell potentiometer reading in degrees Fahrenheit. One thermocouple was put into the flame itself, one in the outside of the

outer liner, and three at an outlet of the chamber as shown in figure A-9.

Diesel fuel was not used in this series of tests because its ability to ignite readily was doubted. The methyl alcohol proved to be very good, while the kerosene seemed to produce a flame too hot for start ups on the turbine.

A.6 Initial Modifications to the Turbo Charger

For easy adaptation of the combustion chamber to the turbo charger, figure A-10, the right hand end was rotated through 90° as shown. Thus the compressor outlet and the turbine inlet were placed in the same plane.

The turbo charger was then mounted on a frame and then on a dolly so it could easily be moved in under the exhaust stack in the ram-jet room (figure A-12).

The combustion chamber was then attached to the turbine inlet with the air "nozzle" gun still attached as in figure A-5. This allowed a check on the ability of the fuels to ignite and the critical temperature at the nozzle ring inlet. A water line was also connected to the jacketing on the turbine as a good safety precaution.

The control system was as described before, except the revolution per minute indicator was added (see section 2.1.1 for details). This instrument was originally gear driven through a 5 to 1 reduction, but after a few hours of trials, the gears failed and were replaced by fibre friction disks as shown in figure 2-6, which have worked satisfactorily ever since. It was later found that the R.P.M. readings shown by this instrument were approximately twice the actual value.

A.7 Initial Trials

Due to the repetition of several runs in the initial trials, a summary has been made in table A-1. It should be remembered that the error in the revolutions per

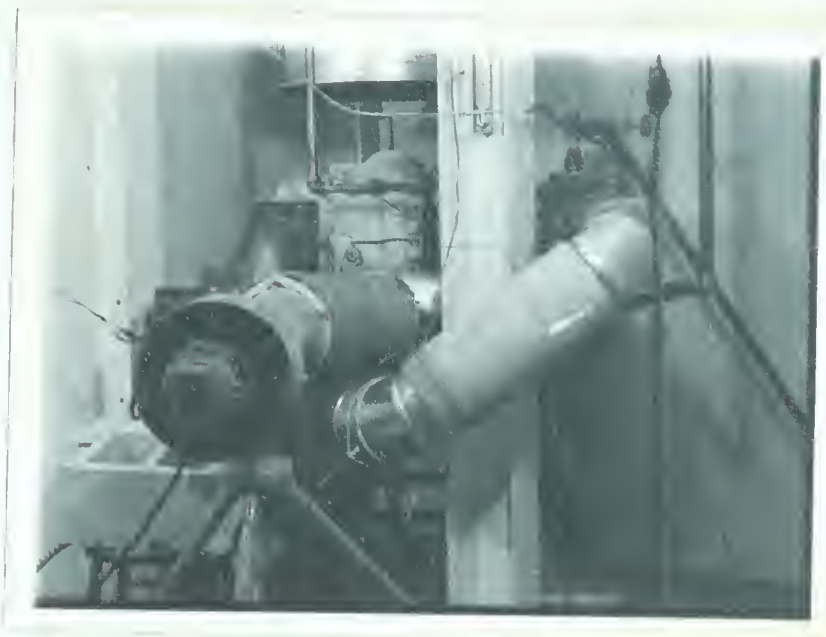

FIGURE A-11 GENERAL VIEW OF TURBINE DURING INITIAL TRIALS

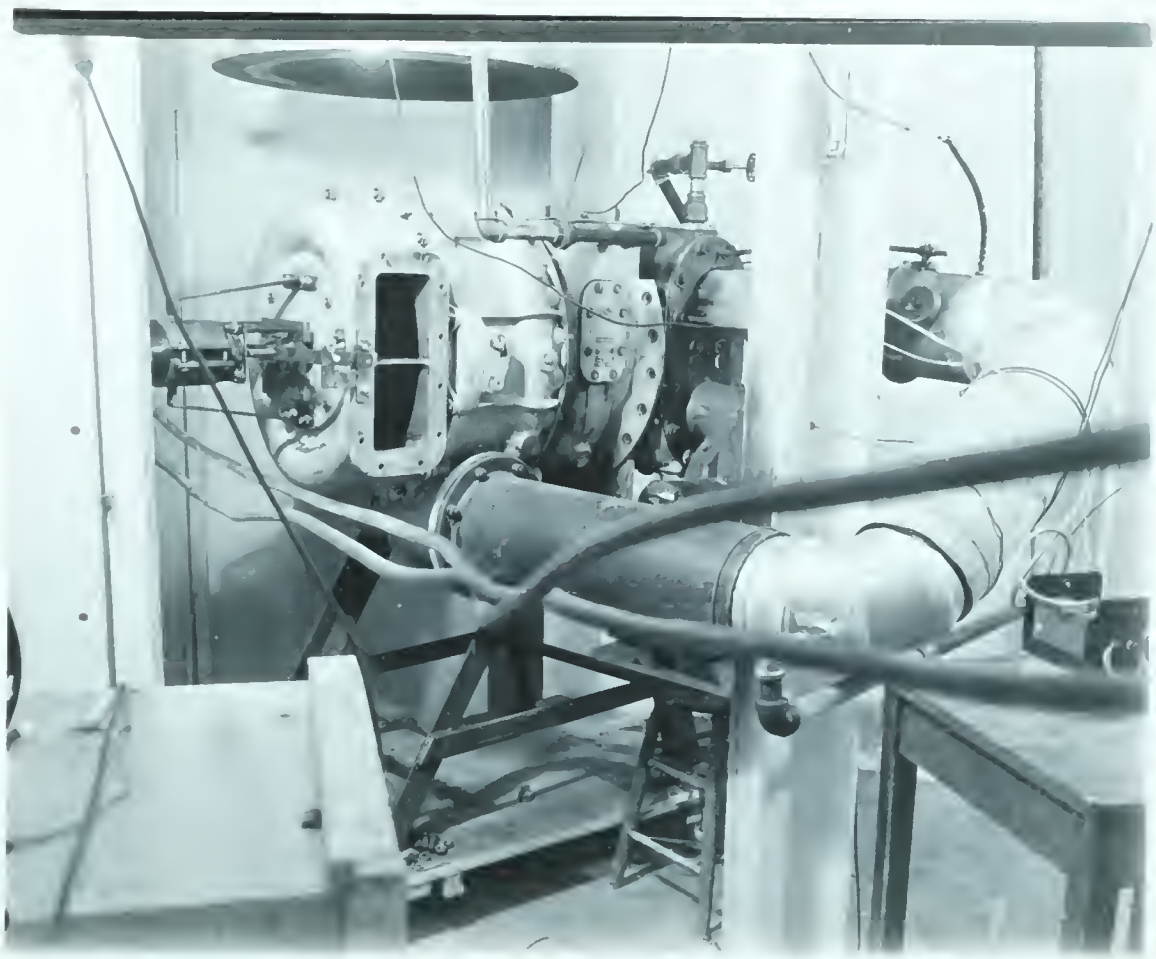

FIGURE A-12 GENERAL VIEW OF TURBINE BEFORE ADDITION OF SECOND COMBUSTION CHAMBER

minute indicator had not been found at this time so that, as in the case of series 14, the indicated speed was about 7800 RPM, coupled with the 4" of Hg total pressure produced a not unlikely spot in the Brown Boveri compressor curves. Thus things were thought to be working out quite nicely at this time.

TABLE A-1

SUMMARY OF INITIAL TESTS

Series No.	Purpose	Equipment Arrangement	Observation and Remarks
1	check light up temperature on alcohol	as described in section A-6, no connection between compressor and combustion chamber	Temperature good, (before and after turbine), speed low
2	as in series 1	as in series 1 except the compressed air lines were added for additional boost	temperature good, speed low, no apparent discharge from the compressor
3	to increase the speed of the turbine unit on alcohol	as in series 2 except a new exhaust fan was added to the lower turbine inlet for increased running speed and cooling of the turbine blades, no compressed air	speed up to 1000 RPM actual (2000 RPM observed)
4	attempt to get the turbine to supply its own air on alcohol	nozzle air gun on lower turbine inlet, compressor air duct connected as would be in normal use, no compressed air	ignition fine, temperatures normal, speed 1000 RPM actual
5	to increase its RPM	as in series 4, except exhaust fan in compressor inlet, see figure A-11	temperatures normal, speed 1700 actual. Present supply of alcohol used up.
6	try ignition on kerosene	as series 5 but exhaust fan removed	flame very hot 2300°F. Trouble getting ignition. Rapid cooling speed 1600 RPM actual

TABLE A-1 Continued

Series No.	Purpose	Equipment Arrangement	Observation and Remarks
7	increase running speed on kerosene	no compressed air, exhaust fan into lower turbine inlet, air gun on compressor inlet	trouble with ignition, hot flame, rapid cooling, speed 1425 RPM, flame very unstable, flame out occuring, decrease in speed from series 6
8	as series 7	as series 7, but compressed air added into the duct from the compressor to the combustion chamber	flame stable if compressed air is on, speed 1750 RPM, pump 7 p.s.i., flame out again occuring, duct joints separated
9	as series 7	exhaust fan and nozzle air gun connected in series into the turbine inlet, compressed air as before, secured duct to column as shown in figures A-11 and A-12, also added a static pressure tap into the duct as seen at the top of the above figures	no flame, 1150 RPM - 4.5" of H_2O, with flame, 1750 RPM, 10" of H_2O, pump 7 p.s.i., speed drops if fans off
10	to check the air flow into the compressor using an air anemometer, on kerosene	exhaust fan only on turbine inlet, changed static pressure tube to a total head tube	did 3 runs, no conclusive results, all results similar to above, extreme trouble with ignitor plug wetting out, definitely need higher spinning speed and better source of ignition
11	check general performance on alcohol	Derwent starting motor installed - see figures A-12, also using Derwent ignitor with a model "T" coil providing sprak fed by a dry cell battery, exhaust fan left in lower turbine inlet	cranking speed 2500 RPM on 42 volts, no flame, blew total head manometer out, replaced with mercury, with flame, thermo-

TABLE A-1 Continued

Series No.	Purpose	Equipment Arrangement	Observation and Results
			couples not working, 2" Hg at 2500 RPM, ignitor not working properly
12	as series 11	coil now fed by a 6 volt automotive battery, rest as series 11, thermocouples checked out	did several runs with alcohol starts, switching to kerosene, speeds up to 3750 RPM, pump 21 p.s.i., 3" Hg, speed will not hold with starter off, flame chatters the duct work if compressed air on
13	as series 11	as before except 54 volts on the starter	again did several runs, results similar to series 12 but sparks beginning to emit from the starter
14	as series 11	starter alignment corrected	speed 3900 RPM, pump 25 p.s.i., total pressure 4" Hg, immediate decrease in speed if starter off, duct work joints separating even though tied securely

A.8 Additional Modifications

As the previous set of series runs ended with the second term in the spring of 1962, it was decided that if a really serious attempt was to be made on the turbine, extensive modifications and instrumentation were needed.

Since the ram jet had arrived and was going to be installed in the room presently used, it was decided to move the turbine into the south east corner of the C.F.R. engine room, so that an exhaust duct could be run from the turbine, through the observation hole used in the past, to the exhaust stack in the ram jet room.

Deep consideration was also given to a statement by Brown Boveri mentioning that full use should be made of the gas inlet ports, thus requiring two combustion chambers. This statement was soon confirmed when the turbine was dismantled to check the condition of the nozzle ring and the turbine blades.

Photographs taken at this time are shown in figures A-13 and A-14. In figure A-13, no apparent damage is seen, but in figure A-14, it is evident that effectively only one-half the nozzle ring area had been used, that is the light area, while the other one-half was covered with carbon left over from the turbo charger's use on a diesel engine. Also evident, but not seen here, was that the section of the nozzle ring used was warped from excessive temperatures reached on light ups with kerosene.

Exactly how to add a second combustion chamber was thoroughly discussed, and since equal flow to each chamber could not be insured in any set up, it was decided to make the air flow somewhat in favor of the top chamber, since the steam injection was going to take place in the lower chamber only. The installation decided

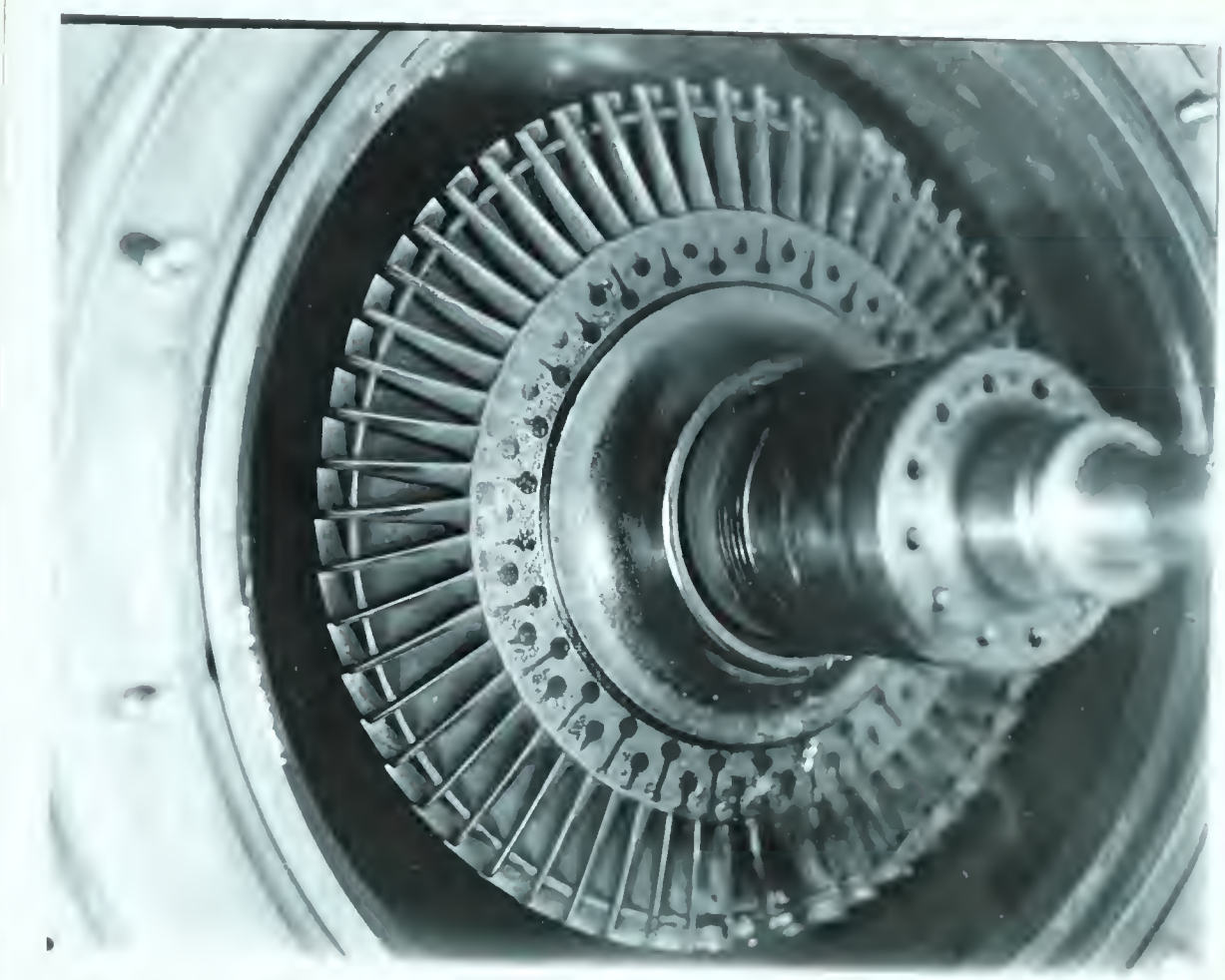

FIGURE A-13 TURBINE BLADES AFTER THE FIRST SERIES OF TRIAL RUNS

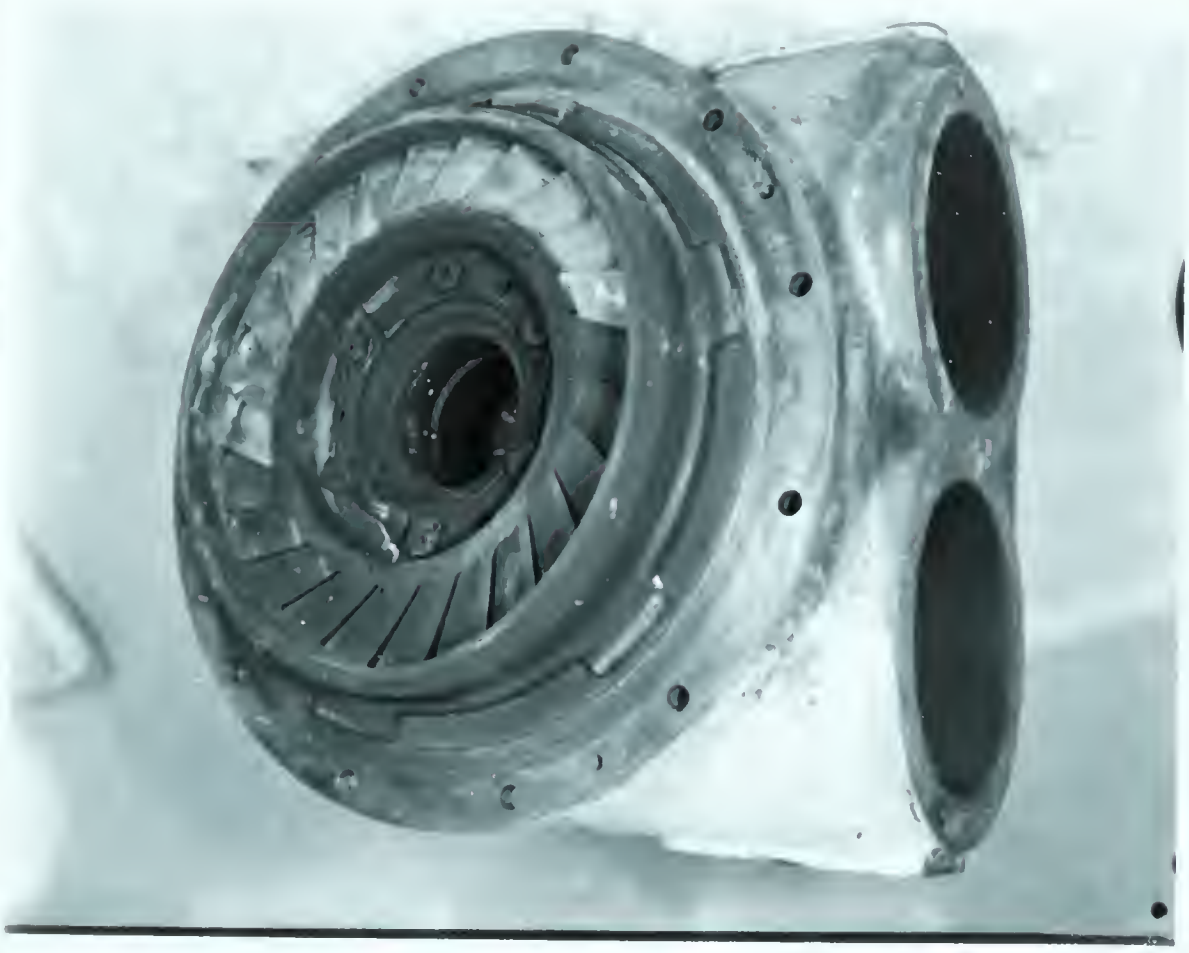

FIGURE A-14 NOZZLE RING AFTER THE FIRST SERIES OF TRIAL RUNS

upon also reduced the cost considerably as standard 8" pipe is quite expensive.

The lower combustion chamber (see figure 2-4) is identical to the top chamber, and a flame jump tube was added between them. It was hoped that this flame tube would help ignite one chamber or the other in starts, or in case of a flame out in one chamber. In actual practice the lower chamber has ignited itself in start up without spark ignition.

Having set up the combustion chamber as in figure 2-4, the duct work from the compressor to the combustion chambers was added as shown in figure 2-2. In order to make combustion chamber removal fairly easy, two bolt flanges were cut from extra chambers and welded in to the 8" pipe, so a mechanical connection exists between the chambers and the pipe as shown in figure 2-4.

Next a 10" circular duct with a pitot tube traversing station was constructed for the air intake to the compressor as shown in figure 2-1. The measuring station was originally calibrated on an heater-air conditioner unit, but proved to be insufficient and was later re-calibrated on the wind box in the Mechanical Engineering air flow laboratory using the Keith fan and the General Electric D.C. motor to drive the fan. The calibration curve obtained is shown in figure 2-12.

The air intake duct was attached to the compressor inlet by a transition piece. This can be seen in figure 2-3.

The pressure tappings and thermocouples were next installed. The pressure tappings consist of a total head tube at the compressor outlet as seen in figure 2-2, and static pressure tappings before each combustion chamber as shown in figure 2-4. These tappings were connected through tygon tubing to U-tube manometers filled with mercury

as seen in the left of figure 2-1.

The thermocouples consist of iron-constantan before and after the compressor and before each combustion chamber, while chromel alumel thermocouples inside stainless steel jackets were used at the hotter locations, before and after the turbine wheel. The locations of these chromel and alumel thermocouples can be seen in figures 2-3, 2-4 and 2-6. All the thermocouples are connected into the before mentioned 40 position potentiometer (see figure 2-13).

The rest of the controls remained the same with the exception of a "T" connection which was installed in the fuel line. This had a quick action shut off valve to feed the lower combustion chamber.

When most of the above had been completed, several run ups were tried on the starter fed by 42 volts. Speeds reaching 4500 RPM actual were obtained but very low pressures occured, and the points in the Brown Boveri chart did not match up well at all when compared with the air flow measurements.

The reason for the increase in the free running speed over the previous values of about 2500 RPM actual (see table A-1) was probably due to less resistance to air flow offered by the two chambers compared to one.

Several of these runs were made with similar results. Finally, the starter lost its power, the batteries being used only 3 times since the last charging. The starter was dismantled and inspected. New bearings were installed, but the starter still lacked power. A check of the batteries showed that they were very weak and since it takes a week to recharge them, a more reliable source of power was sought.

The answer to this problem was found in a 60 H.P. D.C. dynamometer driven by a 3-cylinder, 2-stroke, G.M.C. Diesel engine which the Mechanical Engineering Department has in its internal combustion laboratory. Checking the output of the dynamometer through a load bank, it was found that with maximum field excitation at 600 RPM, 50 volts and 250 amps could be produced, which was about equivalent to the output of the batteries. With minimum field excitation, these values dropped to 30 volts and 100 amps at 600 RPM.

Electrical cable was then run from the dynamometer to the starter through a switch for cutting in and out the power. Since the diesel could not be controlled from the C.F.R. engine room, it was run at 600 RPM and maximum field excitation. This worked well until the shear pin in the starter drive began to break due to the instantaneous maximum power input. To get around this a 12 volt battery was connected into the circuit with a switch as shown in figure A-15.

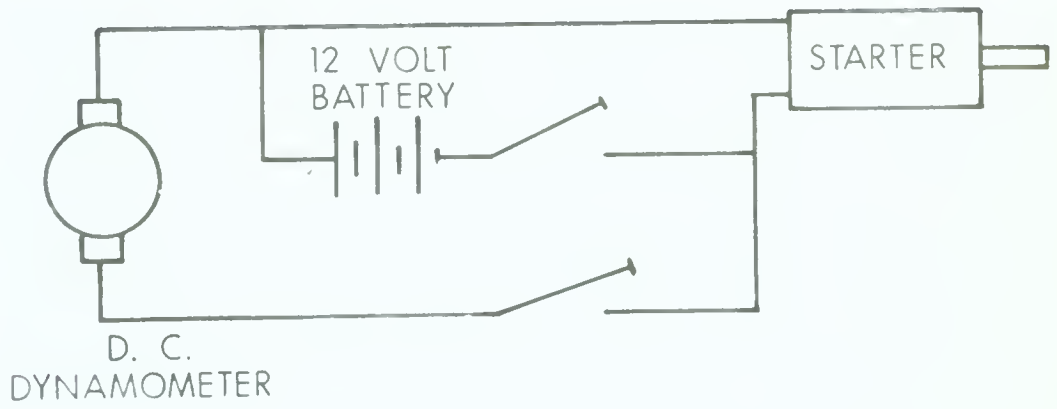

FIGURE A - 15 METHOD OF APPLYING LOW AND HIGH VOLTAGE TO STARTING MOTOR

This allows the turbine to be started easily in 12 volts (2000 RPM actual) and switched to the diesel for maximum run up speed.

A.9 Additional Trials and Success

Again the trials have been tabulated as in section A.7, and it should be noted that there is some overlapping between section A.8 and this section.

It should also be noted that only short summaries of equipment modifications are given here, while a more detailed description of the final arrangement, i.e. series 29, is given in the description of the apparatus, chapter 2.

While additional trials were run after no. 29, they were exclusively thermal efficiency runs and are summarized in chapter 5.

TABLE A-2

ADDITIONAL TRIALS

Series No.	Purpose	Equipment Arrangement	Observations and Remarks
15	check RPM, pressures and air flow	as described in section A-8, starter fed by batteries	3 runs, battery trouble occurred on last 4500 RPM actual, no correlation between speed, air flow and pressures
16	check operation of starter	as series 15, only starter overhauled	speed low, batteries weak
17	check RPM, pressures and air flow	starter now powered by the Diesel engine	2 runs, operation fine, still no correlation
18	check ignition of combustion chamber	as series 17, have "T" connection to lower chamber with shut off valve	several runs, trouble at first obtaining lights on alcohol, speeds around 4500 actual, noticed bottom chamber 400°F. hotter than top chamber
19	check control of chamber temperatures and use of alcohol on lights switching to kerosene	as series 18, only a globe valve added to control lower chamber	several runs, good ignition on both chambers - lighting at speeds over 2500 RPM actual. Can maintain temperature control. Turbine seemed to hold its own at 5000 RPM with starter off. Having trouble with alcohol-kerosene mixture slugging. Shear pins beginning to break.
20	check operation of power change on the starter	12 volt battery connected into starter circuit as in figure A-15	several runs, alcohol-kerosene mixture. Top chamber would light fine, but flame would occur when lighting

TABLE A-2 Continued

Series No.	Purpose	Equipment Arrangement	Observations and Remarks
			bottom chamber. Think not enough pump pressure and too much decrease occurs when valve on lower chamber is opened. Also get high temperatures on light.
21	try to keep temperatures down on start by quickly switching from 12 volts to Diesel	as series 20	starting procedure okay; temperatures controllable; turbine actually run for 2 minutes or so. Exhaust dust was smouldering due to improvised duct with soldered joints. Speed about 6500 RPM actual. No pressure correlation. Checked speed with a stroboscope. Seems accurate.
22	modify lower combustion chamber for steam injection		removed combustion chambers. Noticed a large pool of fuel in lower 8" pipe. Installed a drain valve. Also noticed pipe is full of metal chips and slag from welding. Cleaned out pipes and ground down welds. Also flushed pressure tappings in an effort to obtain proper readings. A new exhaust duct was installed as shown in figure 2-3 with an inspection hole as seen in figure 2-4.
23	to check pressures and speed correlation	as before, only added a temporary manometer very close to tappings. Have also installed air bleed off line complete with manometers and valve control. Bleed off from two holes in schroll case on compressor	pressures reading as before, no correlation

TABLE A-2 Continued

Series No.	Purpose	Equipment Arrangement	Observations and Remarks
24	to check start ups in kerosene lighting both chambers simultaneously	as before, only lower chamber fuel control moved to control panel and a valve has also been installed in the upper chamber fuel line, see figure 2-13	after several attempts, system works fine. Ran diesel engine at 800 RPM for extra boost on starter. Turbine definitely ran, had up to 9500 RPM actual (recorder showing 19,000+). Temperatures easily controllable. Noise level very high. Did not try air-bleed-off line. Correlation between pressure and air flow show about 1/2 RPM shown on the recorder. Checked with a hand tachometer. RPM reading approximately twice actual value. Re-calibrated instrument. Correlation is now excellent. Noticed T max. readings high compared with temperature after turbine wheel.
25	to check air bleed off operation and correlation between T max and after turbine	as before, only made T max thermocouples longer so that the place where the copper wire to the potentiometer joins is out in much cooler air, see figure 2-7	Air bleed does not work very successfully. Temperature readings good. Good correlation on compressor efficiency etc. Pump tripped off several times at about 15,000 RPM even with a 1/2 HP motor. Also noticed casing around turbine wheel leaking water.
26	to check action of fuel pump and water leak	as before, only driving a new pump with a 3 HP motor	Water leak still persists, pump action is no good. The pump jumps momentarily to 200+ p.s.i., causing immediate increase in speed. Bushing seized.

TABLE A-2 Continued

Series No.	Purpose	Equipment Arrangement	Observations and Remarks
			Changed to old pump, works fine. RPM recorder doing funny things. Gear loose on generator.
27	as series 26 but also to check fuel weight apparatus	as above. Fuel weighing by using a balance scale (figure 2-5) with a micro-switch installed under the lever arm figure 2-10) to activate the CFR engine switching mechanism and time clock (figure 2-11)	pump fine, RPM's fine, fuel clock started O.K., did not check to see if would stop
28	to check operation of new air bleed off line and action of fuel weighing	as before, but installed air bleed off as shown in figures 2-2 and 2-8 complete with control valve and manometers	several runs. Air-bleed-off operation fine. Fuel clock works.
29	to check static pressure drop across lower combustion chamber, secondary air temperature in lower chamber, and static exhaust pressure	installed a static pressure tap next to T max thermocouple in the lower chamber as seen in figure 2-6. Also installed an iron-constantan thermocouple in bleed hole in outer liner of lower chamber as shown in figure 2-7.	Everything works fine, only drive gears of RPM recorder wore out. Replaced with fibre friction disks. Work fine. Thermal efficiency about 0.425%. Pump leaking badly. Replaced the gear pump with a piston pump driven by a 1/4 HP, 200 RPM electric motor. Operation fine.